

CHAPTER 10: THE BIG PICTURE: COSMOCHEMISTRY

INTRODUCTION

In the previous eight chapters we acquired a full set of geochemical tools. In this and subsequent chapters, we will apply these tools to understanding the Earth. Certainly any full understanding of the Earth includes an understanding of its origin and its relationship to its neighboring celestial bodies. That is our focus in this chapter.

The question of the origin of the Earth is closely tied to that of the composition of the Earth, and certainly the latter is central to geochemistry. Indeed, one of the primary objectives of early geochemists was to determine the abundance of the elements in the Earth. It is natural to wonder what accounts for these abundances and to ask whether the elemental abundances in the Earth are the same as the abundances elsewhere in the solar system and in the universe. We might also ask why the Earth consists mainly of magnesium, silicon, oxygen, and iron? Why not titanium, fluorine and gold? Upon posing these questions, the realm of geochemistry melds smoothly into the realms of cosmochemistry and cosmology. Cosmochemistry has as its objective an understanding of the distribution and abundance of elements in the Solar System, and, to a lesser degree, the cosmos (the latter is relegated to secondary stature only because the data on objects outside the Solar System are much less complete).

The composition of the Earth is unique: there is undoubtedly no other celestial body that has exactly the same composition of the Earth. Nevertheless, the composition of the Earth is similar to that of the other terrestrial planets: Mercury, Venus, Mars, and the Moon. The Earth also shares a common geochemical heritage with the remainder of the Solar System, and all bodies in the Solar System probably have the same relative abundances of some elements, and the same isotopic compositions of most elements. What we know of the composition of the remainder of the universe suggests that it has a composition that is grossly similar to our Solar System: it is dominated by hydrogen and helium, with lesser amounts of carbon, oxygen, magnesium, silicon and iron, but there are local differences, particularly in the abundances of elements heavier than hydrogen and helium.

The unique composition of the Earth is product of three sets of processes. These include those processes responsible for the creation of elements, that is, nucleosynthetic processes; the creation of the Solar System, and finally the formation of the Earth itself. We will begin by considering nucleosynthesis. Meteorites are the principal record of formation of the Solar System and of the planetary bodies within it, so we devote considerable space to understanding these objects. Perhaps ever since he acquired the capacity to contemplate the abstract, man has wondered about how and when the Earth formed. The answer to the question can be provided by applying the tools of geochemistry to meteorites. We close the chapter by attempting to construct a history of Solar System and planetary formation from the meteorite record.

IN THE BEGINNING...NUCLEOSYNTHESIS

ASTRONOMICAL BACKGROUND

Nucleosynthesis is the process of creation of the elements. While we could simply take for granted the existence of the elements, such an approach is somehow intellectually unsatisfactory. The origin of the elements is both a geochemical and astronomical question, perhaps even more a cosmological one. Our understanding of nucleosynthesis comes from a combination of observations of the abundances of the elements (and their isotopes) in meteorites and from observations on stars and related objects. Thus to understand how the elements formed we need to understand a few astronomical observations and concepts. The universe began some 10 to 20 Ga ago with the Big Bang*, since then the

* The age of the universe is currently a hotly debated topic in astronomy and cosmology. Various lines of evidence appear to be contradictory and are not well explained by current theories. This makes one

CHAPTER 10: COSMOCHEMISTRY

universe has been expanding, cooling, and evolving. This hypothesis follows from two observations: the relationship between red-shift and distance and the cosmic background radiation, particularly the former.

Stars shine because of exothermic nuclear reactions occurring in their cores. The energy released by these processes creates a tendency for thermal expansion that, in general, exactly balances the tendency for gravitational collapse. Surface temperatures are very much cooler than temperatures in stellar cores. For example, the Sun, which is an average star in almost every respect, has a surface temperature of 5700 K and a core temperature thought to be 14,000,000 K.

Stars are classified based on their color (and spectral absorption lines), which is in turn related to their surface temperature. From hot to cold, the classification is: O, B, F, G, K, M, with subclasses designated by numbers, e.g., F5. (The mnemonic is 'O Be a Fine Girl, Kiss Me!'). The Sun is class G. Stars are also divided into Populations. Population I stars are second or later generation stars and have greater heavy element contents than Population II stars. Population I stars are generally located in the main disk of the galaxy, whereas the old first generation stars of Population II occur mainly in globular clusters that circle the main disk.

On a plot of luminosity versus wavelength of their principal emissions (i.e., color), called a Hertzsprung-Russell diagram (Figure 10.1), most stars (about 90%) fall along an array defining an inverse correlation, called the "Main Sequence" between these two properties. Since wavelength is inversely related to the fourth power of temperature, this correlations means simply that hot stars give off more energy (are more luminous) than cooler stars. Mass and radius are also simply related to temperature for these so-called main sequence stars: hot stars are big, small cool stars are small. Thus O and B stars are large, luminous and hot; K and M stars are small, faint, and cool. Stars on the main sequence produce energy by 'hydrogen burning', fusion of hydrogen to produce helium. Since the rate at which these reactions occur depends on temperature and density, hot, massive stars release more energy than smaller ones. As a result they exhaust the hydrogen in their cores much more rapidly. Thus there is an inverse relationship between the lifetime of a star, or at least the time it spends on the main sequence, and its mass. The most massive stars, up to 100 solar masses, have life expectancies of only about 10^6 years, whereas small stars, as small as 0.01 solar masses, remain on the main sequence more than 10^{10} years.

The two most important exceptions to the main sequence stars, the red giants and the white dwarfs, represent stars that have burned all the H fuel in the cores and

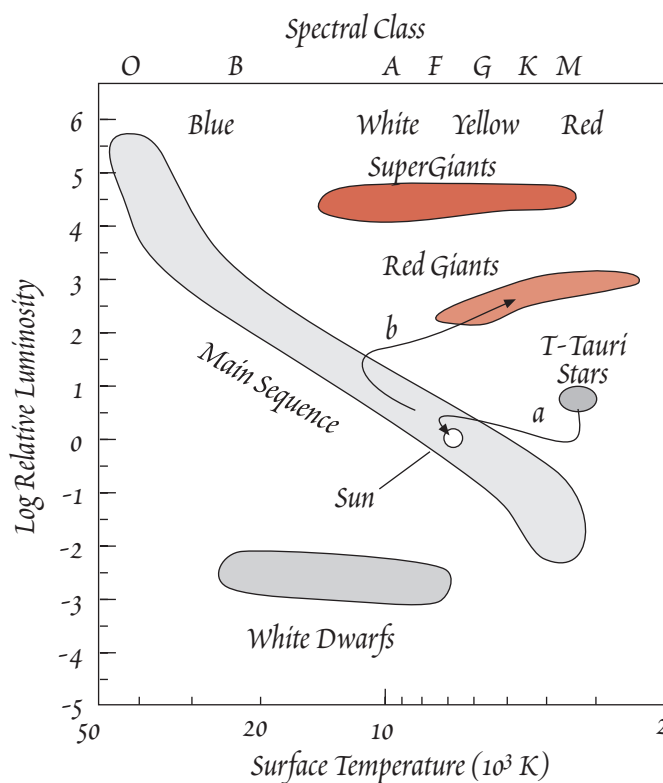


Figure 10.1. The Hertzsprung-Russell diagram of the relationship between luminosity and surface temperature. Arrows show evolutionary path for a star the size of the Sun in pre- (a) and post- (b) main sequence phases.

wonder whether astronomy is not ripe for revolution, in which some of its most fundamental theories might be replaced by entirely new ones, or at least be radically altered.

CHAPTER 10: COSMOCHEMISTRY

have moved on in the evolutionary sequence. H in the core is not replenished because the density difference prevents convection between the core and outer layers, which are still H-rich. The interior part of the core collapses under gravity. With enough collapse, the layer immediately above the He core will begin to “burn” H again, which again stabilizes the star. The core, however, continues to collapse until temperature and pressure are great enough for He burning to begin. At the same time, and for reasons not fully understood, the exterior expands and cools, resulting in a *red giant*, a star that is over-luminous relative to main sequence stars of the same color. When the Sun reaches this phase, in perhaps another 5 Ga, it will expand to the Earth's orbit. A star will remain in the red giant phase for something like 10^6 – 10^8 years. During this time, radiation pressure results in a greatly enhanced solar wind, of the order of 10^{-6} to 10^{-7} , or even 10^{-4} , solar masses per year (the Sun's solar wind is 10^{-14} solar masses per year, so that in its entire lifetime the Sun will blow off 1/10,000 of its mass through the solar wind).

The fate of stars after the red giant phase (when the He in the core is exhausted) depends on their mass. Nuclear reactions in small stars cease and they simply contract, their exteriors heating up as they do so, to become *white dwarfs*. The energy released is that produced by previous nuclear reactions and gravitational potential energy. This is the likely fate of the Sun. White Dwarfs are underluminous relative to stars of similar color on the main sequence. They can be thought of as little more than glowing ashes. Unless they blow off sufficient mass during the red giant phase, large stars die explosively, in supernovae. (Novae are entirely different events that occur in binary systems when mass from a main sequence star is pulled by gravity onto a white dwarf companion.) Supernovae are incredibly energetic events. The energy released by a supernova can exceed that released by an entire galaxy (which, it will be recalled, consists of on the order of 10^9 stars) for days or weeks!

THE POLYGENETIC HYPOTHESIS OF BURBIDGE, BURBIDGE, FOWLER AND HOYLE

Our understanding of nucleosynthesis comes from three sets of observations: (1) the abundance of isotopes and elements in the cosmos, (2) experiments on nuclear reactions that determine what reactions are possible (or probable) under given conditions, and (3) inferences about possible sites of nucleosynthesis and about the conditions that prevail in those sites. The abundances of the element in

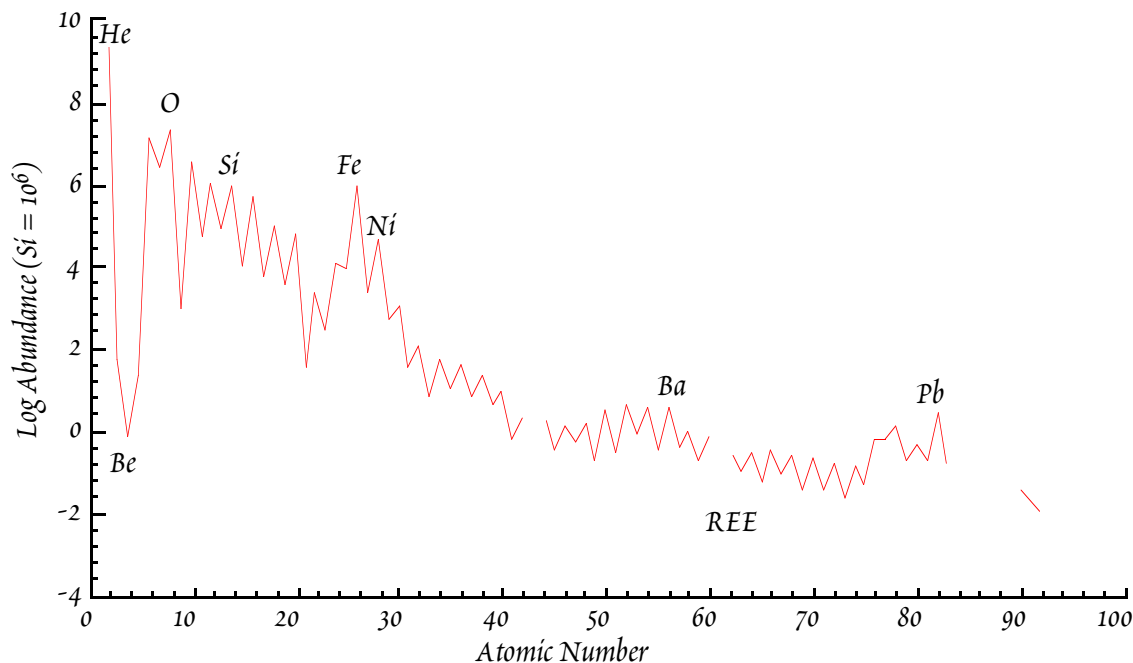


Figure 10.2. Solar system abundance of the elements relative to silicon as a function of atomic number.

CHAPTER 10: COSMOCHEMISTRY

primitive meteorites are by far our most important source of information of elemental abundances. Some additional information can be obtained from spectral observations of stars. The abundances of the elements in the Solar System are shown in Figure 10.2. Any successful theory of nuclear synthesis must explain this abundance pattern. Thus the chemical and isotopic composition of meteorites is a matter of keen interest, not only to geochemists, but to astronomers and physicists as well.

The cosmology outlined above provides two possibilities for formation of the elements: (1) they were formed in the Big Bang itself, or (2) they were subsequently produced. One key piece of evidence comes from looking back into the history of the cosmos. Astronomy is a bit like geology in that just as we learn about the evolution of the Earth by examining old rocks, we can learn about the evolution of the cosmos by looking at old stars. The old stars of Population II are considerably poorer in heavy elements than are young stars. In particular, Population II stars have an Fe/H ratio typically a factor of 100 lower than the Sun. This suggests that much of the heavy element inventory of the galaxy has been produced since these stars formed some 10 Ga ago. There are also significant variations in the Fe/H ratio between galaxies. In particular, dwarf spheroidal galaxies appear to be deficient in Fe, and sometimes in C, N, and O, relative to our own galaxy. Other galaxies show distinct radial compositional variations. For example, the O/H ratio in the interstellar gas of the disk of the spiral galaxy M81 falls by an order of magnitude with distance from the center. Finally, one sees a systematic decrease in the Fe/H ratio of white dwarfs (the remnants of small to medium size stars) with increasing age. On the other hand, old stars seem to have about the same He/H ratio as young stars. Indeed ${}^4\text{He}$ seems to have an abundance of $25\pm 2\%$ everywhere in the universe.

Thus the observational evidence suggests that (1) H and He are everywhere uniform, implying their creation and fixing of the He/H ratio in the Big Bang, and (2) elements heavier than Li were created by subsequent processes. The production of these heavier elements seems to have occurred steadily through time, but the efficiency of the process varies between galaxies and even within galaxies.

Early attempts (~1930–1950) to understand nucleosynthesis focused on single mechanisms. Failure to find a single mechanism that could explain the observed abundance of nuclides, even under varying conditions, led to the present view that relies on a number of mechanisms operating in different environments and at different times for creation of the elements in their observed abundances. This view, which has been called the polygenetic hypothesis, was first proposed by Burbidge, Burbidge, Fowler and Hoyle (1957). The abundance of trace elements and their isotopic compositions in meteorites were perhaps the most critical observations in development of the theory. An objection to the polygenetic hypothesis was the apparent uniformity of the isotopic composition of the elements, but variations in the isotopic composition have now been demonstrated for a few elements in some meteorites. The isotopic compositions of other elements, such as oxygen and the rare gases, vary between classes of almost all meteorites. Furthermore, there are significant variations in isotopic composition of some elements, such as carbon, among stars. These observations provide strong support for this theory.

To briefly summarize it, the polygenetic hypothesis proposes four phases of nucleosynthesis. *Cosmological nucleosynthesis* occurred shortly after the universe began and is responsible for the cosmic inventory of H and He, and some of the Li. Even though helium is the main product of nucleosynthesis in the interiors of main sequence stars, not enough helium has been produced in this manner to significantly change its cosmic abundance. The lighter elements, up to and including Si and a fraction of the heavier elements, but excluding Li and Be, may be synthesized in the interiors of larger stars during the final stages of their evolution (*stellar nucleosynthesis*). The synthesis of the remaining elements occurs as large stars exhaust the nuclear fuel in their interiors and explode in nature's grandest spectacle, the supernova (*explosive nucleosynthesis*). Finally, Li and Be are continually produced in interstellar space by interaction of cosmic rays with matter (*galactic nucleosynthesis*).

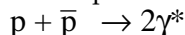
CHAPTER 10: COSMOCHEMISTRY

COSMOLOGICAL NUCLEOSYNTHESIS

Immediately after the Big Bang, the universe was too hot for any matter to exist. But after a second or so, it had cooled to 10^{10} K so that a few protons and neutrons existed in an equilibrium dictated by the following reactions:

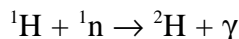


A somewhat worrisome question is why matter exists at all. Symmetry would seem to require production of equal number of protons and anti-protons that would have annihilated themselves by:

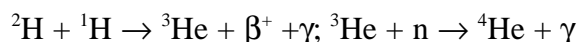
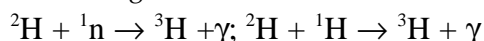


The current theory is that the hyperweak force was responsible for an imbalance favoring matter over anti-matter. The same theory predicts a half-life of the proton of 10^{32} yrs, a prediction not yet verified.

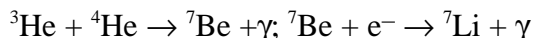
It took another 3 minutes for the universe to cool to 10^9 K, which is cool enough for ${}^2\text{H}$ to form:



At about the same time, the following reactions could also occur:



and



Formation of elements heavier than Li, however, was inhibited by the instability of nuclei of masses 5 and 8. Shortly afterward, the universe cooled below 10^9 K and nuclear reactions were no longer possible. Any free neutrons decayed away (neutrons outside the nucleus are unstable, having a half-life of 10 min). Thus the Big Bang created H, He and Li (${}^7\text{Li}/\text{H} = 10^{-9}$). Some 700,000 years later, the universe had cooled to about 3000 K, cool enough for electrons to be bound to nuclei, forming atoms.

NUCLEOSYNTHESIS IN STELLAR INTERIORS

HYDROGEN, HELIUM, AND CARBON BURNING STARS

For quite some time after the Big Bang, the universe was a more or less homogeneous, hot gas. "Less" turns out to be critical. Inevitably (according to fluid dynamics), inhomogeneities in the gas developed. These inhomogeneities enlarged in a sort of runaway process of gravitational attraction and collapse. Thus were formed protogalaxies, perhaps 0.5 Ga after the Big Bang. Instabilities within the protogalaxies collapsed into stars. Once this collapse proceeded to the point where density reaches 6 g/cm and temperature reaches 10 to 20 million K, nucleosynthesis began in the interior of stars by *hydrogen burning*, or the *pp process*, which involves reactions such as:



There are also other reaction chains that produce ${}^4\text{He}$ that involve Li, Be, and B, either as primary fuel or as intermediate reaction products. Later, when some carbon had already been produced by the first generation of stars and supernovae, second and subsequent generation stars with masses greater than about 1.1 solar masses produced He by another process as well, the *CNO cycle*:



In this process carbon acts as a sort of nuclear catalyst: it is neither produced nor consumed. The net effect is consumption of 4 protons and two positrons to produce a neutrino, some energy and a ${}^4\text{He}$ nucleus.

[†] The ν (nu) is the symbol for a neutrino.

* γ (gamma) is used here to symbolized energy in the form of a gamma ray.

[‡] Here we are using a notation commonly used in nuclear physics. The notation:

is equivalent to:

$${}^{12}\text{C}(p,\gamma) {}^{13}\text{N}$$

$${}^{12}\text{C} + p \rightarrow {}^{13}\text{N} + \gamma$$

CHAPTER 10: COSMOCHEMISTRY

The $^{14}\text{N}(p,\gamma)^{15}\text{O}$ is the slowest in this reaction chain, so there tends to be a net production of ^{14}N as a result. Also, though both ^{12}C and ^{13}C are consumed in this reaction, ^{12}C is consumed more rapidly, so this reaction chain should increase the $^{13}\text{C}/^{12}\text{C}$ ratio.

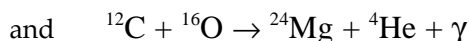
The heat produced by these reactions counterbalances gravitational collapse and these reactions proceed in main sequence stars (Figure 10.1) until the hydrogen in the stellar core is consumed. How quickly this happens depends, as we noted earlier, on the mass of the star.

Once the H is exhausted in the stellar core, fusion ceases, and the balance between gravitational collapse and thermal expansion is broken. The interior of the star thus collapses, raising the star's temperature. The exterior expands and fusion begins in the shells surrounding the core, which now consists of He. This is the *red giant* phase. If the star is massive enough for temperatures to reach 10^8 K and density to reach 10^4 g/cc in the He core, *He burning* can occur:



The catch in this reaction is that the half-life of ^8Be is only 10^{-16} sec, so 3 He nuclei must collide essentially simultaneously, hence densities must be very high. He burning also produce O, and lesser amounts of ^{20}Ne and ^{24}Mg , in the red giant phase, but Li, Be, and B are skipped: they are not synthesized in these phases of stellar evolution. These nuclei are unstable at the temperatures of stellar cores. Rather than being produced, they are consumed in stars.

There is a division of evolutionary paths once helium in the stellar core is consumed. Densities and temperatures necessary to initiate further nuclear reactions cannot be achieved by low-mass stars, such as the Sun, (because the gravitational force is not sufficient to overcome coulomb repulsion of electrons) so their evolution ends after the Red Giant phase, the star becoming a white dwarf. Massive stars, those greater than about $4 M_{\odot}$ [¶], however, undergo further collapse and the initiation of *carbon and oxygen burning* when temperatures reach 600 million K and densities 5×10^5 g/cc. However, stars with intermediate masses, between 4 and $8 M_{\odot}$, can be entirely disrupted by the initiation of carbon burning. For stars more massive $8 M_{\odot}$, evolution now proceeds at an exponentially increasing pace (Figure 10.3) with reactions of the type:



Also, ^{14}N created during the hydrogen burning phase of second generation stars can be converted to ^{22}Ne . A number of other less abundant nuclei, including Na, Al, P, S and K are also synthesized at this time, and in the subsequent process, *Ne burning*.

During the final stages of evolution of massive stars, a significant fraction of the energy released is carried off by neutrinos created by electron-positron annihilations in the core of the star. If the star is sufficiently oxygen-poor that its outer shells are reasonably transparent, the outer shell of the red giant may collapse during last few 10^4 years of evolution to form a *blue giant*.

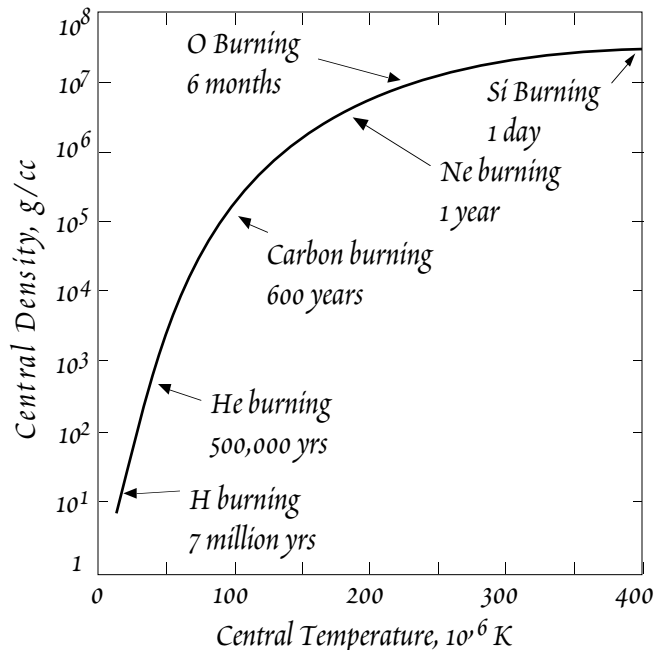


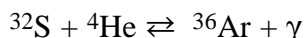
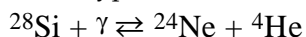
Figure 10.3. Evolutionary path of the core of star of 25 solar masses (after Bethe and Brown, 1985). Note that the period spent in each phase depends on the mass of the star: massive stars evolve more rapidly.

[¶] The symbol \odot is the astronomical symbol for the Sun. M_{\odot} therefore indicates the mass of the Sun.

CHAPTER 10: COSMOCHEMISTRY

THE E-PROCESS

Eventually, a new core consisting mainly of ^{28}Si is produced. At temperatures near 10^9 K and densities above 10^7 g/cc a process known as *silicon burning*, or the *e process*, (for equilibrium) begins, and lasts for a week or less, again depending on the mass of the star. This process includes reactions of the type:



While these reactions can proceed in either direction, there is some tendency for the build up of heavier nuclei with masses 32, 36, 40, 44, 48, 52 and 56. Partly as a result of the e-process, these nuclei are unusually abundant in nature. In addition, because a variety of nuclei are produced during C and Si burning phases, other reactions are possible, synthesizing a number of minor nuclei.

The star is now a cosmic onion of sorts, consisting of a series of shells of successively heavier nuclei and a core of Fe (Figure 10.4). Though temperature increases toward the interior of the star, the structure is stabilized with respect to convection and mixing because each shell is denser than the one overlying it.

Fe-group elements may also be synthesized by the e-process in Type I supernovae*. Type I supernovae occur when white dwarfs of intermediate mass (3-10 solar masses) stars in binary systems accrete material from their companion. When their cores reach the so-called Chandrasekhar limit, C burning is initiated and the star explodes.

THE S-PROCESS

In second and later generation stars containing heavy elements, yet another nucleosynthetic process can operate. This is the slow neutron capture or *s-process*. It is so called because the rate of capture of neutrons is slow compared to the *r-process*, which we will discuss below. It operates mainly in the red giant phase (as evidenced by the existence of ^{99}Tc and enhanced abundances of several s-process nuclides in red giants) where neutrons are produced by reactions such as:

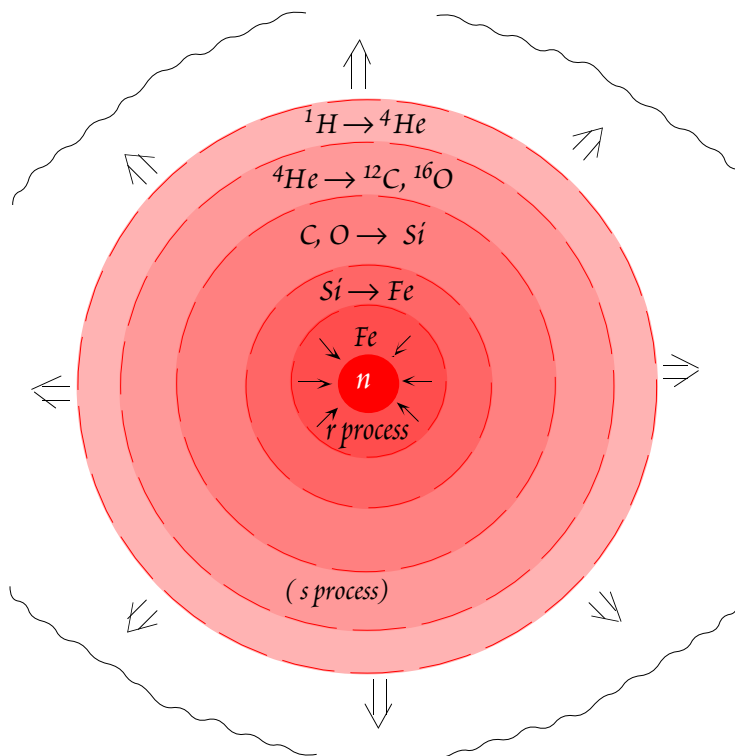
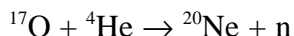
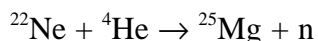
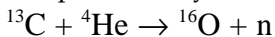


Figure 10.4. Schematic diagram of stellar structure at the onset of the supernova stage. Nuclear burning processes are illustrated for each stage.

*Astronomers recognize two kinds of supernovae: Type I and Type II. A Type I supernova occurs when a white dwarf in a binary system accretes mass from its sister star. Its mass reaches the point where carbon burning initiates and the star is explosively disrupted. The explosions of massive stars which we are considering are the Type II supernovae.

CHAPTER 10: COSMOCHEMISTRY

(but even H burning produces neutrons, so that the *s*-process operates to some degree even in main sequence stars). These neutrons are captured by nuclei to produce successively heavier elements. The principle difference between the *s* and *r* process, discussed below, is the rate of capture relative to the decay of unstable isotopes. In the *s* process, a nucleus may only capture a neutron every thousand years or so. If the newly produced nucleus is not stable, it will decay before another neutron is captured. As a result, the *s*-process path closely follows the valley of stability on the chart of the nuclides and nuclear instabilities cannot be bridged.

Explosive Nucleosynthesis

The *e*-process stops at mass 56. In Chapter 8 we noted that ^{56}Fe had the highest binding energy per nucleon, i.e., it is the most stable nucleus. Thus fusion can release energy only up to mass 56; beyond this the reactions become endothermic, i.e., they consume energy. Once the stellar core has been largely converted to Fe, a critical phase is reached: the balance between thermal expansion and gravitational collapse is broken. The stage is now set for the catastrophic death of the star: a supernova explosion, the ultimate fate of stars with masses greater than about 8 solar masses. The energy released in the supernova is astounding. In its first 10 seconds, the 1987A supernova (Figure 10.5) released more energy than the entire visible universe, 100 times more energy than the Sun will release in its entire 10 billion year lifetime.

When the mass of the iron core reaches 1.4 solar masses (the Chandrasekhar mass), further gravitational collapse cannot be resisted even by coulomb repulsion. The supernova begins with the collapse of this stellar core, which would have a radius of several thousand km (similar to the Earth's radius) before collapse, to a radius of 100 km or so. The collapse occurs in a few tenths of a second.

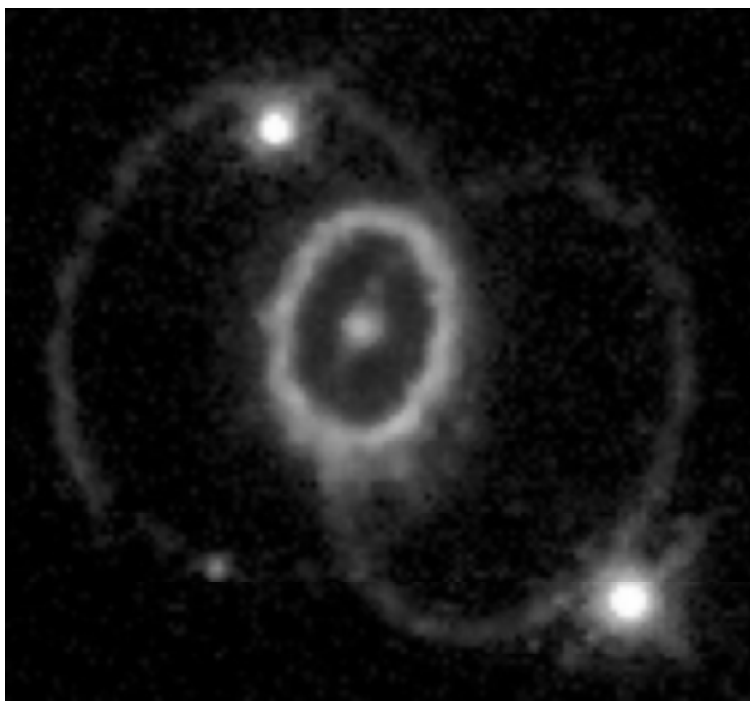
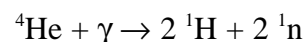
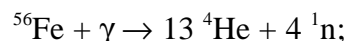


Figure 10.5. Rings of glowing gas surrounding the site of the supernova explosion named Supernova 1987A photographed by the wide field planetary camera on the Hubble Space Telescope in 1994. The nature of the rings is uncertain, but they may be probably debris of the supernova illuminated by high-energy beams of radiation or particles originating from the supernova remnant in the center.

When matter in the center of the core is compressed beyond the density of nuclear matter (3×10^{14} g/cc), it rebounds, sending a massive shock wave back out. As the shock wave travels outward through the core, the temperature increase resulting from the compression produces a breakdown of nuclei by photodisintegration, e.g.:



Thus much of what took millions of years to produce is undone in an instant. However, photodisintegration produces a large number of free neutrons (and protons), which leads to another important nucleosynthetic process, the *r*-process.

Another important effect is the creation of huge numbers of neutrinos by positron-electron annihilations, these particles having "condensed" as pairs from gamma rays. The energy carried away by neutrinos leaving the

CHAPTER 10: COSMOCHEMISTRY

supernova exceeds the kinetic energy of the explosion by a factor of several hundred, and exceeds the visible radiation by a factor of some 30,000. The neutrinos leave the core at nearly the speed of light. Though neutrinos interact with matter very weakly, the density of the core is such that their departure is delayed slightly. Nevertheless, they travel faster than the shock wave and are delayed less than electromagnetic radiation. Thus neutrinos from the 1987A supernova arrived at Earth (some 160,000 years after the event) a few hours before the supernova became visible.

When the shock wave reaches the surface of the core, the outer part of the star is blown apart in an explosion of unimaginable violence. But amidst the destruction new nucleosynthetic processes occur. As the shock wave passes through outer layers, it may 'reignite' them, producing explosive Ne, O and C burning. These processes produce isotopes of S, Cl, Ar, Ca, Ti, and Cr, and some Fe.

THE R-PROCESS

The neutrons produced by photodisintegration in the core are captured by those nuclei that manage to survive this hell. Because the abundance of neutrons is exceedingly high, nuclei capture them at a rapid rate; so rapid that even an unstable nucleus will capture a neutron before it has an opportunity to decay. The result is a build up of neutron-rich unstable nuclei. Eventually the nuclei capture enough neutrons that they are not stable even for a small fraction of a second. At that point, they β^- decay to new nuclides, which are more stable and capable of capturing more neutrons. This is the *r*-process (rapid neutron capture), and is the principle mechanism for building up the heavier nuclei. It reaches a limit when nuclei beyond $A \approx 90$ are reached. These heavy nuclei fission into several lighter fragments. The *r*-process is thought to have a duration of 1 to 100 sec during the peak of the supernova explosion. Figure 10.6 illustrates this process.

The *r*-process produces broad peaks in elemental abundance around the neutron magic numbers (50, 82, 126, corresponding to the elements Sr & Zr, Ba, and Pb). This results because nuclei with magic numbers of neutrons are particularly stable, and have very low cross sections for capture of neutrons, and because nuclei just short of magic numbers have particularly high capture cross sections. Thus the

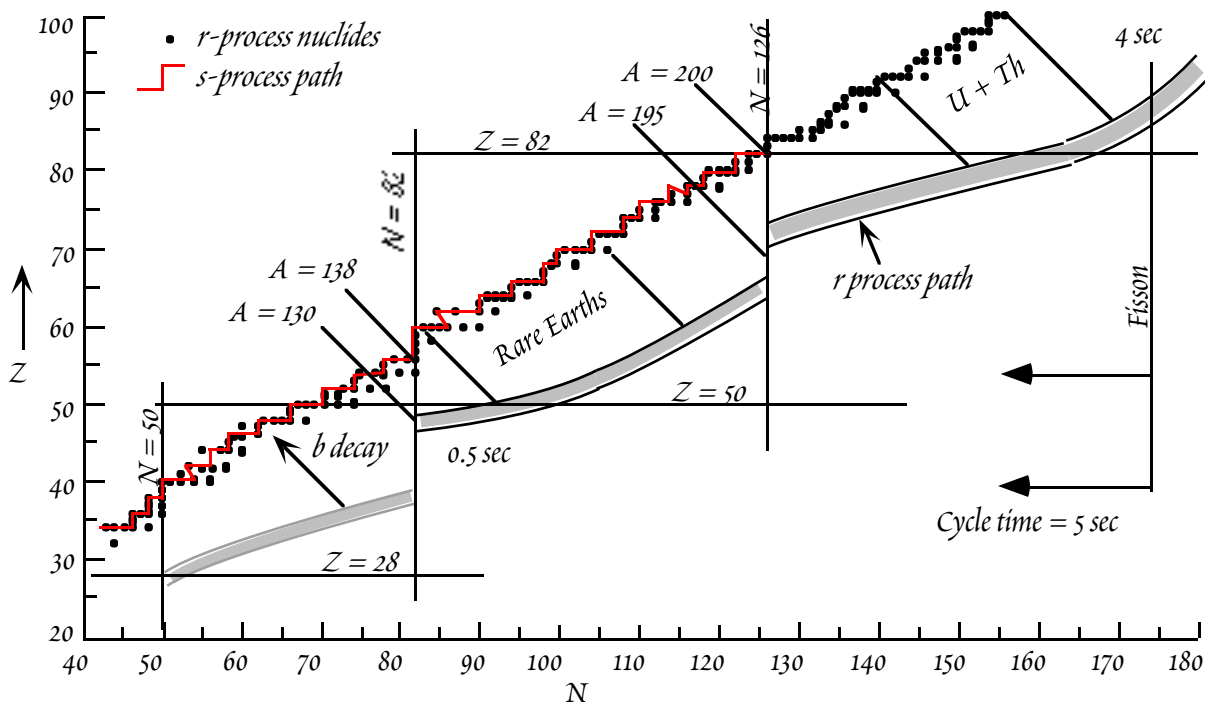


Figure 10.6. Diagram of the *r*-process path on a *Z* vs. *N* diagram. Dashed region is *r*-process path; solid line through stable isotopes shows the *s*-process path.

CHAPTER 10: COSMOCHEMISTRY

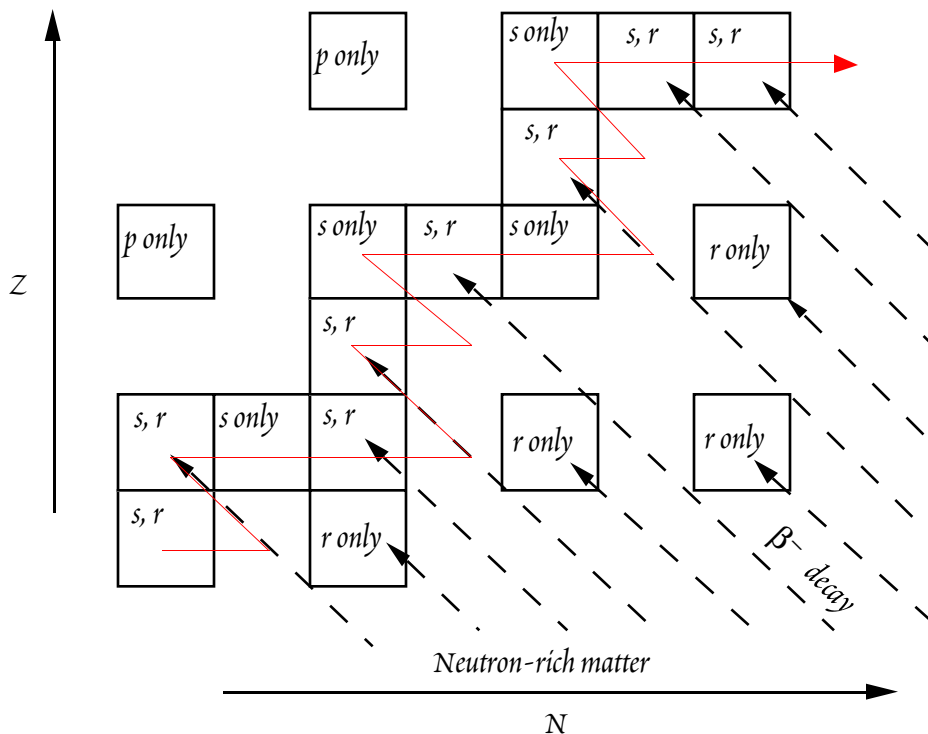


Figure 10.7. Z vs. N diagram showing production of isotopes by the r- s- and p-processes. Squares are stable nuclei; wavy lines are beta-decay path of neutron-rich isotopes produced by the r-process; solid line through stable isotopes shows the s-process path.

magic number nuclei are both created more rapidly and destroyed more slowly than other nuclei. When they decay, the sharp abundance peak at the magic number becomes smeared out.

THE p-PROCESS

The r-process tends to form the heavier (neutron-rich) isotopes of a given element. Proton capture, or the *p-process*, also occurs in supernovae and is responsible for the lightest isotopes of a given element. The probability of proton capture is much less than that of neutron capture. You can easily imagine the reason for this: to be captured, the proton must have sufficient energy to overcome the coulomb repulsion and approach to within 10^{-14} cm of the nucleus where the strong force dominates over the electromagnetic one. In contrast even low energy neutrons can be captured by nuclei since the neutron is uncharged and there is no coulomb repulsion. The production of nuclei by the p-process is much smaller than by neutron capture processes, and is significant only for those nuclides that cannot be produced in other ways. These tend to be the lightest isotopes of an element. Because of the improbability of proton capture, these light, p-process-only isotopes tend to be the least abundant.

Figure 10.7 illustrates how these three processes, the s-, r-, and p-process, create different nuclei. Notice the shielding effect. If an isotope with z protons and n neutrons has a stable isobar with $n+x$ neutrons and $p-x$ protons, this isotope is shielded from production by the r-process because β -decay will cease when that stable isobar is reached. The most abundant isotopes of an element tend to be those created by all processes; the least abundant are those created by only one, particularly by only the p-process. The exact abundance of an isotope depends on a number of factors, including its neutron-capture cross section*, and the neutron capture cross section and stability of neighboring nuclei.

* In a given flux of neutrons, some nuclides will be more likely to capture and bind a neutron than others, just as some atoms will be more likely to capture and bind an electron than others. The neutron capture cross section of a nuclide is a measure of the affinity of that nuclide for neutrons, i.e., a measure of the

CHAPTER 10: COSMOCHEMISTRY

Let's return to the exploding star. In the inner part of the stellar core, the reactions we just discussed do not take place. Instead, the core collapses to the point where all electrons are welded to protons to form a ball of neutrons: a neutron star. This inner core is hot: 100 billion Kelvin. And like a ballerina pulling in her arms, it conserves angular momentum by spinning faster as it collapses. The neutron star inside the expanding supernova shell of 1987A may be spinning at 2000 revolutions per second. Neutron stars emit radiation in beacon-like fashion: a *pulsar*. The collapse of cores of the most massive stars, however, may not stop at all. They collapse to a diameter of zero and their density becomes infinite. Such an object is called a singularity. Its gravitational attraction is so great even light cannot escape, creating a *black hole*.

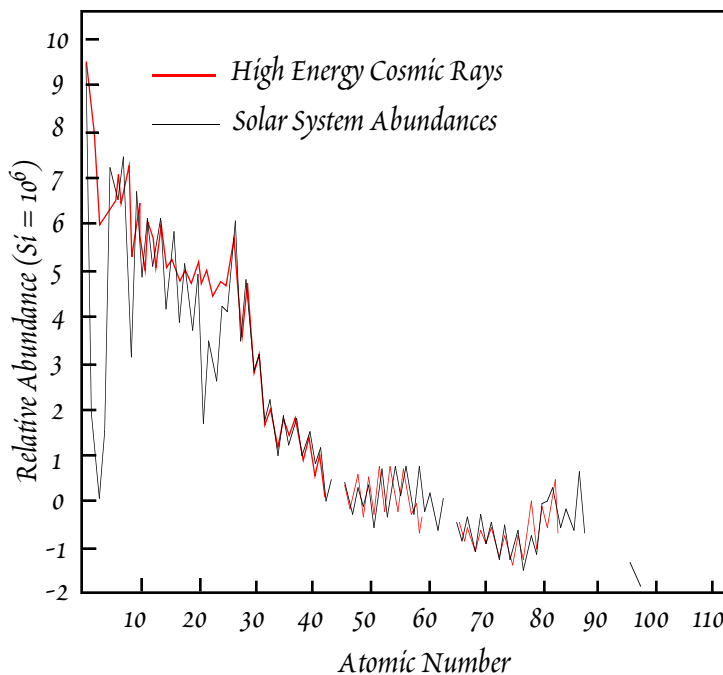


Figure 10.8. Comparison of relative abundances in cosmic rays and the solar system.

NUCLEOSYNTHESIS IN INTERSTELLAR SPACE

Except for production of ${}^7\text{Li}$ in the Big Bang, Li, Be, and B are not produced in any of the above situations. One clue to the creation of these elements is their abundance in galactic cosmic rays: they are over abundant by a factor of 10^6 , as is illustrated in Figure 10.8. They are believed to be formed by interactions of cosmic rays with interstellar gas and dust, primarily reactions of ${}^1\text{H}$ and ${}^4\text{He}$ with carbon, nitrogen and oxygen nuclei. These reactions occur at high energies (higher than the Big Bang and stellar interiors), but at low temperatures where the Li, B and Be can survive.

SUMMARY

Figure 10.9 is a part of the Z vs. N plot showing the abundance of the isotopes of elements 68 through 73. It is a useful region of the chart of the nuclides for illustrating how the various nucleosynthetic processes have combined to produce the observed abundances. First, we notice that even numbered elements tend to have more stable nuclei than odd numbered ones — a result of the greater stability of nuclides with even Z. We also notice that nuclides having a neutron-rich isobar (recall that isobars have the same value of A, but a different combination of N and Z) are underabundant, for example ${}^{170}\text{Yb}$ and ${}^{176}\text{Lu}$. This underabundance results from these nuclides being ‘shielded’ from production by β^- decay of r-process neutron-rich nuclides. In these two examples, ${}^{170}\text{Er}$ and ${}^{176}\text{Yb}$ would be the ultimate product of neutron-rich unstable nuclides of mass number 170 and 176 produced during the r-process. Also notice that ${}^{168}\text{Yb}$, ${}^{174}\text{Hf}$ and ${}^{180}\text{Ta}$ are very rare. These nuclides are shielded from the r-process and are also off the s-process path. They are produced only by the p-process. Finally, those nuclides that can be produced by both the s- and the r-process tend to be the most abundant; for example, ${}^{176}\text{Yb}$ is about half as abundant as ${}^{174}\text{Yb}$ because the former is produced by the r-process only while the latter can be produced by both the s- and the r-process. ${}^{176}\text{Yb}$ cannot be produced by the s-process

probability of that nuclide capturing a neutron in a given neutron flux.

CHAPTER 10: COSMOCHEMISTRY

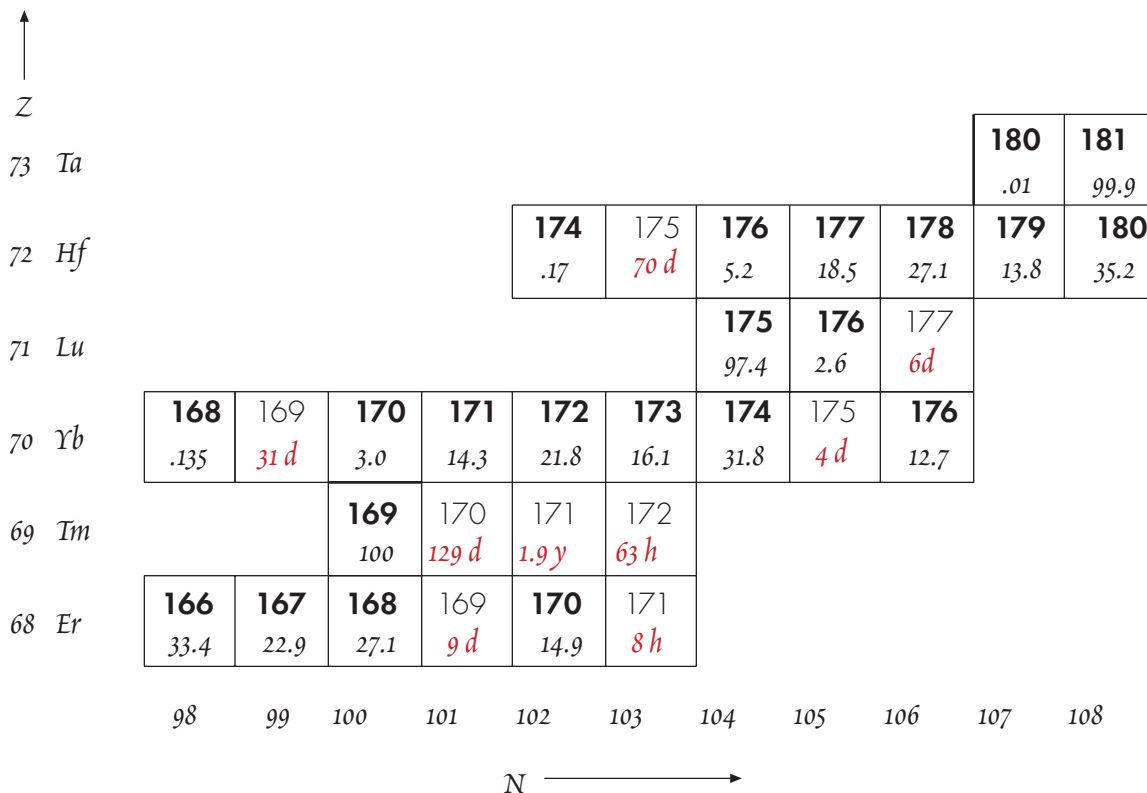


Figure 10.9. View of Part of Chart of the Nuclides. Mass numbers of stable nuclides are shown in bold, their isotopic abundance is shown in italics as percent. Mass numbers of short-lived nuclides are shown in plain text with their half-lives also given.

because during the s-process, the flux of neutrons is sufficiently low that any ¹⁷⁵Yb produced decays to ¹⁷⁵Lu before it can capture a neutron and become a stable ¹⁷⁶Yb.

The heavy element yield of stellar and explosive nucleosynthesis will vary tremendously with the mass of the star. A star of 60 solar masses will convert some 40% of its mass to heavy elements. The bulk of this is apparently ejected into the interstellar medium. Stars too small to become supernovae will convert relatively small fractions of their mass to heavy elements, and only a very small fraction of this will be ejected. One the whole, stars in the mass range of 20-30 solar masses probably produce the bulk of the heavy elements in the galaxy. While such stars, which are already quite large compared to the mean stellar mass, convert a smaller fraction of their mass to heavy elements than truly massive stars, they are much more abundant than the very massive stars.

Novae may also make a significant contribution to the cosmic inventory of a few relatively light elements such as ¹⁹F and ⁷Li, as well as the rarer isotopes of C, N, and O. Novae occur when mass is accreted to a white dwarf from a companion red giant. If the material is mainly hydrogen and accretion is relatively slow, H burning may be ignited on the surface of the white dwarf, resulting in an explosion that ejects a relatively small fraction of the mass of the star.

METEORITES: ESSENTIAL CLUES TO THE BEGINNING

In subsequent sections we want to consider the formation of the Earth and its earliest history. The Earth is a dynamic body; its rock formations are continually being recycled into new ones. As a result, old rocks are rare. The oldest rocks are 4.0 Ga; some zircon grains as old as 4.2 Ga have been found in coarse-grained, metamorphosed sediments. The geological record ends there: there is no trace of the earliest history of the Earth in terrestrial rocks. So to unravel Earth's early history, we have to turn to other bodies in the Solar System. So far, we have samples only of the Moon and meteorites, and a

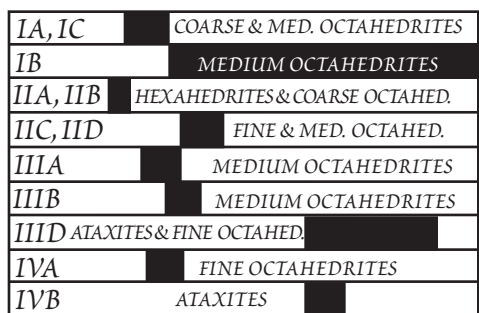
CHAPTER 10: COSMOCHEMISTRY

few rather marginal quality analyses of the surface of Venus and Mars[†]. The Moon provides some clues to the early history of planets; but meteorites provide the best clues as to the formation of planets and the Solar System. We now turn our attention to them.

Meteorites are divided into *Falls* and *Finds*. Falls are meteorites recovered after observation of a fireball whose trajectory can be associated the impact site. (A fireball is a just an intense falling star. Most falling stars are produced by meteoroids so small, a few grams or tens of grams perhaps, that they completely evaporate during their passage through the atmosphere and thus never reach the surface.) Finds are meteorites found but not observed falling. Because finds may have been on the surface of the Earth for very long times, they are often weathered and the compositional information they provide is less reliable than that of falls. An exception of sorts to this is the Antarctic meteorites. Meteorites have been found in surprising numbers in the last 20 years or so in areas of low snow-fall in Antarctica where ice is eroded by evaporation and wind. Meteorites are concentrated in such areas by glaciers. Because of storage in the Antarctic deep freeze, they are little weathered.

Figure 10.10 illustrates the gross features of meteorite classification. Meteorites are classified according to (1) their composition, (2) their mineralogy, and (3) their texture. The classification may seem of little importance, but since the above factors are a reflection of the history of meteorites, un-

IRONS



STONY-IRONS

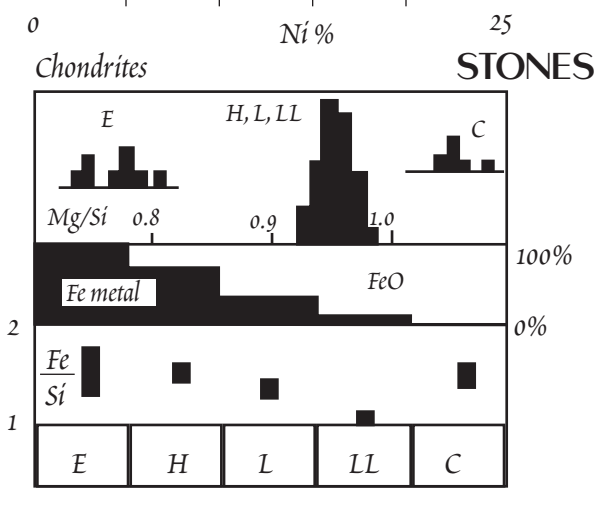
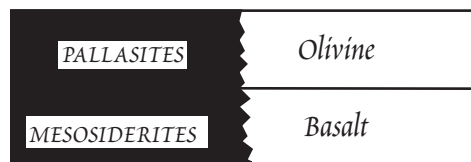


Figure 10.10. Classification of meteorites, illustrating the various textural and chemical parameters that lead to the classification system.

[†] As we shall see, a few meteorites probably come from Mars, providing additional information on the composition of that planet.

CHAPTER 10: COSMOCHEMISTRY

Understanding the classification helps to understand the origin of meteorites and the early Solar System. These classification schemes have evolved over the years and multiple names exist for the same classes, which can lead to some confusion for the uninitiated.

The first order division is between *Stones* and *Irons*. You can pretty well guess what this means: stones are composed mainly of silicates while irons are mainly metal. An intermediate class is the *Stony-Irons*, a mixture of silicate and metal. Figure 10.11 illustrates the relative abundance of the various meteorite types among falls. Stones predominate among falls (irons are more common among finds because they are more likely to be recognized as meteorites, and because they are more likely to be preserved). Stony meteorites are rather friable and disintegrate rapidly in transit through the atmosphere and afterward. Even among the falls, irons are probably grossly overrepresented for these reasons. As of 1978, there were about 3000 meteorites in collections around the world, about 1000 of which were falls. Over 6000 have been added since then by the Antarctic collecting programs.

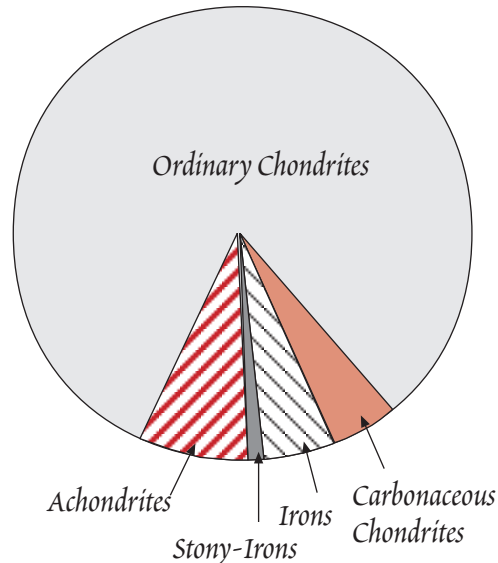


Figure 10.11. Relative abundance of major types of meteorite Falls.

CHONDRITES: THE MOST PRIMITIVE OBJECTS

Let's consider the stones in more detail. They are divided into *chondrites* and *achondrites* depending on whether they contain *chondrules*, at least in principle. Chondrules are small spherical or ellipsoidal particles that were once molten and can constitute up to 80 percent of the mass of chondrites (though the average is closer to perhaps 40%). Chondrites are generally of ultramafic composition. They consist of varying proportions of the following components: a high temperature component consisting of chondrules and other high-temperature inclusions (called refractory inclusions or calcium-aluminum inclusions), large aggregates of metal and sulfides, small aggregates of metal, sulfide and oxides, isolated coarse silicate grains, and a fine-grained, porous mixture of minerals and amorphous material called the matrix. These components formed while dispersed in the solar nebula and they subsequently aggregated to form the meteorite parent bodies (we will discuss the evidence that meteorites are derived from larger parent bodies subsequently). All chondrites have been variably metamorphosed in their parent bodies.

Some are highly brecciated as a result of collisions and impacts on the surface of the parent bodies. The least metamorphosed have a distinctly porous and fluffy texture, as would be expected from the aggregation of nebular dust. An example of a chondrite is shown in Figure 10.12.

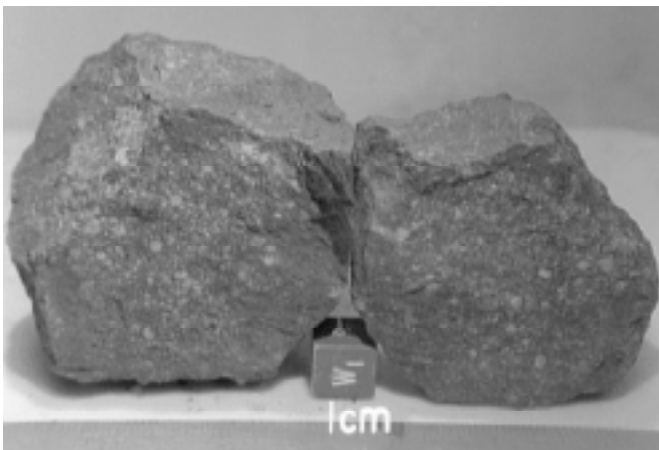


Figure 10.12. A chondritic meteorite from NASA's Antarctic meteorite collection.

CHONDRULES

Chondrules are usually a few tenths of a mm to a few mm in diameter. Mean size varies between chondrite classes (see below), but is typically around 0.5 mm. In the least metamorphosed meteorites,

CHAPTER 10: COSMOCHEMISTRY

they consist of quench crystals (often, but not always monmineralic) and/or glass. Olivine and Ca-poor pyroxene (enstatite, hypersthene) generally constitute over half the volume of the chondrule, with troilite (FeS), kamacite (FeNi alloy), Ca-rich pyroxene (pigeonite, diopside), Mg-Al spinel, chromite, and feldspar being less abundant. Chondrules have remnant magnetism that was presumably acquired as they cooled through their Curie point in the presence of a magnetic field, indicating the presence of such a field in the solar nebula. From the number of compound chondrules (two chondrules fused together) and those having indentations suggestive of collisions with other chondrules, the chondrule density was as high as a few per m^3 at times and places in the solar nebula. While "dents" are observed in chondrules, microcraters produced by high velocity impact are absent. Many chondrules are compositionally zoned, and most chondrules contain nuclei of relict crystals. Many are rimmed with fine-grained dark secondary coatings of volatile-rich material broadly similar in composition to the chondrite matrix.

Chondrules are highly variable in composition. The chondrules within a single meteorite may show more chemical variation than between all classes of chondrites. On the other hand, the mean composition of chondrules is the same in all classes of meteorites. Si, Mg, Al, Ca, Fe, and O are the most abundant elements in chondrules. Minor elements include Na, S, K, Ti, Cr, Mn, and Ni. They are typically depleted in siderophile, chalcophile, and volatile elements relative to the whole chondrite. These depletions, particularly of siderophile and chalcophile elements, appear to have preceded formation of the chondrules, and hence are unrelated to the phenomenon that created the chondrules.

The presence of glass and their spheroidal shape indicates that chondrules represent melt droplets, as has been realized for at least 100 years. However, their origin remains a mystery. The main problem is that at the low pressures that must have prevailed in the solar nebula, liquids are not stable: solids should evaporate rather than melt. In addition, the solar nebula, with an O/H ratio of $\sim 7 \times 10^{-4}$ should have been much too reducing for iron-bearing silicates to exist, yet many chondrules nevertheless have significant Fe^{2+} dissolved in silicates such as olivine. Finally, the source of heat to melt the chondrules is a mystery. Chondrules seem to have been heated quite rapidly and apparently cooled through their crystallization range on time scales of an hour or less, and possibly minutes. Though cooling was rapid, it was considerably slower than the rate that would have resulted from radiative cooling in open space. This conclusion is based on compositional zonation of minerals and experimental reproduction of textures. It is strengthened by other experiments that show chondrules would have evaporated if they existed in the liquid state any longer than this. All these observations indicate they formed very quickly, and may never have reached equilibrium.

Over the past 100 years or so, many mechanisms for chondrule formation have been proposed. These include formation through volcanism on planets and planetesimals or asteroids, impact melting resulting from collisions of planets or planetesimals, condensation from hot nebular gas, and transitory heating of pre-existing nebular or interstellar dust. Most of these hypotheses appear to be inconsistent with the compositional and textural properties of chondrules and there is a building consensus that they formed by transitory heating of 'cool' (< 650 K) nebular dust. The exact mechanism and environment of formation, however, are uncertain. There are several possibilities, including collisions of small (< 1 m) bodies, frictional heating of dust traveling through gas during infall, lightning, energy released by magnetic flares, or reconnection of magnetic field lines, and radiational heating resulting from high velocity outflows during the T-Tauri phase (see below) of the protosun. There are difficulties with all these hypotheses, and it is possible that chondrules were produced by an entirely unrecognized phenomenon in the solar nebula. More thorough reviews of chondrules, their properties, and the problem of their origin may be found in Wood (1988, Kerridge and Matthews (1988), and Taylor (1992).

REFRACTORY INCLUSIONS

There is also much interest in the other high-temperature component, the so-called Refractory Inclusions (RI's) or Ca-Al Inclusions (CAI's), because their compositions are similar to that of the first

CHAPTER 10: COSMOCHEMISTRY

condensates from a high-temperature gas. CAI's range in size from microscopic to 5-10 cm, though most are about the same size as chondrules (typically 0.5 mm). They are enriched, commonly by a factor of 20 or so, in refractory elements such as Ca, Al, Ti, Re and the noble metals, Ba, Th, Zr, Hf, Nb, Ta, Y, and the rare earths. Fe, Mg, and Si are also present, though depleted relative to bulk chondrites. The most common minerals are spinel ($MgAl_2O_4$), perovskite ($CaTiO_3$), melilite ($Ca_2(Mg,Fe,Al,Si)_2O_7$), and hibonite ($Ca(Al,Mg,Ti)_{12}O_{19}$). They can contain microscopic nuggets of refractory siderophile elements (Re, Os, Re, Pt, Ir, W, and Mo) that are mantled with Ni-Fe metal and sulfides. They clearly formed under high temperature, high oxygen fugacity conditions. An alternative origin to the high-temperature condensate scenario is that they are the refractory residues of vaporized material.

It is quite possible that some CAI's are high temperature condensates (particularly the finest ones), while others are refractory residues. There is, however, a broad consensus that they are the products of transitory and local heating events rather than equilibrium condensates from a hot solar nebula. Some CAI's show relative depletions in both the most volatile REE (Eu and Yb) and the most refractory (Er and Lu), suggesting they are the products of multiple cycles of evaporation and condensation. Isotopic anomalies in a number of elements have been identified in some CAI's. This suggests a third possible origin for at least some: they are interstellar grains. Based on radiogenic isotope evidence, CAI's appear to be distinctly older, by several million years or so, than other material in meteorites.

THE CHONDRITE MATRIX

The matrix of chondrites is dark, FeO and volatile-rich material that is very fine-grained (typical grain size is about 1 μm). It can be quite heterogeneous, even on a 10 μm scale. It also varies between meteorite classes, with an order of magnitude variation in Mg/Si, Al/Si and Na/Si. The primary constituents appear to be Fe- and Ca-poor pyroxene and olivine and amorphous material, but Fe-metal and a wide variety of silicates, sulfides, carbonates, and other minerals are also present. In the most volatile-rich meteorites the olivine and pyroxene have been altered to serpentine; in the carbonaceous chondrites, carbonaceous material is present in substantial quantities. One the whole, the composition of the matrix is complementary to that of the chondrules: whereas the latter are depleted in Fe and volatiles, the former are enriched in them. Very significantly, the matrix includes grains of SiC and diamond of anomalous isotopic composition. This material may well be debris of a supernova and may be the oldest solid material in the Solar System. We will discuss these isotopic variations in greater detail in a subsequent section.

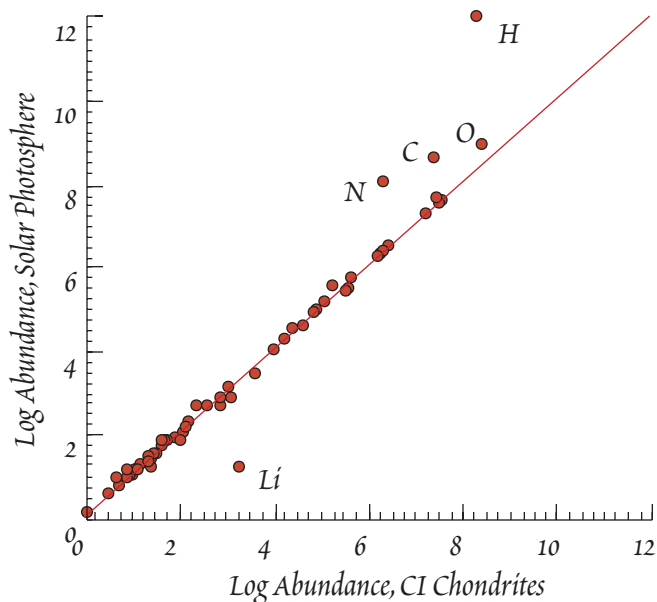


Figure 10.13. Abundances of the elements (in molar units) in the Sun's photosphere vs. their abundances in the carbonaceous chondrite Orgueil (CI1). Abundances for most elements agree within analytical error. The highly volatile elements H, C, N, O and the rare gases (not plotted) are depleted in chondrites relative to the Sun. Lithium is depleted in the Sun.

CHAPTER 10: COSMOCHEMISTRY

CHONDRITE CLASSES AND THEIR COMPOSITIONS

Chondrites are richest in volatiles and have compositions closest to that of the Sun (as determined from spectral studies of its photosphere and the composition of solar wind), though relative to the Sun they are severely depleted in H, He and other highly volatile elements (Figure 10.13). Achondrites, on the other hand, generally have textures similar to terrestrial igneous rocks and compositions suggestive of igneous differentiation. *Chondrites are thus considered the most primitive objects.* Some meteorites lacking chondrules, the CI chondrites, are nevertheless classed as chondrites on compositional grounds. These are the most compositionally primitive objects of all.

Chondrites are subdivided into C (*Carbonaceous*), E (*Enstatite*), and *Ordinary* chondrites. The subclassification into ordinary and E chondrites is based on their iron and nickel content and the degree of oxidation of the iron. The *ordinary chondrites* consist of classes H (High Iron or Bronzite), L (Low Iron or Hypersthene), and LL. The name LL reflects low total iron (and other siderophile metals) and low metallic Fe (and other siderophiles). The E-, or enstatite, chondrites are the most highly reduced, virtually all the iron is present as metal rather than as Fe^{2+} in silicates. The E-chondrites can be further subdivided into EH (high iron) and EL (low iron) classes. Reduction of iron increases the $\text{Si}/(\text{Fe}^{2+} + \text{Mg})$ ratio in silicates and results in enstatite, rather than olivine, being the dominant mineral in these objects. Besides enstatite, metal and sulfides, enstatite chondrites contain a number of other exotic minerals, such as phosphides, carbides and a oxynitride of Si, that indicate they formed under highly reducing conditions. Figures 10.14 and 10.15 illustrate the compositional differences between these chondrite classes.

The diagonal lines on Figure 10.14 are lines of constant total iron content. There has been long debate as to the origin of the variations in iron content. Some have supposed it relates to processes in the parent body, such as loss of iron to form the cores of planetisimals (with iron meteorites representing the cores), but the present consensus among meteorists is that the differences between these groups reflect variations in the oxygen fugacity prevailing at the time and place of condensation of the grains which later coalesced to form meteorite parent bodies. Thus the various chondrite groups probably formed in different regions of the psolar nebula. Because hydrogen is by far the most abundant element in the solar system, oxygen fugacity would be controlled by the amount of hydrogen present. In a region where the H concentration is high, it would bind much of the available O as H_2O , leaving the Fe in a metallic state. Where the H concentration is low, O would be available to oxidize Fe. The H concentration might have varied either radially or vertically through the disk of the solar nebula, providing different environments for chondrite formation.

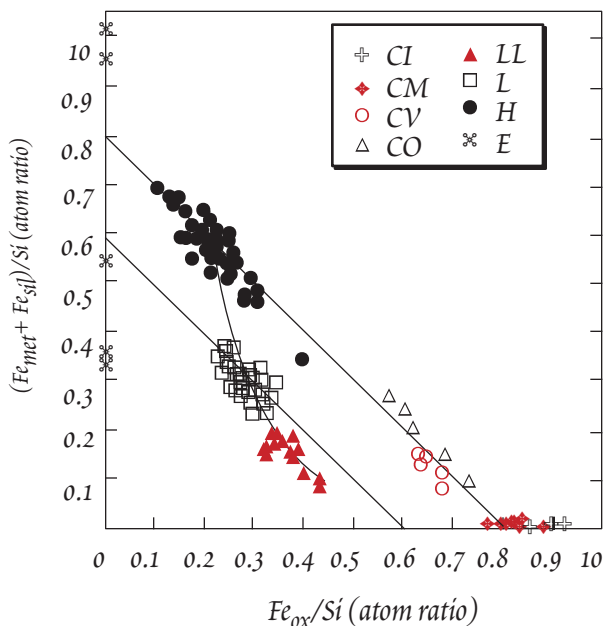


Figure 10.14. Ratio of reduced and oxidized iron to Si in various chondrite groups. The diagonal lines represent constant total iron concentration. After Wasson (1974).

As may be seen in Figure 10.14 and Table 10.1, the variations in oxidation state among ordinary chondrites are paralleled by other chemical variations. Thus, variations in oxygen fugacity alone cannot account for the compositional range seen in these objects.

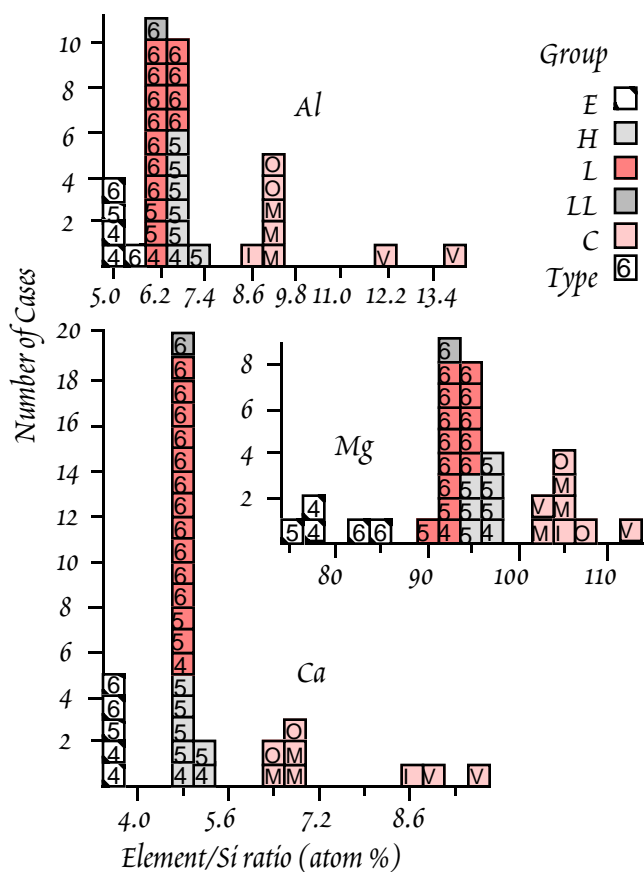


Figure 10.15. Histogram of Al/Si, Mg/Si and Ca/Si ratios in various groups and petrologic types of chondrites. (After Wasson, 1974).

Among the chondrites, and for that matter among all meteorites, *carbonaceous chondrites are the most volatile rich and the most primitive*. They may be further subdivided, but again, we run into some variation in classification. The older classification system divides them into subclasses I, II, and III, reflecting decreasing C and H₂O contents (hence CI are the most primitive). Wasson (1974) initiated a slightly different classification using a type meteorite for the name of the group and dividing the CIII's into two classes. Thus CI = CI (Ivuna), CII = CM (Mighei), CIII = CV (Vigarano) and CO (Ornans). CI are the most primitive objects known. As we noted earlier, CI's lack chondrules. Unfortunately, only one find exists in enough quantity for serious chemical analysis: Orgueil. Table 10.1 lists the general characteristics of the various chondrite groups.

Table 10.2 lists the current best estimate of the abundances of the elements in the Solar System (in units of atoms per 10⁶ Si atoms) and for Orgueil (in various units). While this is the best current summary, it is imperfect and can be expected to improve in the future.

TABLE 10.1. CHARACTERISTICS OF CHONDRITE GROUPS

	Principal ferromagnesian silicate	Fe/(Fe/Mg) of silicate (mole %)	Metallic Fe (wt %)	Mean Mg/Si (molar)	Mean Al/Si (mole %)	Mean Ca/Si (mole %)	Mean δ ¹⁸ O ‰	Mean δ ¹⁷ O ‰	Chondrules Size (mm)	Chondrules Frequency (%)
Carbonaceous										
CI	serpentine	†	0	1.05	8.6	6.2	16.4	8.8	—	—
CM	serpentine	†	0–1	1.05	9.7	6.8	12.2	4.0	0.2	≤15
CO	olivine	9–23	0–5	1.05	9.3	6.8	-1.1	-5.1	0.2	35-45
CV	olivine	6–14	0–8	1.07	11.6	8.4	0	-4.0	1.0	35-45
Ordinary										
H	olivine	16–19	15–19	0.96	6.8	4.9	4.1	2.9	0.3	65-75
L	olivine	21–25	4–9	0.93	6.6	4.7	4.6	3.5	0.7	65-75
LL	olivine	25–32	0.3–3	0.94	6.5	4.7	4.9	3.9	0.9	65-75
Enstatite										
E	enstatite	0.04–1.4	19–25	0.80	5.3	3.6	5.5	2.9	0.5	15-20

† Too fine grained to determine.

CHAPTER 10: COSMOCHEMISTRY

Table 10.2. ABUNDANCES OF THE ELEMENTS

Element	Solar System Abundance*	σ (%)	Concentration in Orgueil (C1) [†]	Element	Solar System Abundance*	σ (%)	Concentration in Orgueil (C1) [†]
1 H	2.79×10^{10}	—	2.02%	44 Ru	1.86	5.4	0.714
2 He	2.72×10^9	—	56 nL/g	45 Rh	0.344	8	0.134
3 Li	5.71×10^1	9.2	1.49	46 Pd	1.39	6.6	0.556
4 Be	7.30×10^{-1}	9.5	0.0249	47 Ag	0.486	6	0.197
5 B	2.12×10^1	24	0.870	48 Cd	1.61	6.5	0.680
6 C	1.01×10^7	—	3.45%	49 In	0.184	6.4	0.0778
7 N	3.13×10^6	—	3180	50 Sn	3.82	9.4	1.68
8 O	2.38×10^7	10	46.4%	51 Sb	0.309	18	0.133
9 F	8.43×10^2	15	58.2	52 Te	4.81	10	2.27
10 Ne	3.44×10^6	14	203 pL/g	53 I	0.9	21	0.433
11 Na	5.74×10^4	7.1	4900	54 Xe	4.7	—	8.6pL/g
12 Mg	1.07×10^6	3.8	9.53%	55 Cs	0.372	6	0.186
13 Al	8.49×10^4	3.6	8690	56 Ba	4.49	4.5	2.340
14 Si	1.00×10^6	4.4	10.67%	57 La	0.446	2.0	0.236
15 P	1.04×10^4	10	1180	58 Ce	1.136	1.7	0.619
16 S	5.15×10^5	13	5.25%	59 Pr	0.1669	2.4	0.09
17 Cl	5.24×10^3	15	698	60 Nd	0.8279	1.3	0.463
18 Ar	1.01×10^5	6	7.51 pL/g	62 Sm	0.2582	1.3	0.144
19 K	3.77×10^3	7.7	566	63 Eu	9.73×10^{-2}	1.6	0.0547
20 Ca	6.11×10^4	7.1	9020	64 Gd	0.330	1.4	0.199
21 Sc	3.42×10^1	8.6	5.86	65 Tb	6.03×10^{-2}	2.2	0.0353
22 Ti	2.40×10^3	5	436	66 Dy	0.3942	1.4	0.246
23 V	2.93×10^2	5.1	56.7	67 Ho	8.89×10^{-2}	2.4	0.0552
24 Cr	1.35×10^4	7.6	2660	68 Er	0.2508	1.3	0.162
25 Mn	9.55×10^3	9.6	1980	69 Tm	3.78×10^{-2}	2.3	0.022
26 Fe	9.00×10^5	2.7	18.51%	70 Yb	0.2479	1.6	0.166
27 Co	2.25×10^3	6.6	507	71 Lu	3.69×10^{-2}	1.3	0.0245
28 Ni	4.93×10^4	5.7	1.10%	72 Hf	0.154	1.9	0.108
29 Cu	5.22×10^2	11	119	73 Ta	2.07×10^{-2}	1.8	0.014
30 Zn	1.26×10^3	4.2	311	74 W	0.133	5.1	0.0923
31 Ga	37.8	6.9	10.1	75 Re	5.17×10^{-2}	9.7	0.0371
32 Ge	1.19×10^2	9.6	32.2	76 Os	0.675	6.3	0.483
33 As	6.56	12	1.85	77 Ir	0.661	6.1	0.474
34 Se	62.1	6.4	18.2	78 Pt	1.34	7.4	0.973
35 Br	11.8	19	3.56	79 Au	0.187	15	0.145
36 Kr	45.0	18	8.7pL/g	80 Hg	0.34	12	0.258
37 Rb	7.09	7	2.3	81 Tl	0.184	9.4	0.143
38 Sr	23.8	8.1	7.80	82 Pb	3.15	7.8	2.43
39 Y	4.64	6.0	1.53	83 Bi	0.144	8.2	0.111
40 Zr	11.4	6.4	6.4	90 Th	3.29×10^{-2}	5.7	0.0289
41 Nb	6.98×10^{-1}	14	0.246	92 U	8.20×10^{-3}	8.4	0.0074
42 Mo	2.55	5.5	0.928				

σ is the estimated uncertainty in the solar system abundances.

* Atoms relative to Si = 10^6

[†] in ppm unless otherwise indicated. Modified from Anders and Grevesse (1989).

CHAPTER 10: COSMOCHEMISTRY

Table 10.3. Distribution of Falls among Chondrites Groups and Types

Group	Petrologic Type					
	1	2	3	4	5	6
Carbonaceous Chondrites						
CI 5						
CM		14				
CV		4	4			
CO			5	1		
Ordinary Chondrites						
H		6	23	53	32	
L			9	11	28	17
LL		6	1	7	20	
Enstatite Chondrites						
E				3	2	6

from Wasson (1974).

Though the principal compositional variations among chondrites probably reflect variations in conditions in the solar nebula, all meteorites have undergone subsequent metamorphism on their parent bodies.† Van Schmus and Wood (1967) divided all chondrites into petrographic types 1 through 6,

Table 10.4. Van Schmus and Wood Petrographic Classification of Chondrites

Class	1	2	3	4	5	6
I. Homogeneity of olivine and pyroxene		Greater than 5% mean deviation		Less than 5% mean deviation	Uniform	
II. Structural state of low-Ca pyroxene		Predominantly monoclinic		Abundant monoclinic crystals	Orthorhombic	
III. Development of secondary feldspar		Absent		Predominantly as micro-crystalline aggregates	Clear, interstitial grains	
IV. Igneous glass		Clear and isotropic primary glass: variable abundance		Turbid if present	Absent	
V. Metallic minerals (Max. Ni content)		Taenite absent or minor (<20%)	Kamacite and taenite present (>20%)			
VI. Average Ni of sulfide minerals		>0.5%	<0.5%			
VII. Overall texture	No Chondrules	Very sharply defined chondrules		Well-defined chondrules	Chondrules readily seen	Poorly defined chondrules
VIII. Texture of matrix	All fine-grained, opaque	Much opaque matrix	Opaque matrix	Transparent microcrystalline matrix	Recrystallized matrix	
IX Bulk carbon content	3 – 5%	0.8 – 2.6%	0.2 – 1%	<0.2%		
X. Bulk water content	18 – 22%	2 – 16%	0.3 – 3%	<1.5%		

† As we shall see, there is evidence that meteorites must have been part of larger planetary bodies

CHAPTER 10: COSMOCHEMISTRY

based on increasing degree of metamorphism and decreasing volatile content. Types 1 and 2 represent low temperature hydrothermal alteration and types 4-6 represent increasing high-temperature metamorphism. Type 3 objects have probably undergone the least metamorphism. Table 10.3 shows the distribution of falls among the classes and petrologic types of chondrites. Table 10.4 summarizes the Van Schmus and Wood classification scheme.

The petrologic types are used together with the above groups to classify meteorites as to origin and metamorphic grade, e.g., CV-2. Types 1 and 2 are missing among the ordinary chondrites, types 1-3 are missing among enstatite chondrites, and class 1 is restricted to CI. CI-1 meteorites have probably not been heated above 300 K since their accumulation into larger bodies.

Differentiated Meteorites

Achondrites

While all the chondrites seem reasonably closely related, the achondrites are a more varied group. A principle distinction from the chondrites, besides the absence of chondrules, is the textural evidence for an igneous origin. Achondrites are generally poorer in volatile and moderately volatile (e.g., the alkalis) elements. The principal Ca-poor classes are the *aubrites* (= enstatite achondrites) and the *urelites* and *diogenites* (= hypersthene achondrites). The aubrites are highly reduced; they resemble enstatite chondrites except the metal and sulfide is missing. Urelites consist of olivine, pyroxene and a few metal grains plus a percent or so carbon, present as graphite and diamond. The principle mineral of diogenites is, as you might have guessed, hypersthene. They resemble the silicate fraction of ordinary chondrites except for a deficiency in olivine. The Ca-rich achondrites include the *Eucrites* and *Howardites*. The eucrites resemble lunar and, to a lesser extent, terrestrial basalts, and are also called *basaltic achondrites*. The howardites are extremely brecciated (most achondrites are brecciated), and are an heterogeneous mixture of eucrite and diogenite material. The brecciated Howardites, the basaltic Eucrites, and the cumulate-textured diogenites may all have come from a single parent body. The angrites (of which there are two, the name of the class being derived from Angra dos Reis) consist mostly of Al-Ti augite (Ca-rich pyroxene) and have a composition indicating a complex igneous differentiation history. Chemical variation in the achondrites is illustrated in Figure 10.16.

A unique group of achondrites, the SNC meteorites have much younger formation ages (~ 1.25 Ga) than virtually all other meteorites. This, and certain features of their bulk compositions and trapped noble gases, led to the interpretation that these meteorites come from Mars, having been ejected by an impact event on that planet. This interpretation, initially controversial, is now the consensus view.

IRONS

Iron meteorites were originally classified based largely on phase and textural relationships. Compositionally, they all consist primarily of Fe-Ni alloys with lesser amounts of (mainly Fe-Ni) sulfides. Octahedral taenite, one of the Fe-Ni alloys, is the stable Fe-Ni metal phase at T > 900°C

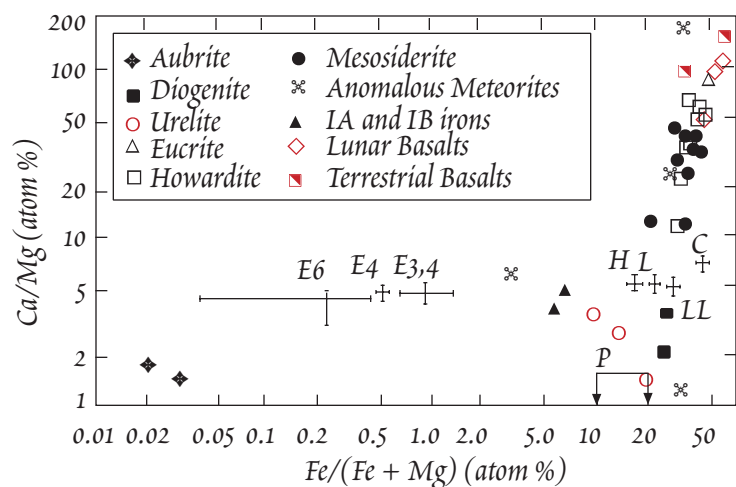


Figure 10.16. Chemical variation among achondrites and terrestrial and lunar basalts. From Wasson (1974).

ranging up to 1000 km in diameter.

CHAPTER 10: COSMOCHEMISTRY

the suite of analyzed irons. There is a general consensus that iron meteorites, with a few notable exceptions, represent the cores of planetary bodies whose diameters ranged from a few tens to a few hundred kilometers, called planetesimals. Cooling rates, estimated from textures and diffusion profiles, are typically in the range of a few 10's of degrees per million years, provide the principle evidence for the planetesimal hypothesis. A few classes of irons, most notably the IAB, may represent impact melts rather than segregated cores (Wasson et al., 1980).

STONY-IRONS

The main classes of stony-irons are the pallasites and the mesosiderites. Pallasites consist of a network of Fe-Ni metal with nodules of olivine. They probably formed at the interface between molten metal and molten silicate bodies, with olivine sinking to the bottom of the silicate magma. Mesosiderites are similar to the achondrites, but contain a large metallic component.

METEORITE MINERALOGY

By and large, meteorites consist of the same minerals we find on Earth. The three most common are olivine, pyroxene and plagioclase. Olivine predominates in carbonaceous chondrites. In reduced chondrites (E's and ordinaries), the Fe reduction means not only the ferromagnesian silicates become more magnesian, they also become more silica-rich, for obvious reasons. Thus pyroxenes dominate the more reduced ordinary chondrites. In extreme cases, these are pure Mg end-members, which are rare on Earth. Hydrated layered silicates (which tend to be extremely fine and difficult to identify) occur and can dominate the matrix of the CI and CM's. Table 10.5 gives an incomplete list of minerals in meteorites. Some of these minerals are extremely rare in the Earth. Indeed in meteorites some are restricted to the CAI's. Another group of minerals you may not be familiar with is those occurring in the irons, principally taenite and kamacite.

RELATIONSHIPS AMONG METEORITES AND METEORITE PARENT-BODIES

The limited variability in composition within meteorite classes and the compositional gaps between different classes suggests all meteorites of a common class share a close genetic history. Relatively young cosmic ray exposure ages, to be discussed below, extensive thermal metamorphism (reach perhaps 1000° C), evidence of melting in achondrites, and slow cooling rates of iron meteorites men-

TABLE 10.5. METEORITE MINERALS

Mineral	Formula	Mineral	Formula
Augite	(Ca, Mg, Fe ²⁺ , Al) ₂ (Si, Al) ₂ O ₆	Oldhamite	CaS
Baddeleyite	ZrO ₂	Olivine	(Mg, Fe) ₂ SiO ₄
Chlorapatite	Ca ₅ (PO ₄) ₃ Cl	Orthopyroxene	(Mg, Fe)SiO ₃
Christobalite	SiO ₂	Pentlandite	(Fe, Ni) ₉ S ₈
Chromite	FeCr ₂ O ₄	Pervoskite	CaTiO ₃
Cohenite	Fe ₃ C	Plagioclase	NaAlSi ₃ O ₈ — CaAl ₂ Si ₂ O ₈
Corrundum	Al ₂ O ₃	Quartz	SiO ₂
Daubreelite	FeCr ₂ S ₄	Rutile	TiO ₂
Farringtonite	Mg ₃ (PO ₄) ₂	Serpentine	Mg ₃ Si ₂ O ₅ (OH) ₄
Graphite, Diamond	C	Sodalite	3NaAlSiO ₄ ·NaCl
Enstatite	MgSiO ₃	Schreibersite	(Fe, Ni) ₃ P
Hibonite	CaO·6Al ₂ O ₃	Spinel	MgAl ₂ O ₄
Ilmenite	FeTiO ₃	Taenite	Fe _{<0.8} Ni _{>0.2}
Kamacite	Fe _{0.93-0.96} Ni _{0.07-0.04}	Tridymite	SiO ₂
Magnetite	Fe ₃ O ₄	Troilite	FeS
Melitite	Ca[Al, Mg][SiAl] ₃ O ₇	Whitlockite	Ca ₃ (PO ₄) ₂
Nepheline	NaAlSiO ₄	Zircon	ZrSiO ₄

CHAPTER 10: COSMOCHEMISTRY

tioned above all indicate that meteorites were once parts of larger *parent* bodies. All meteorites from a given class probably have been derived from the same parent body, though this need not always be the case. Estimates of the radii of parent bodies of various meteorite classes range from 10 to 1000 km. There are some compositional similarities between different classes suggesting a genetic relationship between classes, and possible derivation from the same parent body. Thus the stony-iron mesosiderites are closely related to the achondritic eucrites, howardites and diogenites. These, together with the a subset of pallasites and IIIAB irons may come from the same parent body. Other pallasites seem more closely related to ordinary chondrites and to IAB irons. The achondritic aubrites share with the enstatite chondrites the characteristic of being highly reduced.

Although meteorites represent a wide range of compositions, there is no particular reason to believe that those in collections are representative sample of the compositions of Solar System bodies. As we shall see, most meteorites probably come from the asteroid belt, where they are continually produced by collisions. Meteorites in collections represent only those that have been produced relatively recently. Most likely, they come from only a small fraction of these asteroids, and hence represent only a part of their compositional range.

TIME AND THE ISOTOPIC COMPOSITION OF THE SOLAR SYSTEM

METEORITE AGES

CONVENTIONAL METHODS

Meteorite ages are generally taken to be the age of Solar System. The oft cited value for this age is 4.56 Ga. Before we discuss meteorite ages in detail, we need to consider the question of precisely what event is being dated by radiometric chronometers. In Chapter 8, we found that radioactive clocks record the last time the isotope ratio of the daughter element, e.g., $^{87}\text{Sr}/^{86}\text{Sr}$, was homogenized. This is usually some thermal event. In the context of what we know of early solar system history, the event dated might be (1) the time solid particles were removed from a homogeneous solar nebula, (2) thermal metamorphism in meteorite parent bodies, or (3) crystallization (in the case of chondrules and achondrites), or (4) impact metamorphism of meteorites or their parent bodies. In some cases, the nature of the event being dated is unclear.

The oldest reliable high precision age is from CAI inclusions of *Allende*, a CV3 meteorite. These give a Pb isotope age of 4.568 ± 0.003 Ga. The matrix of Allende seems somewhat younger, although this is uncertain. Thus this age probably reflects the time of formation of the CAI's. Precise Pb-Pb ages of 4.552 Ga have been reported by several laboratories for the *St. Severin* LL chondrite. The same age (4.552 ± 0.003 Ga) has been reported for 2 L5 chondrites. U-Pb ages determined on phosphates in equilibrated (i.e., petrologic classes 4-6) ordinary chondrites range from 4.563 to 4.504 Ga. As these phosphates are thought to be secondary and to have formed during metamorphism, these ages apparently represent the age of metamorphism of these meteorites. Combined whole rock Rb-Sr ages for H, E, and LL chondrites are 4.498 ± 0.015 Ga. However, within the uncertainty of the value of the ^{87}Rb decay constant, this age could be 4.555 Ga (uncertainties normally reported on ages are based only on the scatter about the isochron and the uncertainty associated with the analysis, they do not include uncertainty associated with the decay constant). The age of *Allende* CAI's thus seems 5 Ma older than the best ages obtained on ordinary chondrites. No attempt has been made at high-precision dating of CI chondrites as they are too fine-grained to separate phases.

Pb isotope ages of the unusual achondrite *Angra dos Reis*, often classed by itself as an 'angrite' but related to the Ca-rich achondrites, give a very precise age of 4.5578 ± 0.0004 Ma. Ibitira, a unique unbrecciated eucrite, has an age of 4.556 ± 0.006 Ga. Perhaps surprisingly, these ages are the same as those of chondrites. This suggests that the parent body of these objects formed, melted, and crystallized within a very short time interval. Not all achondrites are quite so old. A few other high precision ages (those with quoted errors of less than 10 Ma) are available and they range from this value down to 4.529 ± 0.005 Ga for *Nueva Laredo*. Thus the total range of the few high precision ages in achondrites is about 30 million years.

CHAPTER 10: COSMOCHEMISTRY

K-Ar ages are often much younger. This probably reflects Ar outgassing as a result of collisions. These K-Ar ages therefore probably date impact metamorphic events rather than formation ages.

The present state of conventional meteorite chronology may be summarized by saying that it appears the meteorite parent bodies formed around 4.56 ± 0.005 Ga, and there is some evidence that high-temperature inclusions (CAI's: calcium-aluminum inclusions) and chondrules in carbonaceous chondrites may have formed a few Ma earlier than other material. Resolving events on a finer time-scale than this has proved difficult using conventional techniques. There are, however, other techniques which help to resolve events in early solar system history, and we now turn to these.

INITIAL RATIOS

The reference 'initial' $^{87}\text{Sr}/^{86}\text{Sr}$ of the solar system is taken as 0.69897 ± 3 , based on the work of Panastassiou and Wasserburg (1969) on basaltic achondrites (BABI: basaltic achondrite best initial). Basaltic achondrites were chosen since they have low Rb/Sr and hence the initial ratio (but not the age) is well constrained in an isochron. Subsequent high precision analyses of individual achondrites yield identical results (earlier reported low *Angra Dos Reis* have subsequently been shown to be in error). CAI's and Rb-poor chondrules from Allende have an even lower initial ratio: 0.69877 ± 3 consistent with the idea that these formed slightly earlier than the meteorite parent bodies.

The initial $^{143}\text{Nd}/^{144}\text{Nd}$ ratio of the solar system is taken as 0.506609 ± 8 (normalized to $^{143}\text{Nd}/^{144}\text{Nd} = 0.72190$) based on the work on chondrites of Jacobsen and Wasserburg (1980). Achondrites seem to have slightly higher initial ratios, suggesting they formed a bit later.

The initial isotopic composition of Pb is taken from the work of Tatsumoto et al. (1973) on troilite from the Canyon Diablo iron meteorite as $^{206}\text{Pb}/^{204}\text{Pb}$: 9.307, $^{207}\text{Pb}/^{204}\text{Pb}$: 10.294, $^{208}\text{Pb}/^{204}\text{Pb}$: 29.476. These values agree with the best initial values determined from chondrites, including Allende chondrules. More recent work by Chen and Wasserburg (1983) confirms these results, i.e.: 9.3066, 10.293, and 29.475 respectively.

EXTINCT RADIONUCLIDES

There is evidence that certain short-lived nuclides once existed in meteorites. This evidence consists of anomalously high abundances of the daughter nuclides in certain meteorites and fractions of meteorites. A list of these extinct radionuclides is presented in Table 10.6. These provide evidence for a nucleosynthetic event shortly before the solar system formed. To understand why, consider the example of ^{129}I . It decays to ^{129}Xe with a half-life of 16 Ma. Hence 16 Ma after they were created, only 50% of the original atoms of ^{129}I would remain. After 2 half-lives, or 32 Ma, only 25% would remain, after 4 half-lives, or 64 Ma, only 6.125% of the original ^{129}I would remain, etc. After 10 half lives, or 160 Ma, only $1/2^{10}$ (0.1%) of the original amount would remain. Anomalously high abundance of ^{129}Xe relative to other Xe isotopes in a meteorite indicates some ^{129}I was present when the meteorite, or its parent body, formed. From this we can conclude that an event that synthesized ^{129}I occurred not more than roughly 10^8 years before the meteorite formed.

These short-lived 'fossil' radionuclides also provide a means of relative dating of meteorites and other bodies. Of the various systems, the $^{129}\text{I} - ^{129}\text{Xe}$ decay is perhaps most useful. Figure 10.19 shows relative ages based on this decay system. These ages are calculated from $^{129}\text{I}/^{127}\text{I}$ ratios, which are in turn calculated from the ratio of excess ^{129}Xe to ^{127}I . Since the initial ratio of $^{129}\text{I}/^{127}\text{I}$ is not known, the ages are relative (the age of the *Bjurböle* meteorite, an L4 chondrite, is arbitrarily taken as 0).

TABLE 10.6. SHORT-LIVED RADIONUCLIDES IN THE EARLY SOLAR SYSTEM

Radio-nuclide	Half-life Ma	Decay	Daughter	Abundance Ratio
^{146}Sm	103	α	^{142}Nd	$^{146}\text{Sm}/^{144}\text{Sm} \sim 0.005$
^{244}Pu	82	α, SF	Xe	$^{244}\text{Pu}/^{238}\text{U} \sim 0.005$
^{129}I	16	β	^{129}Xe	$^{129}\text{I}/^{127}\text{I} \sim 1 \times 10^{-4}$
^{107}Pd	7	β	^{107}Ag	$^{107}\text{Pd}/^{108}\text{Pd} \sim 2 \times 10^{-5}$
^{53}Mn	3.7	β	^{53}Cr	$^{53}\text{Mn}/^{55}\text{Mn} \sim 4 \times 10^{-5}$
^{26}Al	0.7	β	^{26}Mg	$^{26}\text{Al}/^{27}\text{Al} \sim 5 \times 10^{-5}$

CHAPTER 10: COSMOCHEMISTRY

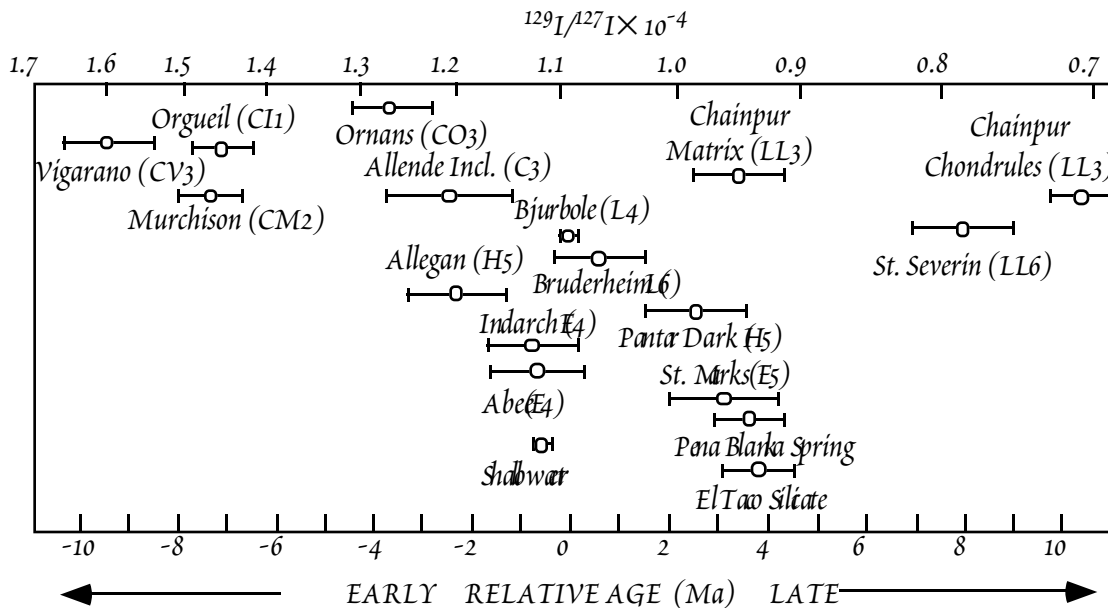


Figure 10.19. Summary of I-Xe ages of meteorites relative to Bjurböle, which is used as a standard because it gives highly reproducible results. Based on data in Swindle and Podosek (1988).

The total range in apparent ages is roughly 20 million years, though most fall within a narrower time span. The ages “date” closure of the systems to Xe and I mobility, but there is considerable debate as to what this represents. Some, perhaps the majority, argue it reflects accretion onto parent bodies or metamorphism. Others argue it somehow dates nebular processes, though the range in apparent ages is much greater than the life span of the solar nebula, which based on theoretical calculations and astronomical observations, is not longer than 1 million years. Perhaps both are involved.

An important point is that the range in ages is narrow and there is little systematic variation in age with meteorite class. Carbonaceous and ordinary chondrites do seem to be slightly older than enstatite chondrites, which might in turn be slightly older on average than LL chondrites. Differentiated meteorites are perhaps slightly younger.

Another important chronometer is isotopic variations of Xe due to fission of ^{244}Pu , half-life 80 Ma (^{244}Pu fissions mainly to the heavier Xe isotopes, ^{132}Xe , ^{134}Xe , and ^{136}Xe , and isotopic variations due to Pu fission are readily distinguished from those due to decay of ^{129}I). When ^{244}Pu decays, a great deal of energy is given off in the process. The newly formed atoms are propelled through the surrounding crystal lattice at high velocities, leaving behind a trail of destruction referred to as a *fission tracks*. Since damaged crystal lattices dissolve more quickly than intact lattices, applying acid to a crystal will etch out and enlarge the fission tracks until they are visible under a microscope. Other naturally occurring radioactive nuclei such as uranium also produce fission tracks, but to a predictable degree. Any excess over this expected number of fission tracks for a known uranium concentration is indicative of the former presence of ^{244}Pu . Such evidence for fossil ^{244}Pu has been found in chondrites, indicating that the chondrite must have formed during the period in which ^{244}Pu still existed in the solar system.

The mere existence of radiogenic ^{129}Xe requires the time span between closure of the presolar nebula to galactic nucleosynthesis and formation of the solar system be no more than about 150 Ma. This time constraint is further reduced by the identification of radiogenic ^{26}Mg , produced by the decay of ^{26}Al . That ^{26}Al is the source of the ^{26}Mg is evidenced by the correlation between ^{26}Mg and the Al/Mg ratio (Figure 10.20). Given the half-life of ^{26}Al of 0.72 Ma, assuming a production ratio for $^{26}\text{Al}/^{27}\text{Al}$ around 10^{-3} to 10^{-4} in nucleosynthesis and an apparent $^{26}\text{Al}/^{27}\text{Al}$ ratios in CAI's of about 10^{-5} suggests a nucleosynthetic event, such as a red giant or supernova, less than 8 Ma before formation of these CAI's. An

CHAPTER 10: COSMOCHEMISTRY

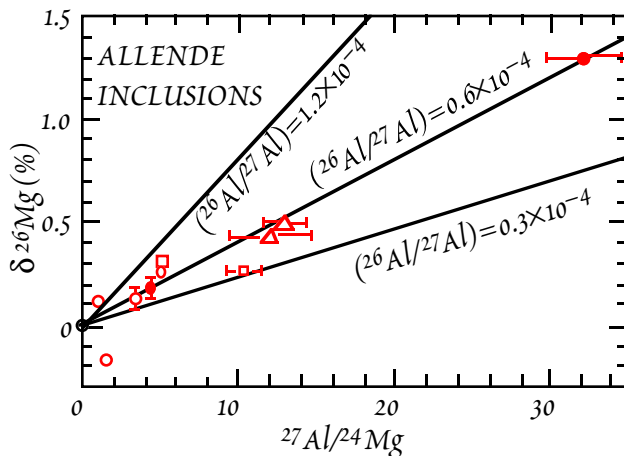


Figure 10.20. Al-Mg evolution diagram for Allende samples. Labeled lines are slopes that would result if the inclusions formed with the stated $^{26}\text{Al}/^{27}\text{Al}$ ratio. $\delta^{26}\text{Mg}$ is the percent deviation from the terrestrial $^{26}\text{Mg}/^{24}\text{Mg}$ ratio; ^{27}Al is the sole stable isotope of Al. After Lee et al. (1976).

variations of Ag from the decay of ^{107}Pd (half-life 6.5 Ma) in iron meteorites indicate core formation in meteorite parent bodies began, and was largely complete, within about 15 Ma of the nucleosynthetic event.

COSMIC RAY EXPOSURE AGES AND THE ORIGIN OF METEORITES

As we saw in Chapter 8, cosmic rays colliding with matter in meteorites and planetary bodies produce new nuclides through spallation. The cosmic rays only penetrate to a limited depth (of the order of a meter or less: there is no cutoff, the flux falls off exponentially), so that only small bodies or the surfaces of larger bodies are exposed to cosmic rays. The rate of production of nuclides by cosmic ray bombardment can be estimated from experimental physics if the cosmic ray flux is known. Thus, assuming a more or less constant cosmic ray flux, the length of time an object has been exposed to cosmic rays, the 'exposure age', can be calculated from the amounts of cosmogenic nuclides. Exposure ages are only accurate to within about a factor of 2, due to all the assumptions that are required in estimating the rate of production of nuclides. Exposure ages for chondrites are shown in Figure 10.21; expo-

important observation is that most CAI's show ^{26}Mg excesses that are consistent with a relatively uniform $^{26}\text{Al}/^{27}\text{Al}$ value of about 5×10^{-5} at the time they formed. Chondrules, on the other hand, rarely show ^{26}Mg excesses, implying the ^{26}Al had decayed by the time they formed, which in turn implies that formation of the CAI's preceded formation of the chondrules by several million years. This is a surprisingly long period and one which theorists have difficulty explaining.

Since ^{41}Ca also should have been produced (half-life 80,000 yrs), and anomalous abundances of its decay product, ^{41}K , have not been found, it seems probable that at least 2 Ma must have elapsed between nucleosynthesis and formation of the CAI's. Isotopic variations of Cr have also been identified in *Allende* inclusions, an enstatite chondrite and iron meteorites. They arise from the decay of ^{53}Mn (half-life: 3.7 Ma). These and isotopic

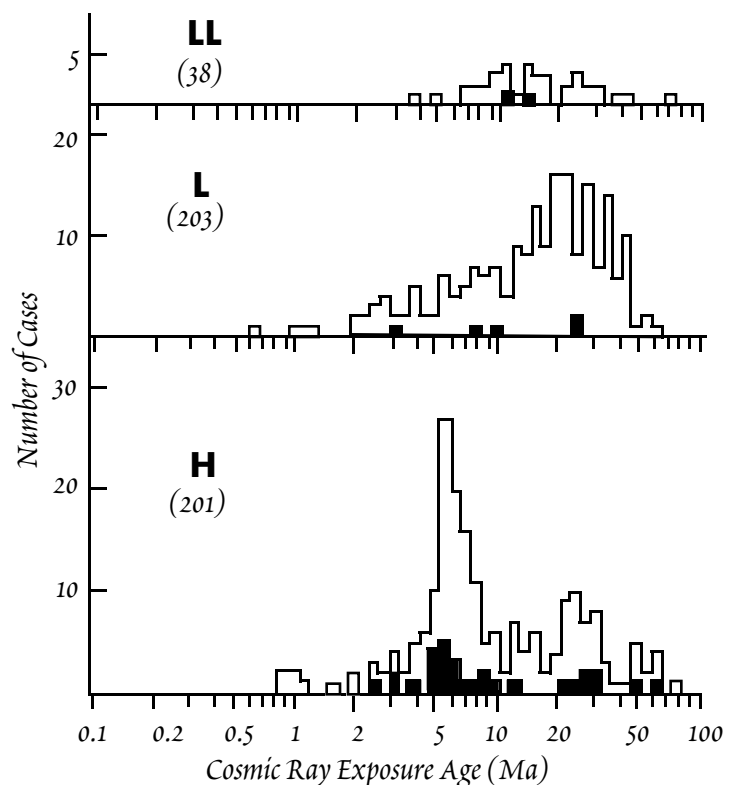


Figure 10.21. Cosmic ray exposure ages of meteorites. Filled histogram is for meteorites with regolith histories (i.e., brecciated meteorites). After Crabb and Schultz (1981).

CHAPTER 10: COSMOCHEMISTRY

sure ages for irons were shown in Figure 8.26 (page 363). As can be seen, the ages for chondrites are considerably less than formation ages. From this we may conclude that meteorites became small bodies accessible to cosmic rays only comparatively recently. Before that, they must have been stored in larger parent bodies where they would have been protected from cosmic ray bombardment. Apparently, meteorites are continually produced by collisions of these larger bodies. Irons tend to have longer exposure ages than stones. This simply reflects their greater strength and resistance to break up. The tendency for exposure ages of individual meteorite classes to cluster suggests many, or perhaps all, members of the class were derived from a single parent body.

Orbits for a few observed falls have been reconstructed, and these reconstructed orbits confirm the suspicion that many meteorites originate in the asteroid belt (Figure 10.22 shows an example of an asteroid). Reflectance spectra of some asteroids can be matched to specific groups of meteorites. Based on spectroscopic studies, Ceres, the largest asteroid (radius of 479 km) as well as several other large asteroids, appears to be compositionally similar CI and CM chondrites. Vestra has a spectra that closely matches that of the eucrites (Figure 10.23) and thus almost certainly has a basaltic crust. Other asteroids, notably those of class "M", appear to be composed of Fe-Ni metal and are analogous to iron meteorites. The reflectance spectra of other asteroids do not match those of any of the meteorite groups, which emphasizes the point made earlier that meteorites represent an incomplete sampling of Solar System material. It is quite interesting and important that the asteroid belt appears to be compositionally zoned, with "igneous" asteroids, analogous to the differentiated meteorites, predominating in the inner part and "primitive" meteorites, analogous to carbonaceous chondrites, dominating in the outer part of the belt.

In the past there had been much speculation about the possibility that carbonaceous chondrites, particularly the CI chondrites, might be derived from comets rather than asteroids. Comets come from the outer reaches of the Solar System, and thus it was thought their compositions might preserve that of the primordial solar nebula. However, the composition of Comet Halley, as determined by the 1986-1987 Giotto probe found that it certainly does not have a "primitive" composition in the sense of matching that of the Sun and CI chondrites. Clearly, comets are composed of chemically processed material, but what these processes might have been is

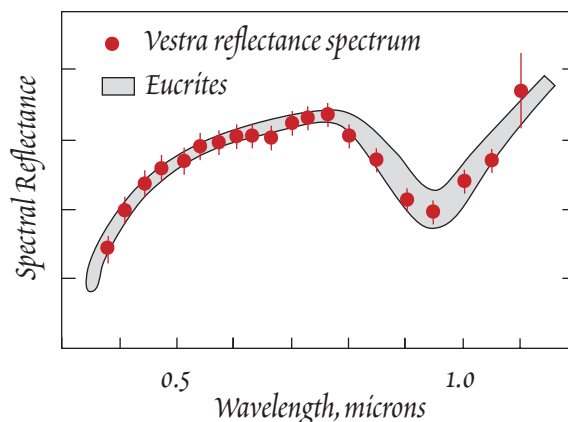


Figure 10.23. Comparison of the laboratory-determined reflectance spectrum of eucrite meteorites (basaltic achondrites) with that of the asteroid Vestra. The close match suggests that the crust of Vestra is basaltic, and similar to eucrites. After McSween (1987).



Figure 10.22. The asteroid Gaspra, photographed by the Galileo spacecraft in 1991. Gaspra is an S-type asteroid, consisting principally of olivine, pyroxenes, and metal with dimensions of about 19 by 12 by 11 kilometers. It appears to be collisional fragment of a larger body.

CHAPTER 10: COSMOCHEMISTRY

uncertain (the Giotto measurements were very imprecise, so perhaps this is not the final work on this subject).

ISOTOPIC ANOMALIES IN METEORITES

NEON ALPHABET SOUP AND INTERSTELLAR GRAINS IN METEORITES

Since Thomson's discovery that elements could consist of more than one isotope in 1912, scientists have realized that the isotopic composition of the elements might vary in the universe. They also realized that these variations, if found, might provide clues as to how the elements came into being. As the only available extraterrestrial material, meteorites were of obvious interest in this respect. However, isotopic analyses of meteorites, by Harold Urey among others, failed to reveal any differences between meteorites and terrestrial materials. This apparent isotopic homogeneity was raised as an objection to the polygenetic hypothesis of Burbidge, Burbidge, Fowler, and Hoyle (1957), since isotopic variations in space and time were an obvious prediction of this model. Within a few years of its publication, however, John Reynolds, a physicist at the University of California, Berkeley, found isotopic variations in noble gases, particularly neon and xenon (Reynolds, 1960).

Noble gases are present in meteorites at concentrations that are often as low as 1 part in 10^{10} . Though they are fairly readily isolated and analyzed at these concentrations, their isotopic compositions are nonetheless sensitive to change due to processes such as radiogenic decay (for He, Ar, and Xe), spallation and other cosmic ray-induced nuclear processes, and solar wind implantation. In addition, mass fractionation can significantly affect the isotopic compositions of the lighter noble gases (He and Ne). Through the late 1960's, all isotopic variations in meteoritic noble gases were thought to be related to these processes. For example, Ne isotopic variations could be described as mixtures of three components, "Neon A" or planetary (similar in composition to the Earth's atmosphere), "Neon B", or solar, and "Neon S", or spallogenic (cosmogenic) (Figure 10.23). The isotopic variations in Xe discovered by Reynolds were nonetheless significant because they were due to the decay of ^{129}I and ^{244}Pu , which must have been only recently (on a cosmic time scale) synthesized.

In 1969, the picture became more complex when evidence of a ^{22}Ne -rich component, named "Neon E" was found in the high temperature (900-1100°C) release fractions of six carbonaceous chondrites (Black and Pepin, 1969). However, the carrier of Neon-E proved difficult to identify. Many scientists participated in an intensive search over nearly 2 decades for the carrier phase of these components. The search quickly focused on the matrix, particularly that of CM2 meteorites. But the fine-grained nature of the matrix, together with the abundance of sticky and refractory organic compounds, made work with the groundmass difficult. In the late 1980's, E. Anders and his colleagues at the University of Chicago (e.g., Tang and Anders, 1988) found that Neon-E is associated with fine-grained (<6 μm) graphite and SiC (silicon carbide) of the matrix. Ne-E actually consists of two isotopically distinct components: Ne-E(L), which was found to reside in graphite, and Ne-E(H) which resides in SiC. The $^{20}\text{Ne}/^{22}\text{Ne}$ ratio of Ne-E(H) is less than 0.01, while that of Ne-E(L) is less than 0.2.

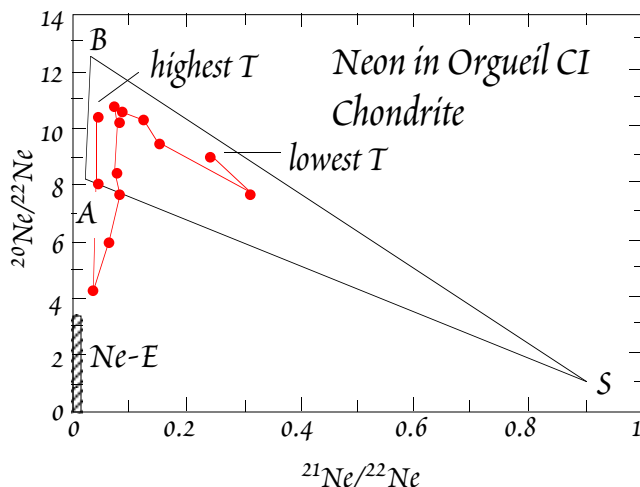


Figure 10.24. Neon isotopic compositions in a step-heating experiment on Orgueil CI chondrite, which produced the first evidence of 'pre-solar' or exotic Ne. The points connected by the line show the changing Ne isotope ratios with increasing temperature. Shaded area was the original estimate of the composition of the pure Ne-E component. Also shown are the compositions of Ne-A ('solar'), Ne-B ('planetary'), and Ne-S ('spallogenic'). After Black and Pepin (1969).

found isotopic variations in noble gases, particularly

CHAPTER 10: COSMOCHEMISTRY

The other key noble gas in this context is xenon. Having 9 isotopes rather than 3 and with contributions from both ^{129}I decay and fission of Pu and U, isotopic variations in Xe are bound to be much more complex than those of Ne. On the other hand, its high mass minimizes mass fractionation effects, so "solar" (more properly solar wind) and "planetary" Xe are isotopically similar. The first evidence of isotopic variations in Xe came in the early 1960's, but these variations were thought to be fissionogenic (at one time it was argued they were produced by fission of short-lived superheavy elements). However, subsequent investigation revealed two distinct components that could not be explained by decay of unstable nuclides. The Xe-HL component, so named because it shows enrichments in both the heaviest and lightest Xe isotopes (Figure 10.25), and the Xe-S component, enriched in ^{128}Xe and ^{130}Xe .

Anders' University of Chicago group eventually identified the carrier of Xe-HL as microdiamonds and that of Xe-S as SiC. These diamonds are extraordinarily fine, averaging only 10 Å in diameter and containing typically only 10^3 or so atoms. Roughly one in every four atoms is at the surface. Because the surface free energy is so large as a result (see Chapter 5), the properties of this material differs significantly from normal diamond. For example, it readily forms a colloid in aqueous solutions of pH > 3. This considerably complicated the effort to isolate it. The other interesting observation is that diamond is unstable at low pressures, and the conditions of interstellar space is are certainly low pressure. The question then arises as to how the could be produced. The best guess at present is condensation from vapor. While diamond is unstable relative to graphite at low pressure, it's formation can be kinetically favored under certain conditions, including condensation from vapor with high hydrogen-carbon ratios.

Once these interstellar grains were isolated, it was possible to study their isotopic compositions in detail, particularly through the use of ion microprobes[‡]. Very large variations in the isotopic composition of carbon and nitrogen, as well as smaller variations in the composition of Si, Mg, Ca, Ti, Sr, and Ba have been found. The characteristics of these interstellar grain are summarized in Table 10.7.

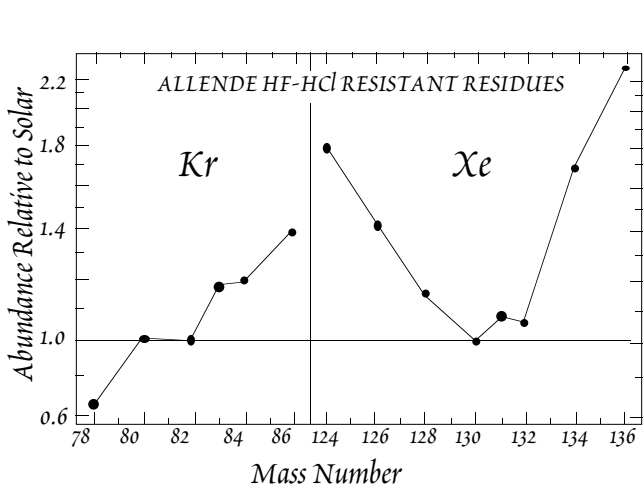


Figure 10.25. The isotopic composition of Kr and Xe of the 'Xe-HL' component in Allende matrix. Xe-HL is characteristically enriched in both the light and heavy isotopes, while the lighter noble gases show enrichment only in the heavy isotopes. After Anders (1988).

In addition, a fourth type of interstellar grain, Al_2O_3 , has also been isolated from the matrix of carbonaceous chondrites.

Discovery of isotopically anomalous interstellar grains has inspired theorists to attempt to explain them, and there has been considerable progress on understanding stellar and explosive nucleosynthesis in the past few years as a result. However, even the very limited treatment of nucleosynthetic processes in stars earlier in the chapter is sufficient to allow us to identify the environment in which some of these grains were produced. Thus, if we examine a chart of the nuclides, we quickly see that the lightest Xe isotope, ^{124}Xe is a p-process-only nuclide, while the heaviest Xe isotope, ^{136}Xe , is a r-process-only nuclide (in addition to production by fission, which, however, produces other Xe isotopes as well). The p- and r-processes occur in supernovae, thus Xe-HL, as

[‡] Ion microprobes fire a narrow beam of ions (often O or Ar) at a surface. This produces ions from the surface that can be analyzed in an attached magnetic sector mass spectrometer. This is known as secondary ionization mass spectrometry or SIMS). Because the ion beam can be focused very finely (a few microns in diameter), very small areas can be analyzed.

Table 10.7. ISOTOPIC CHARACTERISTICS OF INTERSTELLAR GRAINS

Phase	Diamond	SiC	Graphite
Isotopic Component	Xe-HL	Xe-S, Ne-E(H)	Ne-E(L)
Enriched in Isotopes	$^{124}\text{Xe}, ^{136}\text{Xe}$	$^{128}\text{Xe}, ^{130}\text{Xe}, ^{22}\text{Ne}$	^{22}Ne
Nuclear Process	p, r	s, $^{22}\text{Na}(\beta^+, \nu)^{22}\text{Ne}$	$^{14}\text{N} + 2\alpha \rightarrow ^{22}\text{Ne}$
Grain Size, μ	0.001	0.03-10	0.8-7
Abundance in C2 chondrites, ppm	400	7	<2
$(^{13}\text{C}/^{12}\text{C})/(^{13}\text{C}/^{12}\text{C})_{\odot}$	0.96	0.03 – 50	0.012 – 50
$(^{15}\text{N}/^{14}\text{N})/(^{15}\text{N}/^{14}\text{N})_{\odot}$	0.66	0.015 – 20	0.55 – 6.7

Modified from Anders and Zinner (1993).

well perhaps as the diamonds that carry it, must have been produced in supernovae. Xe-S is enriched in ^{128}Xe and ^{130}Xe , which are s-process-only isotopes. The s-process, of course, operates mainly in red giants, so we might guess the SiC was produced in red giants. Carbon and nitrogen in the SiC is, in most cases, enriched in ^{14}N and ^{13}C relative to normal solar system nitrogen and carbon. As we noted earlier in the chapter, there tends to be some net production of ^{14}N , and consumption of ^{12}C in the CNO cycle, which operates in main sequence stars, but also in the H-burning shell of red giants. As it turns out, our guess of red giants as sources of this SiC would be a good one. Theoretical studies show a close match between the observed isotopic patterns and those produced in the red giant phase (also called asymptotic giant branch) of medium-sized stars (1-3 M_{\odot}). These studies show that such stars could also produce the ^{107}Pd and ^{26}Al that was present when the meteorites formed (e.g., Wasserburg et al., 1995).

The Ne-E(L) in graphite is interesting because it appears to consist of pure, or nearly so, ^{22}Ne . Its origin posed something of a mystery: any process that synthesizes ^{22}Ne should also synthesize other Ne isotopes as well as isotopes of other noble gases. The answer lies in theoretical calculations of nucleosynthesis, which indicate that under conditions for synthesis of ^{20}Ne -poor Ne, most of mass 22 would be ^{22}Na , which has a half-life of 2.6 years. Na could readily separate from Ne and other noble gases by condensation into grains if ambient temperatures are below several hundred degrees C, as would certainly be the case in the interstellar medium. Both novae and the He-burning shells of pre-supernovae stars are possible sources of this material.

OTHER EXOTIC COMPONENTS IN METEORITES

Besides isotopic anomalies apparently produced by decay of short-lived radionuclides such as ^{26}Al , ^{129}I , and ^{244}Pu , and those associated with the interstellar grains in the matrix, other isotopic anomalies have been identified in CAI's. Some of these have been observed only in a few CAI's from *Allende*: Ca, Ba, Sm, Nd, and Sr. They have been termed FUN anomalies: fractionation and unknown nuclear. Other variations are widespread, but appear to be due to fractionation, e.g., Si and Mg. A systematic search by G. Lugmair and colleagues at the University of California at San Diego has revealed that isotopic variations of the iron peak elements (elements clustered around the cosmic abundance peak at Fe), Ca through Zn, are ubiquitous in many CAI's. Variations are up to per mil size relative to terrestrial isotope ratios, and are characterized by overabundance of the most neutron-rich nuclides (^{48}Ca , ^{50}Ti , ^{54}Cr , ^{64}Ni , and ^{66}Zn), often accompanied by underabundance of the most neutron-poor isotopes. In some instances, isotopic variations within single mineral grains have been observed with the ion microprobe. In general, these isotopic variations are most readily explained if the inclusions contain an admixture of neutron-rich e-process material from a supernova.

OXYGEN ISOTOPE VARIATIONS

Another element commonly showing isotopic variations is O. Until 1973, O isotope variations in meteorites were thought to be simply the result of fractionation, as they are on Earth. But when R. Clayton of the Univ. of Chicago went to the trouble of measuring ^{17}O (0.037% of O) as well as ^{18}O and ^{16}O , he found that these variations were not consistent with simple mass-dependent fractionation.

CHAPTER 10: COSMOCHEMISTRY

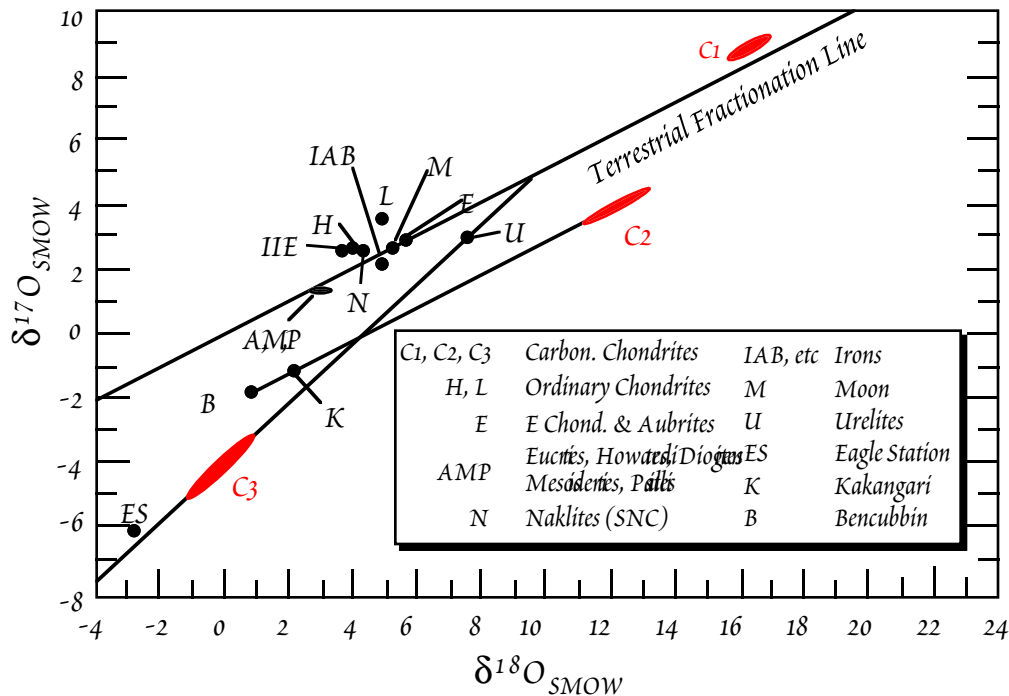


Figure 10.26. Variation of O isotope ratios in meteorites and terrestrial and lunar samples. Most of the data from Allende inclusions is off the plot to the left. From the work of R. N. Clayton.

This is illustrated in Figure 10.26. On a plot of $^{17}\text{O}/^{16}\text{O}$ vs. $^{18}\text{O}/^{16}\text{O}$, variations created by fractionation should plot along a line with slope of 1/2. Terrestrial and lunar samples do indeed define such a line, but other meteorites or their components fall along a line with slope = 1. One interpretation is that this reflects mixing between a more or less pure ^{16}O component, such as might be created by helium

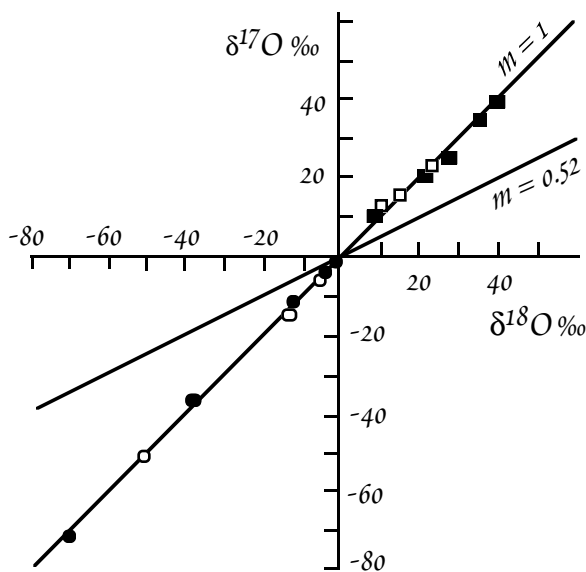


Figure 10.27. Mass independent fractionation during the production of ozone from molecular oxygen. Squares are ozone, dots are oxygen. After Thiemens and Heidenreich (1983).

burning, and a component of 'normal' isotopic composition. However, Thiemens and Heidenreich (1983) conducted experiments in which ozone produced by a high frequency electric discharge showed "mass independent fractionation", i.e., where the ozone was equally enriched in ^{17}O and ^{18}O (Figure 10.27) relative to ^{16}O . The experiment demonstrates that a slope of 1 on the $\delta^{17}\text{O}$ — $\delta^{18}\text{O}$ diagram could be produced by chemical processes. Thiemens suggested this kind of fractionation results from a kinetic fractionation mechanism, which arises because non-symmetric (e.g., $^{16}\text{O}^{17}\text{O}$ or $^{18}\text{O}^{16}\text{O}$) molecules have more available energy levels than symmetric (e.g., $^{16}\text{O}^{16}\text{O}$) molecules (as we saw in Chapter 9, symmetry enters into the calculation of the partition function). However, it is unclear how this mechanism could produce the observed fractionations, and debate still rages as to whether the O isotopic variations are ultimately of chemical or nuclear origin.

Whether the O isotope variations in meteorites are nuclear or fractionation effects, their discovery is one of the most important in the field of

CHAPTER 10: COSMOCHEMISTRY

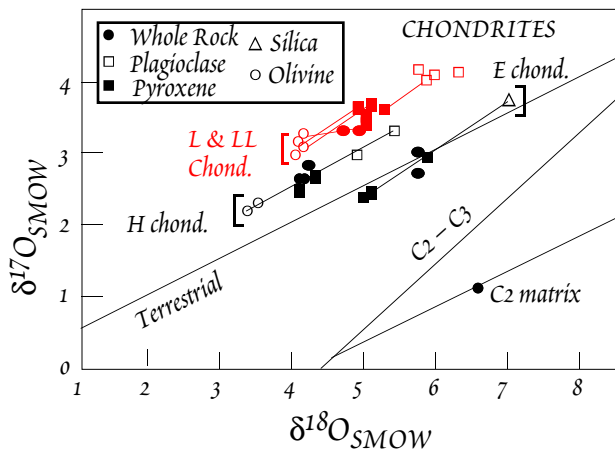


Figure 10.28. O isotope variation among minerals of various meteorite classes (Clayton et al., 1976).

cosmochemistry. What we will call 'mass independent' effects, be they nucleosynthetic or chemical fractionation, almost certainly occurred before meteorites accreted. As Figure 10.28 shows, while variations *between* classes are mostly mass-independent, variations *within* groups of meteorites fall along mass-dependent fractionation lines. This strongly suggests that, for the most part, different groups could not have come from the same parent body and that the different groups probably formed in different parts of the presolar nebula. There are a few exceptions: IIE irons fall on a mass-dependent fractionation line (MDFL) with H-chondrites, IVA irons plot on a MDFL with L and LL chondrites, basaltic and hypersthene achondrites plot on a MDFL with IAB irons and some stony-irons, and the Moon and the Earth plot on a MDFL together with enstatite chondrites and achondrites. This suggests a genetic relationship between these objects, perhaps derivation from a single parent body.

Oxygen isotope compositions of the minerals of the FUN inclusions of *Allende* are erratic and do not fall on any line. These are certainly nuclear effects.

Oxygen isotope compositions of the FUN inclusions of *Allende* are erratic and do not fall on any line. These are certainly nuclear effects.

Mass-independent effects have not been found among isotopes of other elements such as Si, S and Mg (except as noted above), though large mass-dependent fractionations are ubiquitous. Thus oxygen appears unique. The reason may be related to the partition of oxygen between the gaseous and solid phases of the presolar nebula. Over a large temperature range, only about 17% of oxygen will condense, the remainder being in the gas as H₂O and CO. Isotopic variations could arise by reaction between gas and solid of different isotopic composition. Hydrogen and carbon have only two stable isotopes so mass-dependent and mass-independent effects cannot be distinguished.

FORMATION OF THE SOLAR SYSTEM

The idea that the Solar System formed from a cloud of gas and dust is an old one and can be traced back at least to the German philosopher Immanuel Kant (1724-1804), if not to French philosopher and mathematician René Descartes (1590-1650). Like many other aspects of science, however, most of the progress on this problem has been made in the last 50 years. This progress was accelerated by two events in 1969: man's exploration of the Moon and the fall of the Allende meteorite.

There are a number of observations that allow us to place constraints on the way in which the solar system formed. These constraints include astronomical observations of star formation and the physics and chemistry of the solar system itself. Further, any successful model of solar system formation clearly must produce the distribution of mass, angular momentum, and composition, including isotopic composition, that we now observe. The chondritic meteorites, whose various components formed in and accreted from the solar nebula, are also an important constraint on models of solar system formation: a successful model of solar system formation should explain these features.

It must be stated at the outset that no model of solar system has successfully predicted all the relevant observations. This essentially means that our understanding of the process is still incomplete. In this section, we will discuss the various constraints, and outline in a general way the processes involved in solar system formation, emphasizing geochemical aspects. The geochemical goal of models of solar system formation is to predict the composition of the planets. Understanding the composition of the Earth is perhaps the most important aspect of this subject from our perspective.

CHAPTER 10: COSMOCHEMISTRY

ASTRONOMICAL OBSERVATIONS AND THEORETICAL MODELS OF STAR FORMATION

Astronomical observations have established that stars form when fragments of large molecular clouds collapse. Such clouds may have dimensions in excess of 10^6 AU[‡] and masses greater than $10^6 M_{\odot}$ (solar masses). Gravity will tend to make such clouds collapse upon themselves. This tendency may be resisted by thermal motion that tends to expand the cloud, rotational motion that stabilizes it against collapse, and internal pressures generated by magnetic fields. A careful balance between the forces tending to collapse the cloud and forces tending to expand or collapse it can result in the cloud being stable indefinitely.

Density inhomogeneities in the cloud may develop that are gravitationally unstable. The Taurus-Auriga cloud complex is a good example of a region in which low mass stars similar to the Sun are currently forming. The cloud is about 6×10^5 AU across, has a mass of roughly $10^4 M_{\odot}$, a density of 10^2 – 10^3 atoms/cm³, and a temperature around 10 K. Embedded within the cloud are clumps of gas and dust with densities 2 orders of magnitude higher than the surrounding cloud. Within these clumps are luminous protostars. About 100 stars with mass in the range of 0.2–3 M_{\odot} have been formed in this cloud in the past few million years.

In addition to random density perturbations that can spontaneously collapse, two 'events' have been identified as possible triggers of cloud collapse and star formation. The first is shock waves produced by supernovae explosions. As the shock wave propagates through an interstellar cloud, it produces instability that leads to collapse of parts of the cloud. Several such examples are known. A luminous gas cloud in Canis Major is a region of active star formation. The young stars occur in an arc whose radius suggests a shock wave produced by a supernova about a million years ago. The Great Nebula in Orion (Figure 10.29) also has an approximately circular shape, suggestive of a supernova shock wave. In this case, several large supernovae would be necessary to produce the observed motion. Since stars generally form in groups and the longevity of stars depends on their mass, several large stars forming simultaneously could ultimately lead to a series of approximately 'simultaneous' (on an astronomical—geological time scale) supernovae.

The second mechanism of cloud collapse and star formation is the density wave associated with the spiral arms of the galaxy. The spiral arms of galaxies are bright because they contain many young, massive stars (since the lifetime of a massive star will be short, all such stars are astronomically young). It is thought that the arms are actually a standing density, or gravity, wave. The clustering of many stars in the arm pulls in other stars and dust clouds. Eventually, the galactic orbits of these stars and clouds will take them out of the arms, but during the time they are in the arms, they contribute to this self-perpetuating wave of gravitational attraction. We can think of the galactic



Figure 10.29. The Great Nebula in Orion, shown in a Hubble Space Telescope photograph, is cloud of gas and dust within which stars are forming. Credit: NASA.

[‡] AU stands for Astronomical Unit, which is the Earth-Sun distance or 1.49×10^8 km.

CHAPTER 10: COSMOCHEMISTRY

arms as being similar to a traffic jam on the galactic orbital freeway. Though traffic continues to flow through the region of the traffic jam, there is nevertheless a sort of self-perpetuating high concentration of stars in the traffic jam itself. The Sun is thought to pass through an arm about once every 100 Ma on its journey around the galactic center. As clouds are pulled into the arms, they are compressed by collisions with other matter in the arms, leading to collapse of the clouds and initiation of star formation.

These two causes of dust and gas cloud collapse are not mutually exclusive. The time spent by galactic matter in the spiral arms is long enough so that very massive stars will spend their entire lives within the arms. A high concentration of massive stars in the arms means that supernovae will be more common within the arms than elsewhere. These supernovae can contribute to further star formation within the arms.

Model calculations show that once a cloud fragment or clump becomes unstable, it will collapse into a thin disk, the solar nebula, with much of the material collecting as a compact object at the center (the protostar), but much of the angular momentum being contained in the nebular disk. Such protoplanetary disks have recently been photographed by the Hubble Space Telescope (e.g., Figure 10.30). The time scale for collapse of an individual fragment to form a protostar and associated nebular disk depends on the mass of the fragment. For a star of about 1 solar mass, the time scale should be roughly 10^5 to 10^6 years (Cameron, 1995). For very massive stars, the time scale may be two orders of magnitude shorter; for very small stars, it may be two orders of magnitude longer. In most cases, collapse leads to multiple or binary star systems.

Cameron (1995) has divided the evolution of the solar nebula into 4 stages. The first stage is the one we have just described: collapse of a molecular cloud to form a disk-like nebula. At the end of stage 1 a small core of gas and dust that will eventually become the Sun is located at the center of the nebula. One of the most controversial and problematic aspects of models of stellar nebulae is the temperatures attained in the nebula. While early nebular theories (e.g., Cameron, 1962) predicted the inner solar system reached high temperatures, subsequent ones predicted much lower temperatures, 600 K at the orbit of Earth. More recent three-dimensional models of the solar nebula predict temperatures up to 1500 K in the inner solar system (e.g., Boss, 1990), but even these more recent models are greatly simplified and may significantly under- or over-estimated nebular temperatures. Nebular mass is an important factor in the maximum temperatures reached and is not well constrained. A nebula with a mass of $0.04 M_{\odot}$ would reach a maximum temperature of ~ 1400 K at 2-3 AU (the asteroid belt), while one of $0.01 M_{\odot}$ would only reach a temperature of ~ 500 to 800 K (Boss, 1995). Temperatures decrease with distance, as illustrated in Figure 10.31. There is also a strong vertical thermal gradient, so that at 0.1 AU above the nebular midplane temperatures would fall to ~ 500 K.

High temperatures appear to be reached only in the early stages of nebular evolution: calculations show the nebula would cool on a time-scale of 10^5 years (Boss, 1990). The heating is due to release of gravitational energy. The temperature obtained depends on the relative rates of heating and heat loss. The rate of heating depends on the infall rate, i.e., the rate at which gravitational potential energy is converted to thermal energy. The rate of heat dissipation depends to a considerable degree on the density and opacity of the disk. The opacity will depend particularly on the fraction of mass present as condensed matter, i.e., as dust, because dust will strongly absorb radiated energy. As temperatures in the nebula in-

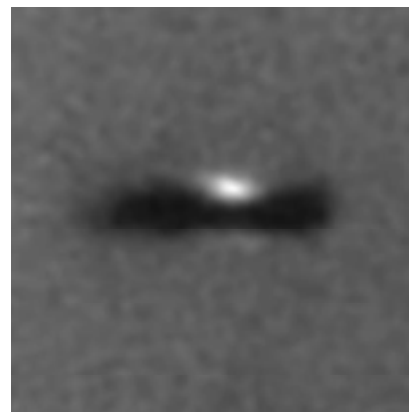


Figure 10.30. Dusty Protoplanetary disk (dark region) surrounding a newly formed star (bright central object) in the Orion Nebula photographed by the Hubble Space Telescope. Credit: Mark McCaughrean (Max-Planck-Institute for Astronomy), C. Robert O'Dell (Rice University), and NASA.

CHAPTER 10: COSMOCHEMISTRY

crease, more and more of the dust will evaporate (pressures are probably quite low in the nebula, in the vicinity of 10^{-4} atm and less). As opacity decreases, more energy will be radiated away, stabilizing, or lowering, temperature. A critical temperatures occur around 1420 K where iron grains evaporate. Above this temperature, there is little dust remaining, so the nebular would be quite transparent. As a result, temperatures probably never exceed 1500 K. However, much of the material that experiences this strong heating within the inner nebula at this stage may ultimately accrete to the Sun, so the relevance of this early heating for the chemical composition of planets and meteorites has been questioned.

Another matter of controversy is the mass of the nebula. Estimates for the mass of the nebula surrounding a star the size of the Sun, range from $0.01 M_{\odot}$ (the mass of material with solar abundances necessary to yield the mass and composition of the planets as observed—their mass is about 0.0015 solar masses) to about $1 M_{\odot}$, in excess of the mass of the Sun. Most recent models seem to favor relatively low mass nebulas. For example, Cameron (1995) uses a value that is several times the minimal value.

In Cameron's stage 2 of nebular evolution, the mass of nebula is roughly steady state, with the mass lost by accretion to the growing Sun being balanced by infall from the cloud. The Sun accretes most of its mass during this stage. One of the most difficult problems in understanding the origin of the Solar System is how the Sun ended up with most of the mass while the planets ended up with most of the angular momentum. This problem has puzzled physicists for more than a century. Indeed, it has been so vexing that some physicists have argued that the planets were formed from a captured nebula rather than one that formed with the Sun (to do so, however, requires that the chemical evidence be totally ignored). Some progress may have been made on this problem in the last few years, however. If the Sun is not located at the center of mass of the system, and if the nebula is sufficiently dense that its gravity is significant, the density waves can develop within the nebula. These density waves are much like the spiral arms of galaxies. What is important is that it appears they can transport both mass inward and angular momentum outward. These theoretical models may have a counterpart in observational astronomy. The density wave calculations indicate that mass can be added to stars in clumps. Some accreting stars can experience sudden increases in luminosity, which is thought to be due to sudden increases in the rate at which mass is accreted to the star. Such stars are known as FU Orionis stars and their outbursts may result from density waves delivering clumps of nebular material to their surfaces.

Because of both radioactivity within the nebula (^{26}Al is probably the most important radionuclide in the nebula at this point) and radiation from the growing Sun, significant ionization may occur within the nebula. If so, magnetic fields will play an important role in nebular processes. These can also transfer angular momentum outward and contribute to radial mixing of the nebula. Another characteristic of FU Orionis stars is that they eject significant amounts of gas at high velocity normal to the plane of the nebula. These "bipolar outflows" also appear to be due to magnetic coupling between the star and the nebula. The rate of outflow is quite high, as much as 10% of the rate of accretion of material from the nebula to the Sun.

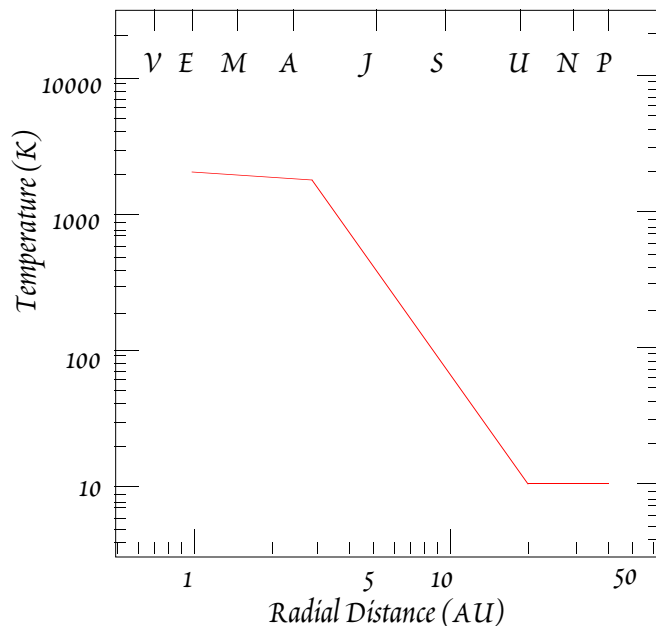


Figure 10.31. Variation of temperature with distance in a 3D computational model of the solar nebula by Alan Boss (1990).

CHAPTER 10: COSMOCHEMISTRY

Solar accretion rates are rapid during stage 2, the FU Orionis stage, and its duration is short. Cameron estimates accretion rates of $10^{-5} M_{\odot}$, and as high as $10^{-4} M_{\odot}$, during periods of rapid accretion, and a duration of this stage of 50,000 years. Much of the material that was in the inner Solar System (and that experienced strong heating in stage 1) is accreted to the Sun in this stage.

Cameron's third stage of nebular evolution is the T Tauri stage. T Tauri stars are young stars. They have cool surfaces (4000 K), but have luminosities several times that of the Sun. They are often surrounded by dusty disks, that characterized by very enhanced solar winds directed radially outward; mass losses of $10^{-8} M_{\odot}/\text{yr}$ are typical (the present solar wind amounts to a loss of $10^{-14} M_{\odot}/\text{yr}$). Like the FU Orionis stars, there are bipolar jets, but they are smaller. The strong solar winds inhibit accretion of additional material to the Sun. At the beginning of this stage accretion rates have decreased to about $10^{-7} M_{\odot}/\text{yr}$ and they drop by another order of magnitude by the end of this stage (Cameron, 1995). The T Tauri solar winds were sufficiently strong that the wind pressure on particles with radii of a few cm and smaller would exceed the gravitational force of the Sun. As a result, the winds begin to sweep any gas and dust that has not accumulated into large particles out of the solar nebula, beginning with the region closest to the Sun and working slowly outward.

It is during this stage, which lasts several million years, that planetismals and planets form. The rate at which dust, which is largely in the submicron size to begin with, accumulates into large bodies depends strongly on a number of parameters that are poorly constrained. These include turbulence, sticking efficiency, and relative velocities. Computer simulations of the process by Cameron (1995) show that grains grow most rapidly in size when they are some distance above (or below) the nebular plane. They then settle to the plane of the nebula. The simulations also suggest that once this coagulation process begins, it proceeds very rapidly. Within time of 10^3 to 10^5 years (fastest in the region of Earth, slowest in the beyond Neptune), most of the mass of the solid material in the nebula is in meter to kilometer size bodies. According to calculations by Wetherill and Stuart (1993), planetismals only slightly larger than this (10 km radius) would accumulated into "planetary embryos", bodies the size of the Moon or Mercury, within 10^5 years.

By stage 3, the nebula had lost most of its original heat. Cameron (1995) proposed the recombination reactions in the solar wind kept the inner solar system sufficiently warm, however, that water ice does not condense. Other processes may have kept the inner solar system warm as well. Jupiter, and to a lesser degree Saturn, may accumulate much of their mass during this stage of nebular evolution (Cameron, 1995). Indeed, the gas-rich nature of these planets appears to require that they form early, before the T Tauri winds dissipate the nebular gas. Though Jupiter is gas-rich, it is nevertheless depleted in gas relative to the Sun, so some dissipation of nebular gas apparently occurred before the assembly of the giant planets was complete. The location of the "snow line", i.e., the distance at which temperature falls below the point where water ice condenses (170 K) may have been located roughly at the orbit of Jupiter during stage 3. Sticking efficiency of grains is greatly enhanced if the grains are coated with frost (of H_2O , CO_2 , NH_4 , etc.). Thus the position of the "snow line" at the orbit of Jupiter may have accelerated the process of planet formation in this region. The early formation of a rocky planet of roughly 10 earth masses would have then been able to capture enough gas to become Jupiter.

The early formation of Jupiter probably has the effect of preventing the formation of a planet within the asteroid belt. This could occur either because Jupiter itself robs the belt of material, or because Jupiter perturbs the orbits of planetary embryos in the asteroid region so that they are ejected from the Solar System. Evolution of planetary embryos into planets in the inner solar system is not affected by Jupiter, but does take longer because of mutual perturbation to high velocity orbits (Wetherill and Stuart (1993).

The Sun has completely accreted by the end of Cameron's stage 3. During stage 4, there is little additional accretion of material to the nebula, which is slowly dissipated by photoevaporation beyond the orbit of Saturn and from inside out by the T Tauri solar winds. As the solar winds drive out the nebula, the inner edge of the remaining nebula, called the bow, becomes a location where formation of planetismals is particularly likely as particles are driven to the bow from both directions. The es-

CHAPTER 10: COSMOCHEMISTRY

estimated time for this stage is 3 to 30 million years. By the end of this period, the nebula has dissipated and planet formation is well underway and perhaps complete.

FORMATION OF CHONDRITIC METEORITES AND PROCESSES IN THE SOLAR NEBULA

After long debate, it is now recognized that compositional variation between classes of chondrites primarily (though not necessarily exclusively) reflects differences in conditions and composition of the nebula in the region where the various parent bodies formed rather than metamorphic processes occurring within parent bodies. Thus the composition and petrography of chondrites provide an important constraint on conditions and processes in the solar nebula.

It is now generally agreed that planetary bodies did not condense from a hot solar nebula, rather they accreted from a cool one. Nevertheless, much of the chemical variation in chondrites appears to be related to volatility. The inner part of the solar nebula may have reached high enough temperatures for much of the dust to sublime. Although this episode appears to have preceded formation of planetesimals and planets by a considerable period, some of the material that later accreted to chondrite parent bodies may have experienced high temperatures in the early nebula. The nature and composition of CAI's and chondrules within meteorites are clear evidence that there were transient local heating events within the nebula. For these reasons, it is useful to consider the sequence in which the elements would condense from a hot nebular gas.

THE CONDENSATION SEQUENCE

The theoretical condensation sequence has been calculated from thermodynamic data, largely by Larimer, Grossman, and Lewis, all of whom have worked with E. Anders at the University of Chicago (e.g., Larimer, 1967; Grossman, 1972). The condensation temperature of an element reflects its vapor pressure, its tendency to react with other elements to form compounds in the gas or solid solutions or alloys in the solid, and its abundance in the gas. Let's consider two examples of condensation sequence calculations. First, consider iron, which is a particularly simple case since it condenses as Fe metal:



Assuming ideality, the partial pressure of iron is simply its mole fraction in the gas times the total pressure (P_T). Since hydrogen is by far the dominant element in the gas, the mole fraction can be approximated as 2 times the solar Fe/H ratio (the 2 arises from hydrogen's presence as H_2). Thus the partial pressure of Fe is written as:

$$p_{\text{Fe}} = \frac{[\text{Fe}]_{\odot}}{1/2[\text{H}]_{\odot}} \times P_T \quad 10.2$$

where $[\text{Fe}]_{\odot}$ and $[\text{H}]_{\odot}$ are the solar abundances of Fe and H and P_T is total pressure. Once condensation begins, we can express the equilibrium constant for this reaction as the ratio of the partial pressure of Fe in the gas to the concentration in the solid:

$$K = \frac{p_{\text{Fe}}}{[\text{Fe}]_s} \quad 10.3$$

where $[\text{Fe}]_s$ is the concentration in the solid and $[\text{Fe}]_g$ is the concentration in the gas.

Condensation begins when the partial pressure of Fe exceeds the vapor pressure of solid Fe. Since:

$$G = -RT \ln K \quad (3.98)$$

the equilibrium constant can also be written as:

$$\ln K = -\frac{\Delta H_v}{RT} + \frac{\Delta S_v}{R} \quad 10.4$$

ΔH_v and ΔS_v are the enthalpy and entropy of vaporization. Once condensation of an element begins, its partial pressure drops by $(1 - \alpha)$ where α is the fraction condensed. Hence, equation 10.2 becomes:

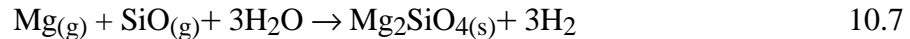
$$p_{\text{Fe}} = \frac{(1 - \alpha) [\text{Fe}]_{\odot}}{1/2[\text{H}]_{\odot}} \times P_T \quad 10.5$$

CHAPTER 10: COSMOCHEMISTRY

Combining 10.3, 10.4, and 10.5, the equation describing condensation is:

$$\ln(1 - \alpha) = -\frac{H_V}{RT} + \frac{S_V}{R} - \ln \frac{[Fe]_O}{1/2[H]_O} - \ln P_T + \ln [Fe]_s \quad 10.6$$

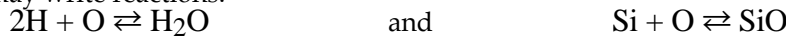
Now consider elements such as Mg and Si, which form compounds in the gas and solid, which complicates the calculation considerably. The reaction for the condensation of forsterite is:



The equilibrium constant for this reaction is:

$$K = \frac{a_{Mg_2SiO_4} P_{H_2}^3}{P_{Mg}^2 P_{SiO} P_{H_2O}^3 P_T^3} \quad 10.8$$

The first step is to compute partial pressures of the gaseous species. For example, for SiO and H₂O above, we may write reactions:



and calculate equilibrium constants for them from the free energies of these species, e.g.:

$$K = \frac{P_{SiO}}{P_{Si} P_O} \quad 10.10$$

Values of K can be computed from thermodynamic data. For each element, an additional constraint is imposed by the total abundance of that element in the gas. Thus for example:

$$[Si]_g + [Si] + [SiO] + [SiO_2] = [Si]_O - [Si]_s \quad 10.11$$

where [Si]_s is the total of silicon in condensed phases. Combining equilibrium constant equations such as 10.10 with mass balance equations such as 10.11 leads to a series of simultaneous equations. These can be solved by successive approximation using a computer. Values of equilibrium constants such as 10.8 can then be computed from ΔH and ΔS using equation 10.4.

Further complications arise when solid solutions form. For example, the forsterite term in 10.7 is 1 if forsterite is treated as a pure phase. If the solid solution with fayalite is considered, then the value of the activity must also be calculated. Values for activity coefficients are difficult to obtain, and ideal solid solution is generally assumed. Thus the activity of forsterite in 10.8 would be replaced by its mole fraction. Solid solution results in the condensation of an element at a higher temperature than if a pure component were the condensed phase.

Some elements, such as Au and Cu, will condense primarily either by reaction with already condensed Fe metal grains, or by condensing with Fe metal. At lower temperatures (around 670 K for P_T = 10⁻⁴ atm), the Fe metal will react with H₂S gas to form FeS. Moreover, from the onset of condensation a small but increasing amount of the Fe will react with H₂O gas to form FeO that dissolves in the silicates. A marked increase in the Fe content of silicates occurs around 400-500 K.

Figure 10.32 shows 2 theoretical sequences calculated by Larimer (1967) and subsequently refined by Grossman (1972). In the 'fast cooling' sequence, matter does not react with nebular gas after it has condensed. At any given time and temperature, the solid phases are a mixture of material condensed over a range of temperature. In the 'slow cooling' sequence, condensed material continually reacts and re-equilibrates with the gas as temperature drops, so that at any time, only an assemblage in equilibrium with the gas at that temperature is present. Figure 10.33 illustrates the minerals expected at a given temperature somewhat more clearly. The condensation sequence depends critically on total pressure and H pressure; the sequence shown is for relatively low total and H pressure. At relatively high pressure, metallic Fe liquid is the first phase to condense.

In a nutshell, the sequence goes like this. The first minerals to condense would be Re and the most refractory of the platinoid metals (Os, Ir, Ru), which would condense as metallic phases. Since these are extremely rare elements, they would likely form very small grains. Interestingly, small nuggets of such metal, called "Fremdlinge" (the German word for "strangers"), are found as inclusions in CAI's. There has been some speculation that they may have served as nuclei for the CAI's. Following this would be condensation of oxides and silicates of Ca, Al and Ti. They should be rich in refrac-

CHAPTER 10: COSMOCHEMISTRY

tory trace elements such as U, Th, Zr, Ba and the REE. This match closely the composition of the CAI's, suggesting the possibility that CAI's are high temperature condensates. The CAI's have about 20 times the 'chondritic' abundances of the refractory elements, suggesting they reflect $1/20 = 5\%$ condensation.

In detail, the CAI's are a varied lot. Some may indeed represent early condensate, but most are probably residual: i.e., the remaining solid after 95% of the dust has evaporated. There is evidence that some CAI's were once liquid, though this is difficult to reconcile with pressures in the nebula, which should have been too low for such liquids to be stable. Some CAI's show evidence of several cycles of evaporation and condensation.

Next in the condensation sequence should come metallic Fe-Ni and compounds richer in the moderately refractory elements such as Mg and Si: olivines and pyroxenes. If the cooling takes place under equilibrium conditions the high temperature assemblage should react to form anorthite as well, and at lower temperature when Na condenses, plagioclase. These phases are the ones that predominate in chondrules, with the important caveat that chondrules are metal poor. Since these phases condense at temperatures similar to Fe-Ni metal, some process must have separated metal from silicates before formation of the chondrules.

The Fe should also largely react out to form more Fe-rich olivine and pyroxene. At lower temperature, S condenses and reacts with Fe to form sulfides. At even lower temperature, the Fe reacts with O to form magnetite and the silicates react with water in the gas to form hydrated silicates. Sulfates, carbonates and organic compounds will also form around these temperatures.

If equilibrium conditions prevail, only the last named compounds would exist when condensation was complete, but all might exist if disequilibrium prevails.

The CI chondrites seem to be very similar in composition and petrography to equilibrium condensates (down to 300 K or so), or, more accurately, accretions of equilibrium condensates. The other carbonaceous chondrites approximate to varying degrees aggregates of disequilibrium condensates. In particular, the CV and CO's chondrites contain both the highest temperature condensates (CAI's) and lowest temperature material (hydrated silicates) and much of everything expected to condense in

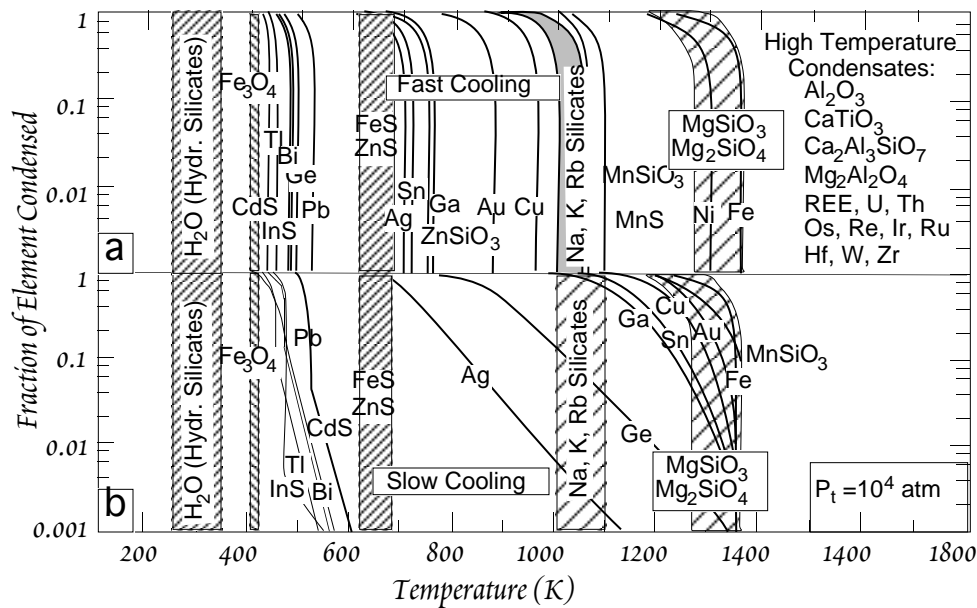


Figure 10.32. Condensation sequence of a gas with solar composition. In slow cooling diffusional equilibrium is assumed. Fast cooling leads to disequilibrium and condensation of pure elements and compounds.

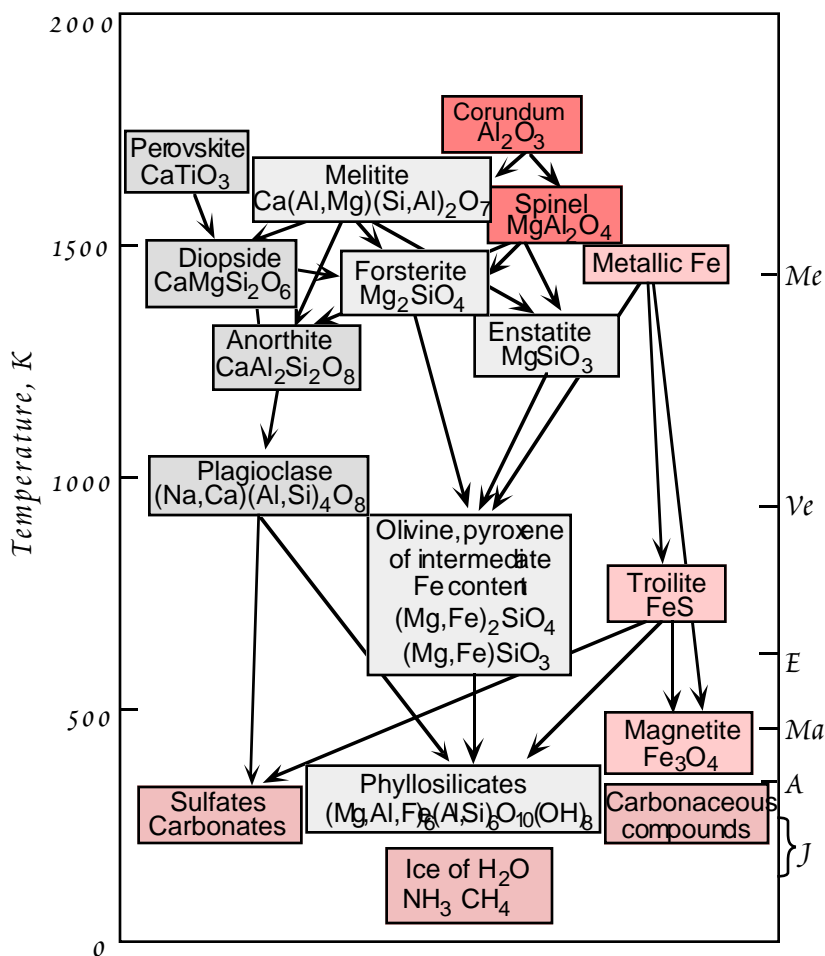


Figure 10.33. Simplified mineralogical condensation sequence.

between. CV and CO are depleted in the more volatile elements and compounds (such as water, but also the moderately volatiles such as Ga and Ge, alkalis).

THE COSMOCHEMICAL CLASSIFICATION OF THE ELEMENTS

The chemical variations in meteorites seem to be dominated by two processes: (1) condensation and evaporation and (2) oxidation and reduction. This leads to a natural classification of the elements into 4 groups based on how they are affected by these processes. The division relative to volatility is based on the condensation sequence discussed above. There are two benchmarks: the condensation of the Mg-silicates and Fe-Ni metal at 1300-1400 K (depending on pressure) and the condensation of FeS at 670 K. Those elements with condensation temperatures higher than or equal to the former are classed as *refractory*, those condensing between the Mg-

silicates and FeS are classed as *moderately volatile*, and those condensing below this temperature are classed as *highly volatile* (Larimer, 1988). Those elements generally found in metal phases in meteorites are classed as *siderophile*. This classification is illustrated in Figure 10.34. There is a some similarity to Goldschmidt's classification that we discussed in Chapter 7. The refractory elements are mostly *lithophile*, the highly volatile elements include all the *atmophile* elements, and the moderately volatiles include many *chalcophile* elements. The similarity results in part because Goldschmidt used the distribution in meteorites as part of the basis for his classification.

Anders noted that the chemistry of the carbonaceous chondrites can be approximated as two component mixtures: a volatile-rich matrix and volatile-poor chondrules and CAI's. CI chondrites consist only of matrix, while CV chondrites contain ~30% chondrules and CAI's, and are ~40% depleted in volatiles as a result. This mixing hypothesis can also be applied to ordinary chondrites, though less well. Here the cosmochemical grouping comes more into play. Figure 10.35 illustrates how several of the chondrite groups can be explained as mixtures of various identifiable components. The refractory elements are associated with chondrules and CAI's. The siderophile elements are, of course, associated with Fe metal. The association of the moderately volatile elements is somewhat more complex: those with chalcophile tendencies are associated with FeS, those with lithophile tendencies (e.g., the alkalis) are associated with silicates in the matrix. The highly volatile elements are associated exclusively with the matrix. Thus much of the compositional variation in chondrites appears to

CHAPTER 10: COSMOCHEMISTRY

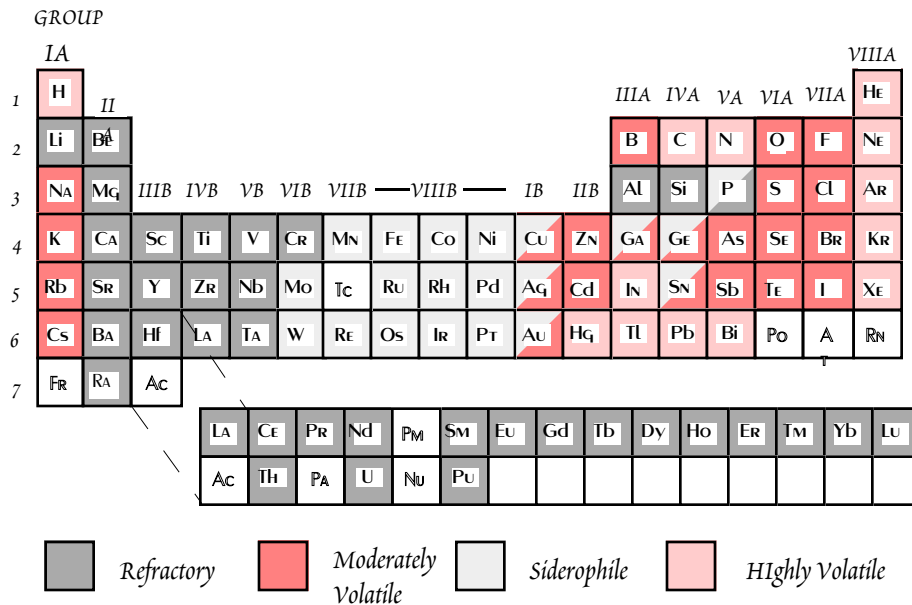


Figure 10.34. The cosmochemical periodic table (after Larimer, 1988).

result from mixing of different components that formed under different conditions in the solar nebula. However, the concentrations of the most volatile elements and compounds (e.g., water) vary between petrographic types, whereas no variation with petrographic type occurs for the moderately volatile elements. Variation in the moderately volatiles may be nebular in origin, whereas some of the variation in the highly volatiles may reflect parent body metamorphism.

CONSTRAINTS ON CONDITIONS IN THE SOLAR NEBULA

In summary, most of the compositional variation between classes of chondritic meteorites falls into 4 categories: variation in the amount of refractory material (as evidence by, for example, Al/Si ratios), variation in the content of volatile material such as water, variation in the amount of siderophile material, and variation in oxygen fugacity.

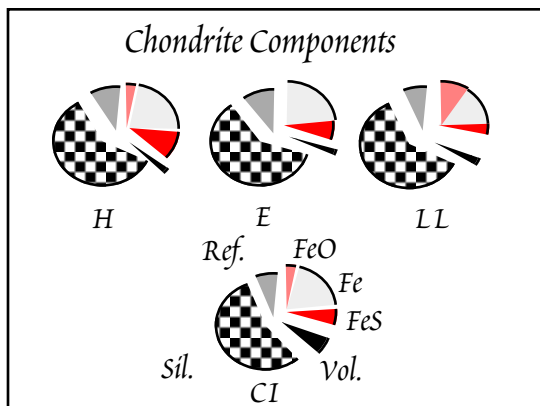


Figure 10.35. Ordinary chondrites as mixtures of nebular components. The CI chondrites contain 'solar' abundances of the condensable elements, all contained in the matrix. From Larimer (1988).

The nature of meteorites place on the formation of the solar system, which are summarized below. These constraints are not all mutually consistent, and cannot all be explained in the context of our present understanding of solar system formation.

- The evidence for pervasive ¹²⁹I suggests nucleosynthesis no more than 10⁸ years before the solar nebula collapsed. This is rather a long time on the scale of galactic processes, so it would be perhaps more surprising if ¹²⁹I were absent.
- The evidence of ²⁶Al in CAI's indicates that newly synthesized material was injected into the molecular cloud that ultimately formed the Solar System not more than about 10⁷ years before the CAI's formed. This is supported by evidence of the existence of ¹⁰⁷Pd and ⁵³Mn, as well as the recent discovery of evidence of ⁴¹Ca (half-life: 10⁵ yr). The most likely site of synthesis of this material is red giant stars.

CHAPTER 10: COSMOCHEMISTRY

- The matrix of carbonaceous chondrites contains a collection of interstellar dust. Most of this material was apparently produced well before the solar system formed. This dust includes diamonds that are either the ash of a supernova explosion, or were implanted with Xe produced in a supernova. That this material has retained its distinct noble gas isotopic signature indicates it was never heated above ~700 K.
- The pervasive presence of chondrules requires that temperatures in the nebula locally reached 1700 K or more. However, chondrules clearly cooled rapidly (time scales of an hour or less), so that these high temperatures were transient. At least locally, much of the nebular dust would have been processed through such events, since chondrules can constitute up to 80% of the mass of some meteorite classes.
- CAI's also require high temperatures and suggest that, at least locally, 95% of the nebular dust was evaporated. Studies have shown that a few of the CAI's also cooled fairly rapidly (0.5-50 K/hr), though others may have remained at high temperature for longer periods. They may have formed in the inner solar system where temperatures were high. Regardless of whether CAI's are condensates or refractory residues, some process must have separated them from the gas before cooling, otherwise lower temperature components should have condensed as well.
- Most CAI's show ^{26}Mg anomalies, indicating they formed while ^{26}Al still existed. With rare exceptions, chondrules do not show ^{26}Mg anomalies, indicating they formed after ^{26}Al had decayed. From this we may conclude that the CAI's formed several million years before the chondrules.
- Planetismals that were the parent bodies of achondrites and irons underwent sufficient heating to melt and differentiate. The oldest achondrites do not appear to be significantly younger than many chondrites. Thus planetismals formed, melted, and differentiated within a few million years of the formation of chondrites.
- Oxygen isotope ratios vary between essentially all meteorites and planetary bodies, implying that the entire nebula was never entirely homogenized, and therefore was never entirely gaseous for a significant length of time. Despite the oxygen isotope heterogeneity, and isotope anomalies in rare interstellar grains, the isotopic composition of most elements investigated in homogeneous throughout all classes of meteorites. This dichotomy has yet to be satisfactorily explained.
- Variations in the chemical composition of chondrites clearly indicates chemical inhomogeneities within the solar nebula.
- Oxygen fugacity clearly varied within the solar nebula. Since the gas is dominated by H and O constitutes a significant fraction of condensed matter, this may reflect variation in the ratio of gas to dust. This could have been caused by a number of processes, such as turbulent eddies or differential settling of grains to the nebular mid-plane. Variation in siderophile content of meteorites could also preferential transport of metal grains due to differences in densities or magnetic properties.

SUMMARY: RECIPE FOR CHONDRITIC METEORITES

We have seen that chondrites are a mix of a variety of materials formed under different conditions, probably in different places in the solar nebula. Figure 10.36 is a cartoon illustrating the processes involved in formation of chondrites and their components. Most CAI's seem to be refractory residual solids heated to ~1700 K. This heating may have occurred in the inner part of the solar nebula and was probably transient and local. Chondrules, on the other hand, experienced melting as a result of rapid heating and subsequent quick cooling. The matrix represents the nebular dust, some, or all of which never experienced severe heating.

CHAPTER 10: COSMOCHEMISTRY

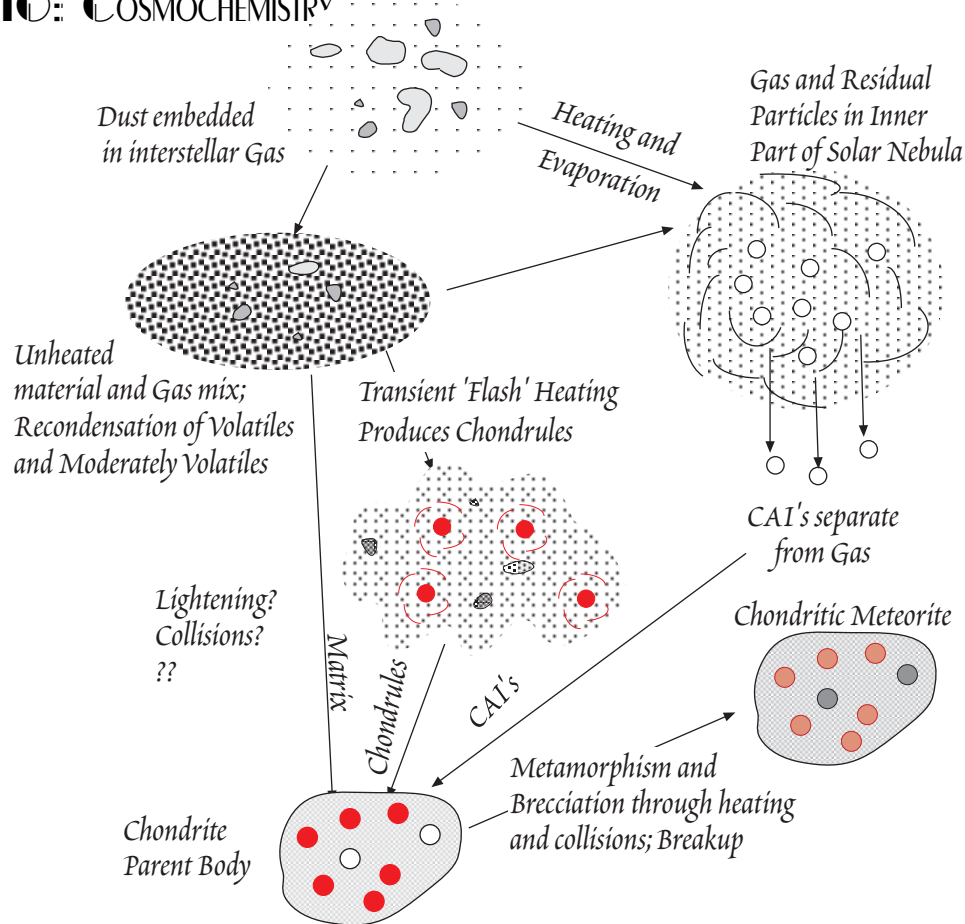


Figure 10.36. Cartoon illustrating the processes involved in the formation of chondrites and their components. Modified from McSween (1987).

FORMATION OF THE PLANETS

Table 10.8 lists the some data regarding the planets. Many planetary scientists do not consider Pluto a planet: it is better than an order of magnitude smaller than Mercury and smaller than some of the major satellites of Jupiter, Saturn, and Neptune, and has a very anomalous orbit. On the other hand, the Moon is so large, nearly a quarter of the size of Mercury, that it is sometimes counted as a planet. The planets can be divided into three groups based on their size, density and composition. These are:

- The terrestrial planets:
 - Mercury
 - Venus
 - Earth-Moon
 - Mars
- The giant planets:
 - Jupiter
 - Saturn
- The outer icy planets:
 - Uranus
 - Neptune
 - (Pluto-Chiron)

The terrestrial planets consist primarily of silicates and Fe-Ni metal, the giant planets consist primarily of H and He, and the icy planets consist of outer gaseous shells with mantles of ices of H₂O,

CHAPTER 10: COSMOCHEMISTRY

CH₄ and NH₃ and silicate-metal cores. In a gross way, this compositional pattern is consistent with radial decrease in nebular temperature (e.g., Figure 10.31): the terrestrial planets lost, or never had, their complement of the highly volatile elements (e.g., H, He) and are also depleted in moderately volatile elements (e.g., K, Pb). From what can be judged from reflectance spectra, the asteroids also fit this pattern: the inner asteroids (sunward of 2.7 AU) are predominantly igneous and compositionally similar to the achondrites, which are highly depleted in volatile and moderately volatile elements. The outer asteroids (beyond 3.4 AU) appear to be similar to carbonaceous chondrites.

Comparing the volatile inventory of Mars with that of Earth, Mars at first appears depleted in volatile elements. It has a much smaller atmosphere than the Earth (surface pressures are 0.006 atm). Like Venus, the Martian atmosphere is dominated by CO₂, with N₂ as the second most abundant component. Judging from the presence of erosional features on the Martian surface, it appears that liquid water once existed on the Martian surface. To attain the necessary temperatures, Mars would have had to have had CO₂ pressures at its surface of 5 to 10 atm. This early atmosphere has been lost, a consequence of the smaller gravitational field of Mars. Thus the depletion of highly volatile elements on Mars may be a secondary feature.

There is evidence that Mars is richer in moderately volatile elements than the Earth. Both analyses of Martian soil and the composition of SNC meteorites suggest a K/U ratio about twice that of the Earth. Sr-Nd isotope systematics (Figure 10.37) of SNC meteorites define an array shifted to higher ⁸⁷Sr/⁸⁶Sr ratios compared with that of the Earth, implying a higher Rb/Sr ratio for Mars. Pb isotope ratios of these meteorites indicate a ²³⁸U/²⁰⁴Pb ratio of 5 for Mars, compared with the terrestrial value of ~8. Thus Martian moderately volatile/refractory element ratios appear to be systematically higher than terrestrial ratios.

The comparison of Venus with the Earth is particularly interesting. Though the two planets are of similar size, the Venetian atmosphere is almost 100 times more massive than that of the Earth.

TABLE 10.8. DATA REGARDING THE SUN, THE PLANETS, AND THEIR MAJOR SATELLITES

	Mass (kg)	radial distance (AU)	radius (km)	density (g/cc)	1 atm density (g/cc)	Principal atmospheric components
Sun	1.99×10 ³⁰		6.96×10 ⁵	1.4		
Mercury	3.35 ×10 ²³	0.39	2.44×10 ³	5.42	5.3	—
Venus	4.87 ×10 ²⁴	0.72	6.05×10 ³	5.24	3.95	CO ₂ , N ₂ , Ar
Earth	5.98 ×10 ²⁴	1.0	6.38×10 ³	5.52	4.03	N ₂ , O ₂ , Ar
Moon	7.35 ×10 ²²		1.74×10 ³	3.3	3.4	—
Mars	6.42 ×10 ²³	1.6	3.39×10 ³	3.93	3.7	CO ₂ , N ₂ , Ar
asteroids	4 ×10 ²¹	2.8	≤10 ³			
Jupiter	1.90 ×10 ²⁷	5.2	6.99×10 ⁴	1.31		H, He
Io	8.63 ×10 ²²		1.82×10 ³	3.42		—
Europa	4.71×10 ²²		1.55×10 ³	3.03		—
Ganymede	1.51 ×10 ²³		2.63×10 ³	1.98		—
Callisto	1.06 ×10 ²³		2.40×10 ³	1.83		—
Saturn	5.69 ×10 ²⁶	9.6	5.95×10 ⁴	0.69		H, He
Titan	1.38 ×10 ²³		2.58×10 ³	1.88		N ₂ , CH ₄
Uranus	8.73 ×10 ²⁵	19.1	2.54×10 ⁴	1.30		H, He, CH ₄
Neptune	1.03 ×10 ²⁶	30.8	2.13×10 ⁴	1.76		H, He, CH ₄
Triton	2.14×10 ²² (?)		1.35×10 ³	2.08		—
Pluto	2.88×10 ²²	39.4	1.15×10 ³	~2.0		—
Chiron	1.74×10 ²¹		5.93×10 ²	~2.0		—
<i>Anhydrous Chondrites</i>					3.4-3.9	

CHAPTER 10: COSMOCHEMISTRY

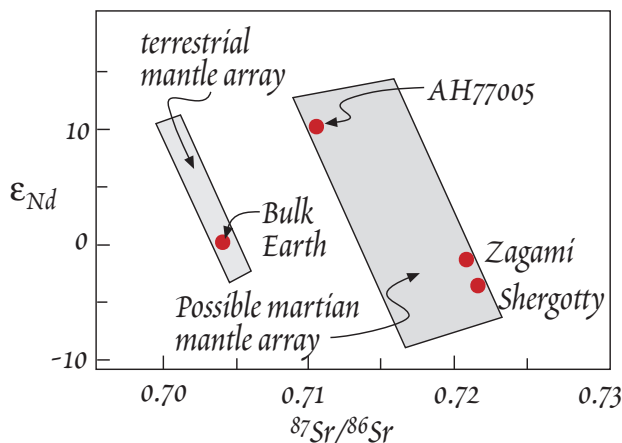


Figure 10.37. Comparison of terrestrial and martian Sr-Nd isotope systematics. The martian array is based on the assumption that SNC meteorites come from Mars. Mars appears to have higher $^{87}\text{Sr}/^{86}\text{Sr}$ and therefore higher Rb/Sr. After Taylor (1992).

that of Earth is about 300. Since ^{40}Ar is produced by radioactive decay, it is related to the planetary K/Ar ratio. The terrestrial $^{40}\text{Ar}/^{36}\text{Ar}$ is high because the Earth captured relatively little primordial Ar; most of the Ar in the terrestrial atmosphere has been produced by decay of ^{40}K . Apparently, Venus captured much more primordial Ar and has a much lower K/Ar ratio than the Earth. Thus on Venus, the amount of ^{40}Ar produced by decay of ^{40}K is smaller compared to the primordial ^{36}Ar .

Although the Earth is depleted in noble gases relative to Venus, it appears to be richer in H_2O (Prinn and Fegley, 1989). Furthermore, the Earth and Venus appear to have similar K/U ratios, implying similar depletions in the moderately volatile elements (Taylor, 1991).

Thus in detail, we find the compositional differences between planets cannot simply be explained by radially decreasing temperature. The noble gas-rich nature of Venus is just one example. Another example is Mercury. Considering its density, Mercury appears to be much richer in iron than the other terrestrial planets, which is difficult to explain simply a temperature effect (since Fe condenses temperatures similar to Mg silicates). In the outer Solar System, we find that although Uranus and Neptune are further from the Sun, they are poorer in H and He than Saturn and Jupiter. Jupiter and Saturn appear to have H/C and N/H ratios that are about a factor of 2 lower than the solar values, and thus only modestly depleted in H. C/H ratios in Uranus and Neptune, however, are 25 times the solar value. Interestingly, while Uranus and Neptune have solar H/He ratios, the atmospheres of Jupiter and Saturn are depleted in He relative to H. However, this probably reflects internal fractionation of these elements within these planets. He becomes saturated in the H_2 -dominated fluid that in outer part of Jupiter, exsolves and sink in the metallic H core, where it is more soluble.

Thus factors other than radial decrease in nebular temperature appear to also have been involved in creating the variety of chemical compositions we see in the Solar System. Some of these factors appear to be at least partly understood. For example, the compositional differences between the giant and icy planets may have been a matter of timing. The cores Jupiter and Saturn apparently formed earlier than those of Uranus and Neptune and thus were able to capture nearly their complete share of nebular gas. Uranus and Neptune apparently formed after much of the gas had dissipated.

The details of the accretion process may also have played an important role in governing the final composition of the planets. As we shall discuss below, there is something close to a consensus among planetary scientists and cosmochemists that the Moon formed as a result of a giant impact of a very large body on the Earth. Such an impact is consistent with current models of planetary accretion, which predict that the final stages of their assembly involve the collision of large planetary em-

Whereas the Venus's atmosphere is dominated by CO_2 , that of the Earth is dominated by N_2 and O_2 . However, the differences in both atmospheric mass and the abundance of CO_2 may reflect the difference in geological processes, and biological processes, on the two planets. Both planets appear to have similar relative abundances of carbon and nitrogen (Prinn and Fegley, 1989). In the case of the Earth, however, most of the surficial carbon is locked up in carbonates and organic carbon in rocks. This is in part due to biological activity, as is the presence of O_2 in the terrestrial atmosphere. There are, however, other differences that are more fundamental. The Venetian atmosphere is richer in noble gases than is the terrestrial one. Furthermore, the $^{40}\text{Ar}/^{36}\text{Ar}$ ratio of the Venetian atmosphere is about 1.15, whereas

CHAPTER 10: COSMOCHEMISTRY

bryos (e.g., Wetherill, 1990). The energy released in the hypothesized giant impact is enormous and could have been sufficient to melt much of the Earth, and much of its volatile elements may have been lost as a result. In contrast, the accretionary histories of Venus and Mars were apparently such that they retained much of their volatile inventory (although the slow backward rotation of Venus suggests it also suffered a late impact). In this respect, we note that the Earth with a satellite that is a significant fraction of its own size is unique. Venus has no moon and the moons of Mars are merely captured asteroids.

A large impact may also explain the peculiar composition of Mercury. Mercury appears to consist of a large Fe-Ni core and a relatively thin silicate mantle. Benz et al. (1988) proposed that Mercury formed with a much larger silicate mantle, but that much of this mantle was lost as a result of a collision with a body roughly 20% the size of the present Mercury.

In summary, the temperature gradient in the solar nebula, the timing of planet formation, and accretionary histories may all play a role in determining planetary composition. This is not to say any real understanding of planet formation has been achieved. How much of the volatile depletion of the terrestrial planets should be attributed to their accretionary history and how much to high temperatures in the inner solar nebula remains unclear. And while there is a consensus that the gas-rich nature of Jupiter and Saturn is due to their formation before the nebular gas was lost, we can only guess as to why they formed early. The inner Solar System heat source is also a mystery. The heat generated by collapse of a molecular cloud should have dissipated early, before T-Tauri winds swept out the nebular gas. If so, the moderately volatile elements should have recondensed. Perhaps planetesimal formation got underway while the inner Solar System was still hot. If so, volatiles would not have been accumulated by them. Any recondensed moderately volatile elements may have remained in small particles that were swept out by later T Tauri winds. The available evidence suggests, however, that planetismals did not form until later. ^{26}Mg anomalies suggest an interval of several million years between the formation of CAI's, the oldest known "event" and chondrule formation, which probably preceded planetesimal formation. This should have been enough time for the inner Solar System to cool to the point where moderately volatile elements would condense. At the least, the absence of ^{26}Mg anomalies in achondrites indicates ^{26}Al was effectively extinct by the time the parent bodies of these meteorites differentiated, implying it occurred millions of years after CAI formation. This observation also eliminates ^{26}Al as a heat source for melting and differentiation of achondrite parent bodies.

Perhaps there was another heat source. Radiation and solar wind from the Sun during its T Tauri stage have been suggested. But while this may be sufficient to keep the inner Solar System warm enough to prevent ice from condensing, it seems considerably less likely it would be sufficient to keep elements such as K from condensing. Rubin (1995) argues that collisional heating was sufficient to produce the metamorphism of meteorite parent bodies. This requires that these bodies be large. If so, they one must ask how the carbonaceous chondrite parent bodies, which apparently include large asteroids such as Ceres, avoided such heating.

Clearly, much remains to be learned about the early history of the Solar System. Progress has, however, been particularly rapid in the last 10 or 20 years. This progress in part been technologically driven, as astronomers work with increasingly powerful telescopes capable of looking at the full electromagnetic spectra, theorists obtain ever more powerful computers, and geochemists develop more powerful analytical tools. Yet the fall of the Allende meteorite in 1969, with its abundant and large CAI's, and man's exploration of the Moon beginning in the same year were perhaps the sparks for this revolution. Hopefully, exploration of other planetary bodies in the future, as well as continued technological advances, will help move us toward the solution to the difficult problems that remain.

THE MOON: ITS CHEMISTRY, HISTORY AND RELATION TO EARTH

The Moon is the one planetary sized body about whose early history we have gained some understanding. This history may have been partly shared by Earth, and is therefore worth considering. A consensus about the origin of the Moon may be emerging 25 years after the Apollo landings. Most investigators now believe the Moon originated as the result of the impact of a large body, similar in size, perhaps to Mars on the Earth. This event probably occurred near the end of the main accretionary period.

THE GIANT IMPACT HYPOTHESIS

The impact hypothesis was initially suggested to explain the angular momentum, which is much greater than that of other planets, and other "anomalous" features of the Earth-Moon system, including the relatively large mass of the Moon and the high inclination of its orbit (Hartmann and Davis, 1975). It also is able to explain many of the unusual compositional features of the Moon.

Table 10.9 compares the composition of the Earth and the Moon. There are several notable differences. First, the Moon is depleted in moderately volatile elements (Na, K) compared to the Earth. Second, although the silicate part of the Moon (mantle + crust) is richer in iron than the silicate Earth, the bulk lunar composition is poorer in iron than the terrestrial one. This reflects the small size of the lunar core, only about 2% of the mass of the planet. The lunar depletion in Fe compared to the Earth extends to all siderophile and chalcophile elements as well. The Moon is also much more depleted in the highly volatile elements as well. In the words of Newsom and Taylor (1989), it is "bone dry". Conversely, the Moon is enriched the refractory lithophile elements, having nearly twice the Al and Ca as the Earth. Despite these compositional differences, the Moon and Earth have the same oxygen isotope composition, which strongly suggests they formed from the same part of the solar nebula.

Fairly detailed models of the impact have been produced (e.g., Newsom and Taylor, 1989). The model that best explains the features of the Earth-Moon system can be best summarized as follows. During the latest stages of accretion, the Earth was struck at low angle, and relatively low velocity (5 km/s) by a body slightly larger than Mars. The impactor presumably shared the depletion in highly and moderately volatile elements that characterizes the terrestrial planets. Metallic cores had already formed in both the Earth and the impactor. The collision disrupts the impactor and partially disrupts the Earth's mantle, and much of the resulting debris goes into orbit around the Earth. Most of the disrupted core of the impactor quickly (a matter of hours) accretes to the Earth and the silicate material in orbit more slowly coalesces to form Moon. About 85% of the material forming the Moon is derived from the impactor, the remainder from the Earth's mantle. A small core then segregates from the largely molten Moon. Most of the core of the impactor quickly sinks through the disrupted mantle of the Earth to coalesce with the existing terrestrial core. The depletion of siderophile elements in the Moon is thus a result of its formation from the silicated portions of the impactor and Earth, in which the siderophile were already depleted by core formation. The volatile element depletion of the Moon is a consequence of the evaporation of these elements during impact.

Table 10.9. Comparison of the Compositions of the Earth and Moon

	Bulk Earth	Bulk Moon	Silicate Earth	Silicate Moon
SiO ₂	30.38	43.4	45.0	44.4
TiO ₂	0.14	0.3	0.201	0.31
Al ₂ O ₃	3.00	6.0	4.45	6.14
FeO	5.43	10.7	8.05	10.9
MgO	25.52	32	37.8	32.7
CaO	2.40	4.5	3.55	4.6
Na ₂ O	0.24	0.09	0.36	0.09
K ₂ O	0.02	0.01	0.029	0.01
Fe	28.43	2.166	87.5	
Ni	1.75	0.134	5.4	
S	1.62		5	
core%	32.5%	2.3%		
mantle	67.5%	97.7%		

Terrestrial composition from McDonough and Sun (1995), assuming the light element in the core is S. Lunar composition from Taylor (1992).

Table 10.10. REPRESENTATIVE COMPOSITIONS OF LUNAR ROCKS

	Highland Anorthosite	Highland Anorth. Gabbro	Mare Qz Tholeiite	Low-K Mare Basalt	Fra Mauro KREEP
SiO ₂	44.3	44.5	46.1	40.5	48.0
TiO ₂	0.06	0.39	3.35	10.5	2.1
Al ₂ O ₃	35.1	26.0	9.95	10.4	17.6
FeO	0.67	5.77	20.7	18.5	10.9
MnO	—	—	0.28	0.28	—
MgO	0.80	8.05	8.1	7.0	8.7
CaO	18.7	14.9	10.9	11.6	10.7
Na ₂ O	0.8	0.25	0.26	0.41	0.7
K ₂ O	—	—	0.07	0.10	0.54
P ₂ O ₅	—	—	0.08	0.11	—
Cr ₂ O ₃	0.02	0.06	0.46	0.25	0.18
Total	100.5	99.9	100.3	99.7	99.4

GEOLOGY AND HISTORY OF THE MOON

The Moon can be divided into three geologic provinces: the highlands, mountainous regions apparently consisting largely of anorthosite, the uplands, areas of mild relief covered by a blanket of ejecta from the large impacts, and the Mare, the large craters which have been filled with basalt. Much of the surface of the Moon is covered with fine debris of impacts, called the regolith, consisting of rock and mineral fragments, glass, and some meteorite particles. For the most part, it seems to be locally derived; thus the regolith in the Mare differs from that of the highlands, though large impacts would have showered debris over large regions. Basalt from the Mare encompasses a variety of magma types, including both incompatible-element rich and incompatible-element poor types and both quartz-normative and olivine normative tholeiites. Highland rocks include anorthosite (nearly monomineralic calcic plagioclase), anorthosite gabbro (plagioclase and pyroxene with lesser amounts of olivine), dunite, and K-rich basalts. The highlands are extremely brecciated; most of these rock types have been found only as clasts in breccias. Table 10.10 shows some representative compositions of lunar rocks, and Figure 10.38 shows rare earth patterns of the same rock types.

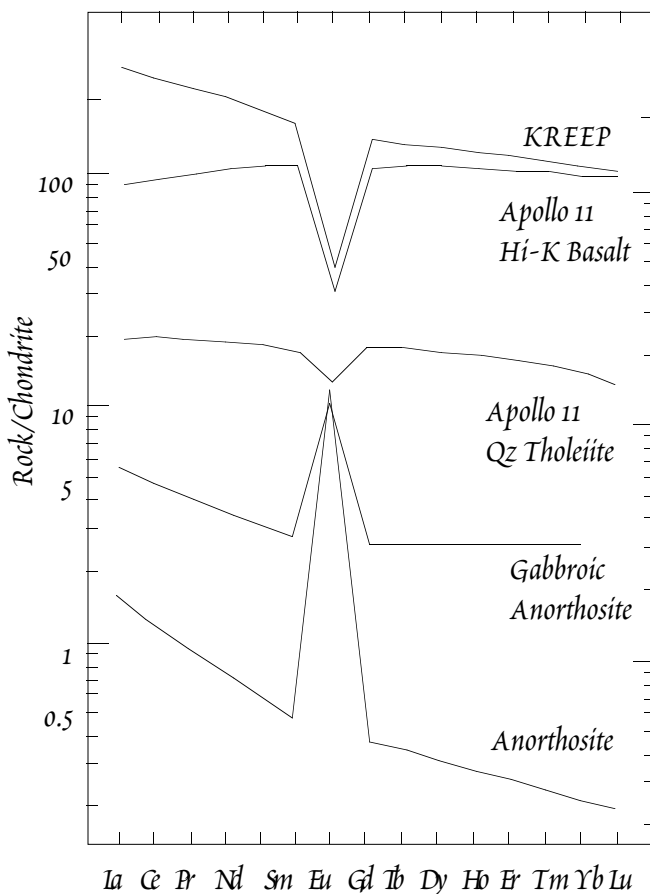


Figure 10.38. Rare earth patterns of representative lunar rocks. From Taylor (1975).

Most of the lunar Mare are thought to have been created between 4.2 and 3.8 Ga. Preexisting large impact craters were de-

CHAPTER 10: COSMOCHEMISTRY

stroyed in this time period. Subsequently, the Mare were flooded by basalt to a depth of 5 to 10 km. These were partial melts generated at 100 or so km depth. The flooding occurred over an extensive time: 3.9 to 3.1 Ga. Mare flooding was the last major lunar geologic event. Subsequent to that time, the only activity has been continual bombardment by meteorites and asteroids, which continued to produce minor disruption of the surface and build up of the regolith, and rare volcanism.

Figure 10.39 illustrates the highlights of lunar history. The oldest lunar rocks are nearly as old as meteorites. These are clasts of anorthositic highland rocks found in breccias. This suggests lunar differentiation began about 4.5 billion years ago. But most highland rocks have ages between 3.9 and 4.0 Ga. For the most part, these ages are interpreted as (and sometimes can be shown to be) the time of impact metamorphism. Apparently the Moon suffered very heavy bombardment by meteorites and asteroids as late as 3.9 Ga. The clustering of ages around this time gives rise to the idea of a 'late heavy bombardment' of the Moon. Alternatively, the age pattern could have been produced by decreasing impact rate between 4.5 to 3.9 Ga. According to this hypothesis, impact rates were so high in the first 500 Ma, that the probability of a rock surviving without having its age "reset" by impact metamorphism would be very low. Thus only a fraction would survive to record older ages. Around 3.9 billion years, the impact rate dropped to the point where the probability was such that most rocks would escape further impact metamorphism. Whether there was a 'late heavy bombardment' is still disputed.

One of the more important conclusions derived from study of the Moon is that it underwent very extensive melting just after its formation, perhaps forming a magma ocean 100 km deep. It is also possible that it was entirely molten, the energy supplied by the giant impact would have been sufficient to accomplish this. The anorthosite of the highlands is thought to have originated by plagioclase flotation in the magma ocean, i.e., anorthosite icebergs. The lunar crust seems to have been largely in place within 100 to 200 Ma after the Moon's formation. Fractional crystallization of this magma ocean and flotation of plagioclase accounts for the general Eu depletion (Figure 10.38) observed in basalts derived from the lunar mantle. A particularly incompatible-element enriched basalt, called KREEP (K, REE, P: potassium, rare earth elements and phosphorus enriched) is thought to reflect extreme differentiation of the magma ocean.

There is almost complete agreement that extensive melting on the Moon occurred very early. Given this, and the much greater amounts of energy released by accretion of the Earth, it is hard to see how the Earth would not also have experienced extensive melting. The energy supplied by the giant impact would have been sufficient to melt the entire mantle of the Earth, though this depends on exactly how this energy is dissipated.

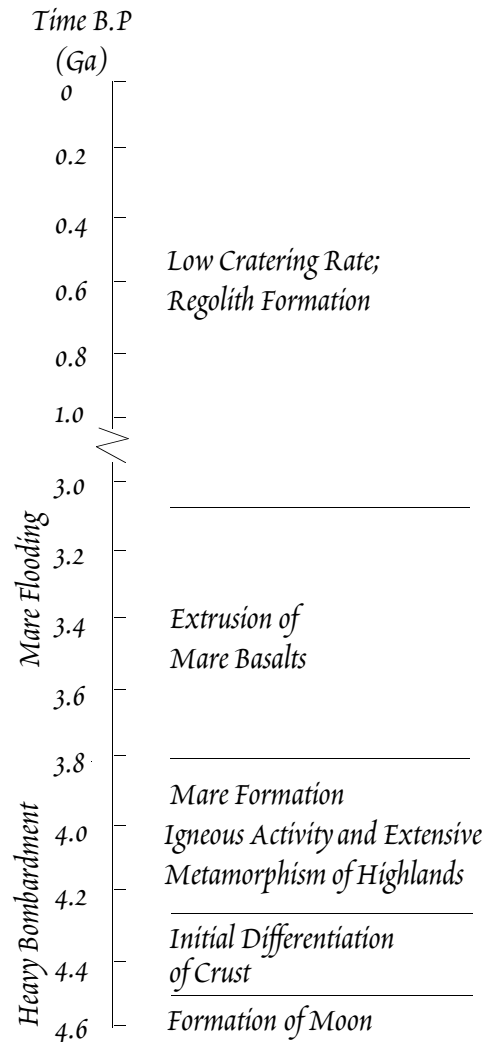


Figure 10.39. Highlights of lunar chronology

CHAPTER 10: COSMOCHEMISTRY

REFERENCES AND SUGGESTIONS FOR FURTHER READING:

- Anders, E. and E. Zinner. 1993. Interstellar grains in primitive meteorites: diamond, silicon carbide, and graphite. *Meteoritics*. 28: 490-514.
- Anders, E. and N. Grevesse. 1989. Abundances of the elements: Meteoritic and solar, *Geochim. Cosmochim. Acta*, 53: 197-214.
- Anders, E., 1988. Circumstellar material in meteorites: noble gases, carbon and nitrogen, in *Meteorites and the Early Solar System*, ed. by J. F. Kerridge and M. S. Matthews. Tucson: Univ. of Arizona Press
- Benz, W., W. L. Slattery and A. G. W. Cameron. 1988. Collisional stripping of Mercury's mantle. *Icarus*. 74: 516-528.
- Boss, A. P. 1990. 3D solar nebular models: implications for Earth origin, in *Origin of the Earth*, ed. by H. E. Newsom and J. H. Jones. Oxford: Oxford Univ. Press.
- Burbidge, E. M., G. R. Burbidge, W. A. Fowler, and F. Hoyle. 1957. Synthesis of the elements in stars, *Rev. Mod. Phys.*, 29: 547-650.
- Cameron, A. G. W. 1962. The formation of the sun and planets. *Icarus*, 1: 13-69.
- Cameron, A. G. W. 1995. The first ten million years in the solar nebula. *Meteoritics*. 30: 133-161.
- Chen, J. H. and G. J. Wasserburg. 1983. The least radiogenic Pb in iron meteorites. *Fourteenth Lunar and Planetary Science Conference, Abstracts*, Part I, Lunar & Planet Sci. Inst., Houston, pp. 103-104.
- Clayton, R. N., N. Onuma, and T. K. Mayeda. 1976. A classification of meteorites based on oxygen isotopes, *Earth. Planet. Sci. Lett.*, 30: 10-18.
- Cowley, C. R. 1995. *Cosmochemistry*. Cambridge: Cambridge University Press.
- Crabb, J., and L. Schultz. 1981. Cosmic-ray exposure ages of the ordinary chondrites and their significance for parent body stratigraphy, *Geochim. Cosmochim. Acta*, 45: 2151-2160.
- Grossman, L., 1972. Condensation in the primitive solar nebula, *Geochim. Cosmochim. Acta*, 36: 597-619.
- Hartmann, W. K. and D. R. Davis. 1975. Satellite-sized planetismals and lunar origin. *Icarus*. 24: 504-515.
- Jacobsen, S. and G. J. Wasserburg. 1980. Sm-Nd isotopic evolution of chondrites, *Earth Planet. Sci. Lett.*, 50, 139-155.
- Kerridge, J. F., and M. S. Matthews (editors). 1988. *Meteorites and the Early Solar System*, Univ. of Arizona Press, Tucson, 1269pp.
- Larimer, J. W., 1967. Chemical fractionations in meteorites — I: condensation of the elements, *Geochim. Cosmochim. Acta*, 31, 1215-1238.
- Larimer, J. W., The cosmochemical classification of the elements, in *Meteorites and the Early Solar System*, edited by J. F. Kerridge and M. S. Matthews, p. 375-389, Univ. Arizona Press, Tucson, 1988.
- Lee, T., D. A. Papanastassiou and G. J. Wasserburg, 1976. Demonstration of ²⁶Mg excess in Allende and evidence for ²⁶Al, *Geophys. Res. Lett.*, 3: 41-44.
- McDonough, W. F. and S.-S. Sun. 1995. The composition of the Earth. *Chem. Geol.* 120: 223-253.
- McSween, H. Y., Jr. 1987. *Meteorites and their Planet Bodies*, New York: Cambridge University Press.
- Newsom, H. E. and J. H. Jones (editors). 1990. *Origin of the Earth*, Oxford: Oxford Univ. Press.
- Newsom, H. E. and S. R. Taylor. 1989. Geochemical implications of the formation of the Moon by a single giant impact. *Nature*. 338: 29-34.
- Papanastassiou, D. A., and G. J. Wasserburg. 1969. Initial strontium isotopic abundances and the resolution of small time differences in the formation of planetary objects. *Earth Planet. Sci. Lett.*, 5: 361-376.
- Podosek, F. A. 1970. Dating of meteorites by high temperature release of iodine correlated ¹²⁹Xe, *Geochim. Cosmochim. Acta*, 34: 341-365.
- Prinn, R. G. and B. Fegley. 1989. Solar nebula chemistry: origin of planetary, satellite and cometary volatiles. in *Origin and Evolution of Planetary and Satellite Atmospheres*, ed. S. K. Atreya, J. B. Pollack and M. S. Mathews. Tucson: Univ. of Arizona Press.

CHAPTER 10: COSMOCHEMISTRY

Rubin, A. E. 1995. Petrological evidence for collisional heating of chondritic asteroids. *Icarus*. 113: 156-167.

Talyor, S. R. 1991. Accretion in the inner nebula: the relationship between terrestrial planetary compositions and meteorites. *Meteoritics*. 26: 267-277.

Tang, M. and E. Anders. 1988. Isotopic anomalies of Ne, Xe, and C in meteorites. II. Interstellar diamond and SiC: Carriers of exotic noble gases, *Geochim. Cosmochim. Acta*, 52, 1235-1244, 1988.

Tatsumoto, M., R. J. Knight, and C. J. Allègre. 1973. Time differences in the formation of meteorites ad determined from the ratio of lead-207 to lead-206, *Science*, 180: 1279-1283.

Taylor, S. R. 1975. *Lunar Science: A Post-Apollo View*. Pergamon Press, New York, 372 pp.

Taylor, S. R. 1992. *Solar System Evolution: A New Perspective*. Cambridge: Cambridge University Press.

Thiemens, M. H., and J. E. Heidenreich. 1983. The mass independent fractionation of oxygen — A novel isotopic effect and its cosmochemical implications, *Science*, 219: 1073-1075.

Van Schmus, W. R., and J. A Wood. 1967. A chemical petrologic classification for the chondritic meteorites. *Geochim. Cosmochim. Acta*, 31: 747-765.

Wasserburg, G. J., M. Busso, R. Gallino and C. M. Raiteri. 1994. Asymptotic giant branch stars as a source of short-lived radioactive nuclei in the solar nebula. *Astrophys. J.* 424: 412-428.

Wasson, J. T., 1974. *Meteorites*, Springer-Verlag, Berlin, 316 pp.

Wasson, J. T., 1985. *Meteorites: Their Record of Early Solar System History*, New York: W. H. Freeman.

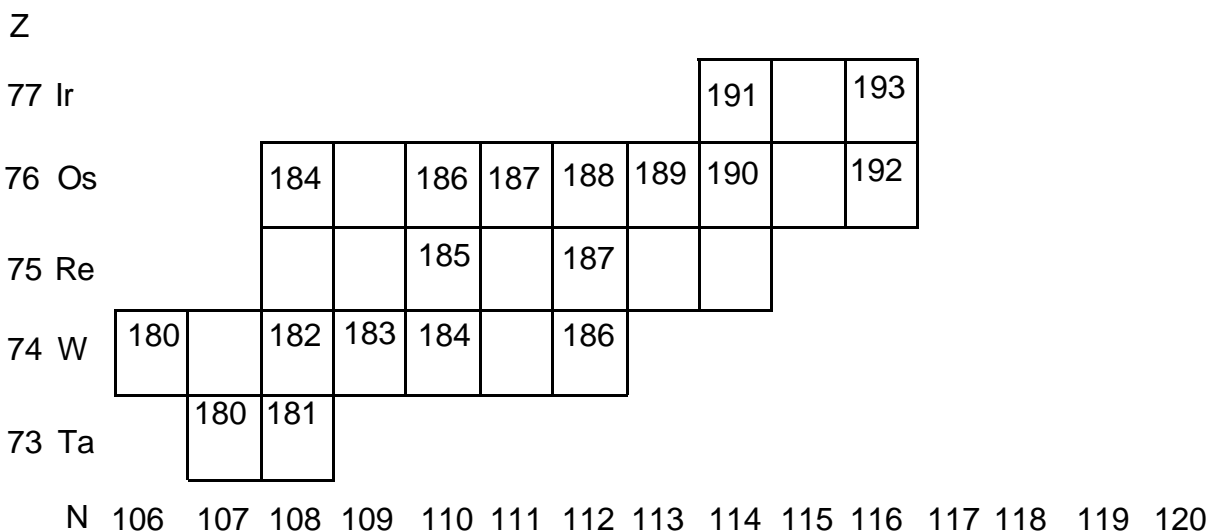
Wetherill, G. W. 1990. Formation of the Earth, *Ann. Rev. Earth Planet. Sci.*, 18: 205-256.

Wetherill, G. W. and G. R. Stewart. 1993. Formation of planetary embryos: effects of fragmentation, low relative velocity, and independent variation of eccentricity and inclination. *Icarus*. 106: 190-209.

Wood, J. A.. 1988. Chondritic meteorites and the solar nebula, *Ann. Rev. Earth Planet. Sci.*, 16, 53-72.

PROBLEMS

1. On the part of the chart of the nuclides below, identify the mode of origin (S, R, or P process) of the stable isotopes of W, Re, Os, and Ir by writing S, R or P in the box for each (remember some nuclides can be created by more than one process). Identify those isotopes you feel should be most abundant and those least abundant. On the chart below, mass numbers are given for only the stable isotopes. As a start, assume the S-process path starts at ¹⁸¹Ta. Assume the unstable isotopes will decay before capturing a neutron during the S-process.



CHAPTER 10: COSMOCHEMISTRY

2. One calcium-aluminum inclusion in the Allende meteorite has $\delta^{26}\text{Mg}$ values which imply a $^{26}\text{Al}/^{27}\text{Al}$ ratio of 0.46×10^{-4} at the time of its formation. A second inclusion apparently formed with a $^{26}\text{Al}/^{27}\text{Al}$ ratio of 1.1×10^{-4} . The half-life of ^{26}Al is 7.2×10^5 years. Assuming both these inclusions formed from the same cloud of dust and gas and that the $^{26}\text{Al}/^{27}\text{Al}$ ratio in this cloud was uniform, what is the time interval between formation of the two inclusions?
3. Assuming that the oxygen in C3 chondrites are a mixture of oxygen having an oxygen isotope composition lying on the terrestrial fractionation line in Figure 10.23 and pure ^{16}O , how much ^{16}O would have to be added to oxygen lying on the terrestrial fractionation line to reproduce their oxygen isotopic composition?
4. Using the partition coefficients in Table 6.5, estimate the fraction of plagioclase that would have to fractionally crystallize from a lunar magma ocean to produce the Eu anomaly of KREEP shown in Figure 10.32. Hint: concern yourself only with the Eu/Sm ratio.
5. Make a plot of the log of the fraction of Os condensed from a gas of "solar" composition as a function of temperature (e.g., a plot similar to Figure 10.27). Assume a total pressure of 10^{-4} atm, ΔH_v° of 738 kJ/mol, ΔS_v° of 139 J/mol, and the solar system abundances in Table 10.2. Assume the solid is pure Os metal. (HINT: about 50% will be condensed at 1737 K.)